EXCITED STATES
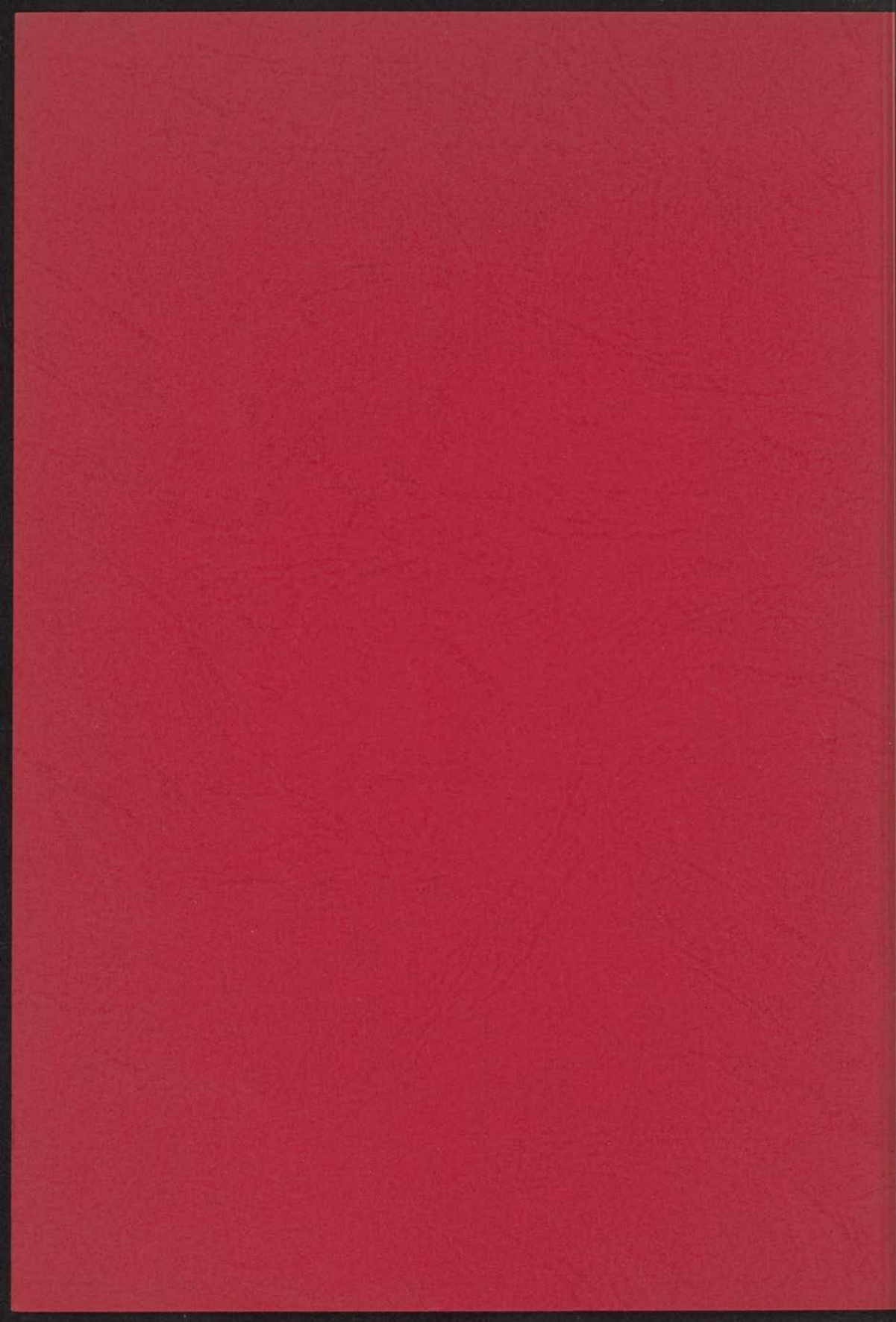# OF ATOMS AND MOLECULES

I LOW-ENERGY ELECTRON SPECTROSCOPY
II QUANTUMCHEMICAL CALCULATIONS ON CONJUGATED SYSTEMS

F.W.E. KNOOP

EXCITED STATES
OF ATOMS AND MOLECULES

I LOW-ENERGY ELECTRON SPECTROSCOPY
II QUANTUMCHEMICAL CALCULATIONS ON CONJUGATED SYSTEMS

STELLINGEN

behorende bij het proefschrift van

F.W.E. KNOOP

I.

Het door Allinger en Stuart gehanteerd energiecriterium ter selectie van de meest essentiële aangeslagen configuraties in Molecular Orbital berekeningen voldoet slecht. Een criterium gebaseerd op storingsrekening geeft wel goede resultaten.

N.L. Allinger, Th.W. Stuart, J. Chem. Phys. **47** (1967) 4611.
Dit proefschrift, hoofdstuk III.

II.

Bij de door Chamberlain en Whittle gevolgde methode voor de bepaling van de C-H bandsterkte in benzeen, welke gebaseerd is op de vorming van CHF_3 moleculen door reactie van benzeen met CF_3 radicalen, is onvoldoende aandacht besteed aan optredende nevenreacties.

G.A. Chamberlain, E. Whittle, Trans. Far. Soc. **67** (1971) 2077.

III.

In drempelexcitatie spectra van benzeen met electronen werd tot nu toe de absorptie bij $\sim$ 4.8 eV gekarakteriseerd als een overgang naar de eerste singulet toestand van benzeen ($^1B_{2u}$). Mede op grond van het gedrag van de excitatiefunctie van deze absorptie bij toenemende electronenenergie is een verklaring als triplet excitatie ($^3E_{1u}$) meer waarschijnlijk.

R.N. Compton, R.H. Huebner, P.W. Reinhardt, L.G. Christophorou, J. Chem. Phys. **48** (1968) 901.
M.J. Hubin-Franskin, J.E. Collin, Int. J. Mass Spectr. **5** (1970) 163.
Dit proefschrift, hoofdstuk V.

IV.

Het model van Joliot en Joliot ter verklaring van het fluorescentie gedrag van chlorophyll in vivo is niet in overeenstemming met de resultaten van experimenten van Tumerman en Sorokin en van Briantais, Govindjee en Merkelo.

A. Joliot, P. Joliot, C.R. Acad. Sc. Paris **258** (1964) 4622.
L.A. Tumerman, E.M. Sorokin, Molecularnaja Biologia **1** (1968) 628.
J.M. Briantais, Govindjee, H. Merkelo, Int. Conf. Photosynthetic Unit, 1970.

V.

Bij excitatie van H_2O door laag energetische electronen is een toekenning als het triplet analogon van de optisch toegestane overgang ($^1B_1$) aan de zwakke absorptieband bij $\sim$ 4.5 eV aan sterke bedenkingen onderhevig.

R.N. Compton, R.H. Huebner, P.W. Reinhardt, L.G. Christophorou, J. Chem. Phys. **48** (1968) 901.
C.R. Claydon, G.A. Segal, H.S. Taylor, J. Chem. Phys. **54** (1971) 3799.
F.W.E. Knoop, H.H. Brongersma, L.J. Oosterhoff, Chem. Phys. Letters **13** (1972) 20.

VI.

Voor het aantonen van de oppervlakte specificiteit met ionenverstrooiing (He^+) maakt Smith gebruik van cadmium sulfide eenkristallen. Het experiment wordt echter juist zo uitgevoerd dat een uitspraak over deze specificiteit onmogelijk is.

D.P. Smith, Surface Science **25** (1971) 171.
H.H. Brongersma, P.M. Mul, Chem. Phys. Letters, accepted for publication.

VII.

Men kan gemakkelijk onderscheid maken tussen singulet-singulet en singulet-triplet aanslag van atomen/moleculen door energieverliesmetingen uit te voeren met resp. H^+- en H_2^+-ionen.

J.H. Moore, J.P. Doering, J. Chem. Phys. **52** (1970) 1692.

VIII.

De toekenning van triplet excitaties door Bowman en Miller aan de laag-energetische absorpties van acetyleen (2.0 eV) en propyn (2.8 eV) bij beschieting met langzame electronen is aanvechtbaar.

C.R. Bowman, W.D. Miller, J. Chem. Phys. **42** (1965) 681.
Dit proefschrift, hoofdstuk VII.

IX.

De quantum opbrengst voor fluorescentie van benzeen zoals bepaald door Smith bij excitatie van benzeen met electronen (25 - 200 eV) is in tegenstelling tot zijn bewering niet in overeenstemming met de resultaten van Parmenter en Schuyler.

W.H. Smith, J. Chem. Phys. **54** (1971) 4169.
C.S. Parmenter, M.W. Schuyler, Chem. Phys. Letters **6** (1970) 339.

X.

De conclusie van Gerrard, Hudson en Mooney dat voor dialkylaminodichloroboranen de toename van het dubbele band karakter van de centrale binding (B-N) direct gecorreleerd is met een vermindering in de frequentie van de strekvibratie is aan sterke twijfel onderhevig.

W. Gerrard, H.R. Hudson, E.F. Mooney, J. Chem. Soc. **1960** 5168.

XI.

Het is aan grote twijfel onderhevig of het huidig standpunt van de vakbonden met betrekking tot de loonpolitiek in het belang is van de werknemers. De loonpolitiek zal meer afgestemd moeten worden op de totale maatschappelijke problematiek zoals de toenemende werkloosheid en de milieuverontreiniging.

EXCITED STATES
OF ATOMS AND MOLECULES

I LOW-ENERGY ELECTRON SPECTROSCOPY
II QUANTUMCHEMICAL CALCULATIONS ON CONJUGATED SYSTEMS

PROEFSCHRIFT

TER VERKRIJGING VAN DE GRAAD VAN DOCTOR
IN DE WISKUNDE EN NATUURWETENSCHAPPEN AAN
DE RIJKSUNIVERSITEIT TE LEIDEN, OP GEZAG VAN
DE RECTOR MAGNIFICUS DR. W.R.O. GOSLINGS, HOOG-
LERAAR IN DE FACULTEIT DER GENEESKUNDE, VOL-
GENS BESLUIT VAN HET COLLEGE VAN DEKANEN
TE VERDEDIGEN OP WOENSDAG 7 JUNI 1972 TE
KLOKKE 15.15 UUR

DOOR

FRITS WILLEM EVERT KNOOP

GEBOREN TE MEDAN
NED. INDIË (THANS INDONESIË) IN 1942

C O N T E N T S

CHAPTER I

INTRODUCTION

Atoms and molecules in their excited states play a prominent part in many kinds of chemical and physical phenomena including photosynthesis, photochemistry, energy degradation in radiation chemistry and astrophysical processes.

Among the electronically excited states especially the triplet state (optically forbidden) is of interest. Both the relatively long life time (10^{-4} - 10 sec) and the presence of two unpaired electrons makes this state a reactive species. Not so long ago only phosphorescence (decay of the (lowest) triplet state to the ground state by emission of light) provided information about the life time and excitation energy of the triplet state. Nowadays flash photolysis (using laser techniques) is general usage. This method enables to study the lowest triplet state and to follow its kinetics where phosphorescence is not observable. Moreover triplet-triplet excitation energies can also be measured (Porter et al., 1954). Another way to determine the energies of triplet states is by measuring the enhanced photon absorption of the ground state to the triplet state due to increased spin-orbit coupling in the molecule by external perturbation. This can be effected using heavy atom solvents ($CHBr_3$, CH_2J_2) or high pressure gases like O_2, NO or other paramagnetic molecules (Evans, 1956).

Nevertheless the number of triplet states observed by optical techniques is rather scanty, even the energy of the lowest triplet state is often not known.

Electron-impact spectroscopy enables the determination of many excited states which have not been observed before by other methods. It appears that the selection rules for the excitation of atoms and

molecules depend strongly on the energy of the incident electron. While at high-energy electron impact the selection rules approach the optical ones, at low-energy electron impact practically all electronic transitions are allowed (chapter II). Triplet transitions appear to be important just above their threshold of excitation.

Threshold excitation processes can be studied by means of the Trapped Electron (T.E.) method as developed by Schulz (1958) and introduced into our laboratory by Brongersma (1968). However, using this technique characterization of the observed transitions is still difficult. In this thesis (chapter IV) a new technique is introduced, the so-called Double Retarding Potential Difference (D.R.P.D.) technique. This method allows to extend our measurements to 10 eV or more above the threshold of excitation. By studying the energy dependence of the excitation function in this energy region, classification of the studied process might be obtained; e.g. triplet transitions are known to peak within 10 eV above their threshold.

Both the T.E. method and the D.R.P.D. method can be applied with the newly constructed spectrometer which is described in chapter IV. Apart from the conventional inlet system, introduction of samples obtained from gases or liquids into the spectrometer, a high-temperature inlet system can be used allowing the measurement of low volatile compounds.

Using these techniques some atoms and molecules are studied which are important from a physical or chemical point of view, e.g. helium; water and related compounds; unsaturated compounds like benzene, 1,3,5 trans-hexatriene, 7,8 dehydro-cholesterol and acetylene. Triplet excitation turns out to be intensive in the measured spectra. Characterization, if necessary, is obtained in most cases by using the D.R.P.D. method.

For support of the assignment and a better understanding of the origin of the excited states, the excitation energies can be calculated (chapter II). In the case of conjugated systems (π-electrons) we performed extensive calculations studying the influence of singly, doubly and multiply excited configurations on the calculated energies. It appears that the predicted energies for hydrocarbons (planar), resulting from calculations in which singly and doubly excited configurations are included, agree with experimental values within 0.2 - 0.3 eV. In order to truncate the large number of excited

configurations a criterion, based on perturbation theory has been
developed which selects out the most essential configurations.
Calculations performed with the selected configurations give results
which are consistent with the outcome of calculations in which no
selection has been made.

C H A P T E R II

E L E C T R O N I M P A C T S P E C T R O S C O P Y

2.1 INTRODUCTION

The collision of an electron and an isolated atom or molecule may give rise to a large number of phenomena. Among them are the scattering without energy transfer (elastic), electron exchange, excitation or de-excitation of the target particle, ionization, negative ion formation, molecular dissociation or a combination of several of these processes.

The quantity which is directly related to the intensity of the studied process is the "cross section". This quantity has the dimensions of an area. The differential cross section $\sigma(\Theta,\phi)$ is determined by the flux of scattered electrons per unit solid angle, while the total cross section is given by

$$\sigma_{tot} = \int \sigma(\Theta,\phi) \sin \Theta \, d\Theta \, d\phi \qquad (2.1)$$

in which the angles (Θ,ϕ) specify the direction of the scattered electron.

From the above mentioned possibilities of interaction between an electron and an atom or molecule we will only consider the excitation process.

Let us first summarize the important differences between photon-impact and electron-impact spectroscopy.

i   At very high incident electron energy, more than 20 keV, the selection rules closely resemble the optical ones. However, at low incident energy, lower than ~ 100 eV, optically forbidden transitions are frequently observed. In particular spin forbidden

transitions (exchange of the incident electron with a molecular electron) will show up rather intensively near the threshold of excitation.

ii   In conventional optical spectroscopy all of the energy of the photon is absorbed by the system through a resonant process. In electron-impact spectroscopy the incident electron will transfer only part of its kinetic energy to the target particle. The study of the energy dependence and/or the angular dependence of the inelastically scattered electron will permit us to identify the transition involved.

iii   In photon-impact spectroscopy the procedure for excitation at energies higher than 7 eV (vacuum UV) is much more complicated due to experimental difficulties. For electron-impact spectros-copy the conditions are independent of energy loss.

iv   In general the resolution of the optical techniques is much better than found in electron-impact spectroscopy.

2.2   EXPERIMENTAL PROCEDURES

2.2.1 <u>Differential cross section measurements</u>

The measurement of differential (angular) cross sections consists of detection of the electrons which have been scattered by single collision with the target particles in a particular direction (θ, ϕ) and have simultaneously undergone a particular energy loss. The energy reso-lution of the incident electron beam and the energy selection of the inelastically scattered electrons are usually defined by the use of electrostatic analysers. From the current possible types, parallel plate condenser (Foner et al., 1961), 127° concentric cylindrical filter (Marmet et al., 1960), 180° hemispherical analyser (Lassettre et al., 1968; Simpson, 1964; Ehrhardt et al., 1968) the last type appears to be superior both in resolution and focusing capacities. Energy resolution of 5 meV at 10^{-9} A can be obtained. The angular dependence of the scattered electron intensity for a particular energy loss is sensitive to the nature of the studied transition thus providing a method for iden-tification of the transition involved (Kuppermann et al., 1968; Doering et al., 1967).

2.2.2 Total cross section measurements

The so-called Trapped Electron (T.E.) method introduced by Schulz (1958) allows the measurement of the total cross section of an excitation process close to threshold (Brongersma et al., 1967; Dowell et al., 1967; Hall et al., 1971). An extensive description of this method is presented in Chapter IV.

Threshold excitation spectra can also be obtained by means of the SF_6 scavenger method (Curran, 1963; Compton et al., 1968; Brion et al., 1968). Zero-energy electrons will attach to SF_6 molecules with high probability producing SF_6^- ions. The resolution obtained with the scavenger technique (~ 200 meV) is nearly the same as found with the T.E. method (100-200 meV).

Recently a new technique, the so-called Double Retarding Potential Difference (D.R.P.D.) method has been introduced by Knoop, Brongersma and Boerboom (1970) which allows to extend the energy region for total cross section measurements from 0 up to 10 eV above the threshold of excitation (see also chapter IV). Thus triplet transitions which are expected to peak within 10 eV from threshold might be identified by measuring the total cross section versus excess energy of the scattered electrons.

To produce the primary beam of electrons in both the T.E. and D.R.P.D. method the Retarding Potential Difference (R.P.D.) technique developed by Fox et al. (1955) is usually applied. Though a better resolution is obtained in comparison with the energy distribution resulting from a simple cathode, the improvement of the final energy spread will be limited due to the transverse energy spread of the incident electrons (60 - 100 meV) which is left unaffected (see also chapter IV).

In order to lower this limit we must look for other and better techniques of producing low energy spread electron beams. A very promising method is the so-called Trochoidal Electron Monochromator technique as developed by Stamatovic and Schulz (1968, 1970). From their work an experimental limit for resolution of the incident electrons results of 10 - 20 meV.

2.3   THEORETICAL METHODS

2.3.1   High energy electron impact

Provided the energy of the incident electron is large compared
with the binding energy of the molecular electrons an approximate method
of wide applicability known as the (first) Born approximation may be
used to calculate cross sections. This method is based on the assumption
that the interaction between the electron and the molecule is weak so
that the wave functions of the incident and scattered electrons can be
represented by plane waves. Defining the initial wave function of the
total system by $\exp(i\vec{k}_o \cdot \vec{r}_1) \cdot \phi_o(\vec{r}_2)$ and the wave function describing
the resulting system after the scattering event by $\exp(i\vec{k}_n \cdot \vec{r}_1) \cdot \phi_n(\vec{r}_2)$,
the scattering amplitude $f_n(\Theta,\phi)$ can be derived as (Born approximation)

$$f_n(\Theta,\phi) = \frac{-2m}{4\pi\hbar^2} \int e^{-i\vec{k}_n \cdot \vec{r}_1} \cdot \phi_n^*(\vec{r}_2) \, V(\vec{r}_1,\vec{r}_2) \, e^{-i\vec{k}_o \cdot \vec{r}_1} \cdot \phi_o(\vec{r}_2) \, d\vec{r}_1 d\vec{r}_2$$

(2.2)

where m is the electron mass, $\vec{r}_1$ and $\vec{r}_2$ are the positions of the inci-
dent electron and the molecular electron, $\vec{k}_o$ and $\vec{k}_n$ are the wave vectors
of the incident electron and the scattered electron, ϕ_o and ϕ_n are the
initial and final wave functions of the molecular electron. $V(\vec{r}_1,\vec{r}_2)$
consists of the interaction energy term of the two electrons and the
attractive potential energy terms of the incident electron with the core.

Neglect of the electron-core interaction will lead to the
expression

$$f_n(\Theta,\phi) = \frac{-2m \, e^2}{\hbar^2 \, \vec{K}^2} \int e^{i\vec{K} \cdot \vec{r}_2} \cdot \phi_n^*(\vec{r}_2) \, \phi_o(\vec{r}_2) \, d\vec{r}_2 \qquad (2.3)$$

where $\vec{K} = \vec{k}_o - \vec{k}_n$

e = electron charge.

At small scattering angles and high incident electron energy the magni-
tude of $\vec{K}$ will be very small. Therefore $\exp(i\vec{K} \cdot \vec{r}_2)$ can be expanded in a
Taylor series. Using the relation

$$\sigma_n(\Theta,\phi) = \frac{k_n}{k_o} |f_n(\Theta,\phi)|^2 \qquad (2.4)$$

and the first term $(i\vec{K} \cdot \vec{r}_2)$ of the Taylor series we can derive for the
total cross section (2.1) of an optically allowed transition

$$\sigma_{tot}(\text{Born}) \sim | < \phi_n | z | \phi_o > |^2 \qquad (2.5)$$

where the z-coordinate of the molecular electron is taken in the direction of $(\vec{k}_o - \vec{k}_n)$. Thus optically allowed transitions will be dominant at high incident electron energies.

The inclusion of electron exchange between the incident and a molecular electron will complicate the picture. At high energies the electron exchange can be accounted for by using the Born-Oppenheimer approximation or by the Ochkur (1964) or Ochkur-Rudge (Rudge, 1965) approximations. For the last two methods a degree of accuracy will be obtained comparable as found in the Born approximation. Using the Ochkur approximation it appears that for singlet-singlet transitions the exchange amplitude $g_n(\theta,\phi)$ is varying from $10^{-2} - 10^{-3}$ of the magnitude of $f_n(\theta,\phi)$ with increasing incident electron energy from 100 - 400 eV. Consequently for excitation of a state that involves change of multiplicity (only $g_n(\theta,\phi)$ contributes) the cross section will fall rapidly with electron energy as it increases above 100 eV or so. Thus triplet excitation cross sections are expected to be vanishingly small in this energy range.

The above mentioned approximations might give good estimates of experimental values at high electron energies (e.g. ten times threshold energy or more) but there is no theoretical justification that these methods will remain good approximations at low energies.

2.3.2   Low energy electron impact

When the speed of the incident electron is about equal or smaller than those of the molecular electrons the wave functions of the incident and scattered electrons can no longer be approximated by plane waves. The approaching electron will polarize the target atom or molecule while on the other hand the wave function of this electron will be largely distorted by the target particle. In the energy region near threshold it is expected that electron exchange processes (triplet excitation) will be very important. Moreover the formation of unstable negative ion states will influence the excitation cross sections near threshold. The total transition probability may be regarded as the result of a direct excitation process (including exchange)

$$e^- + A \rightarrow A^* + e^- \tag{2.6}$$

and an excitation process via a short lived negative ion state

$$e^- + A \rightarrow (A^*)^- \rightarrow A^* + e^- \qquad (2.7)$$

In the last process, as a first step the incident electron excites a
target state which energy is less than the resonant energy. The extra
electron has sufficient energy to escape leaving the target in its
excited state. However, the electron will be temporarily bound due to
a barrier constituted by the attractive polarization energy and the
repulsive centrifugal force. The negative ion decays when the electron
tunnels through the barrier. This gives rise to a so-called shape
resonance in the excitation function of the excited state. The width of
the shape resonance is strongly correlated with the lifetime of the
negative ion state or with the width of the potential barrier. In chap-
ter V examples are given of shape resonances observed in helium and
benzene.

    In addition to these shape resonances, the so-called Feshbach
resonances also show up in electron-impact processes. Those resonances
will occur when the incident electron loses energy in exciting the
target (electronically or vibrationally) and finds itself with in-
sufficient energy to escape from the system while the target remains
in its excited state. Before the electron can be emitted it must
reabsorb energy from the target. The widths of the Feshbach resonances
are in general much smaller than for shape resonances due to the longer
lifetimes. Examples of vibrationally (nuclear) excited Feshbach
resonances are the negative ion states of SF_6 and $C_6H_5NO_2$.

    To calculate excitation cross sections the close coupling approx-
imation or similar methods are commonly used. The close coupling approx-
imation starts from the following expansion of the total wave function
of a N+1 electron system

$$\Psi(\vec{r}_1, \ldots, \vec{r}_N, \vec{r}_{N+1}) = A \sum_i \phi_i(\vec{r}_1, \ldots, \vec{r}_N) \, F_i(\vec{r}_{N+1}) \qquad (2.8)$$

where $\{\phi_i\}$ form the complete set of eigenstates of the target Hamiltonian
and F_i are functions to be determined which describe the motion of the
incident electron. A anti-symmetrizes the complete expansion. Application
of the Hamiltonian of the total system on the wave function (2.8) will
yield a full set of coupled equations for the functions F_i, which are
in general too complicated to be solved so that truncation of the eigen-
function expansion is necessary. Using only the eigenstates which are
essential and strongly interact with each other we might adequately

describe the situation. The close coupling approximation will be good
if the coupling with all states which are neglected is small. For this
reason satisfactory results are obtained only close to threshold.

Two methods which are strongly related to the close coupling
approximation are the Projection Operator formalism developed by
Feshbach (1958, 1962) and the Configuration Interaction method intro-
duced by Fano (1961).

In these methods resonance phenomena are implicitly included
(van Santen, 1971). A method which includes specifically the polari-
zation effect is known as the polarized orbital method (Temkin et al.,
1961).

Because of the complexity of these methods applications have
been limited to simple atoms such as hydrogen and helium (Burke et al.,
1969). Accurate quantitative predictions of molecular excitation cross
sections in the low energy region are not to be expected in the near
future though we should not underestimate the recent progress in this
field. Even qualitative selection rules of molecular transitions for
low energy electron impact are not available partly due to the lack
of experimental data. Goddard et al. (1971) tentatively formulated
some selection rules for electron-impact spectroscopy based on group
theory.

CHAPTER III

CALCULATIONS ON EXCITED STATES
OF CONJUGATED SYSTEMS

3.1 MOLECULAR ORBITAL VERSUS VALENCE BOND THEORY

In quantumchemical studies two methods are commonly used: The
Valence Bond (VB) method and the Molecular Orbital (MO) method.

The VB method which may be regarded as a generalization of the
Heitler-London (1927) model of H_2 is based on localized wave functions.
These wave functions will yield covalent structures corresponding to
the structural formulae of classical chemistry. Therefore results ob-
tained with the VB method are easily understood in the language of
structural formulae which forms the backbone of organic chemistry.
However, it is well known that using this form of VB method excitation
energies are badly approximated and moreover all transitions are pre-
dicted to be forbidden. In order to obtain better results a large
number of ionic (polar) structures must be added (McWeeny, 1955). This
is rather unattractive regarding the amount of labour involved in
actual calculations.

The MO method (Hückel, 1930; Coulson and Longuet-Higgins, 1947)
is almost exclusively used in present-day calculations. As each elec-
tron is described by a non-localized wave function the results
obtained with this method are difficult to correlate with the classi-
cal chemical structures. Compared with the VB method the MO method is
much more appropriate to give in a first approximation reasonably well
predicted excitation energies.

Inclusion of all possible configurations in the MO theory and
all structures (covalent and ionic) in the VB method must yield the
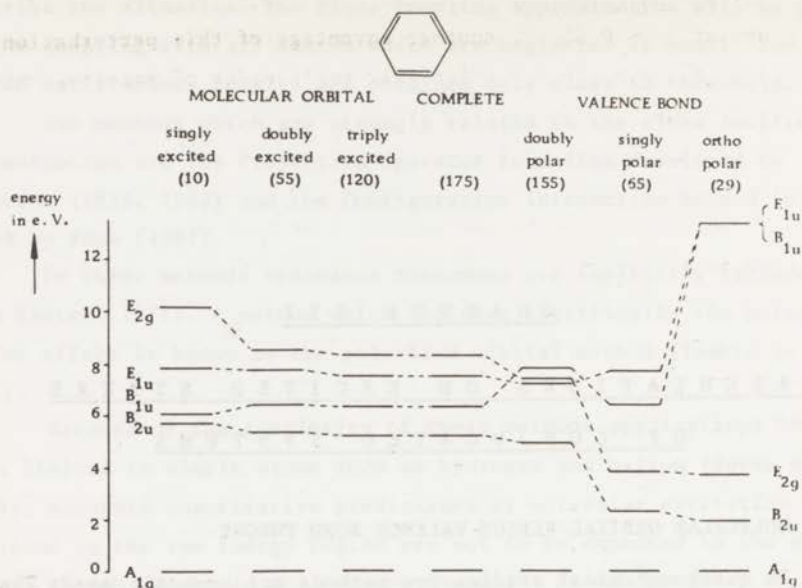
Fig. 3.1 - The energy levels of the excited states of benzene (singlet).
The numbers between parentheses represent the number of con-
figurations (MO method) and structures (VB method). This
figure has been taken from Van der Lugt et al. (1970)

same results. This is shown in the case of benzene (π-electrons only)
in Fig. 3.1. This figure has been taken from Van der Lugt et al. (1970).

3.2 SEMI-EMPIRICAL MOLECULAR ORBITAL CALCULATIONS

The time-independent Schrödinger equation

$$H\Psi = E\Psi \qquad (3.1)$$

is in general too complicated to be solved exactly. Usually magnetic
and relativistic effects are neglected. Moreover the Born-Oppenheimer
approximation is used which implies a separation of nuclear and elec-
tronic motion. Thus the simplified Hamiltonian pertaining to the elec-
tronic motion will look like

$$H = \sum_i - \tfrac{1}{2} \Delta(i) - \sum_{i,\mu} \frac{Z_\mu}{r_{i\mu}} + \sum_{i > j} \frac{1}{r_{ij}}$$

$$\text{(3.2)}$$

$$= \sum_i H^N(i) + \sum_{i > j} \frac{1}{r_{ij}}$$

$-\tfrac{1}{2} \Delta(i)$ = kinetic energy of electron i,

$-\sum_\mu \dfrac{Z_\mu}{r_{i\mu}}$ = potential energy of electron i with respect to nuclei μ,

$\dfrac{1}{r_{ij}}$ = electrostatic repulsion between electrons i and j.

The molecular orbitals are expressed as linear combinations of atomic orbitals (LCAO)

$$\phi_i = \sum_\nu c_{i\nu} \phi_\nu \tag{3.3}$$

If the number of electrons in the molecule is even the ground state of the system is in general described by a closed shell configuration, in which the molecular orbitals ϕ_i are doubly occupied (2n electrons)

$$\Psi_o = |\phi_1(1)\overline{\phi}_1(2)\phi_2(3)\overline{\phi}_2(4)\ldots\ldots\phi_n(2n-1)\overline{\phi}_n(2n)|$$

$$\text{(3.4)}$$

$$= |\phi_1\overline{\phi}_1\phi_2\overline{\phi}_2 \ldots\ldots\phi_n\overline{\phi}_n|$$

in which $\phi_1(i)$ is defined as $\phi_1(i)\alpha(\omega_i)$

$\overline{\phi}_1(j)$ is defined as $\phi_1(j)\beta(\omega_j)$.

The set of molecular orbitals is obtained by means of a self-consistent field (SCF) procedure which originally has been developed by Hartree and Fock in the case of atoms. The Hartree-Fock equation is defined as

$$F(1)\phi_i(1) = \varepsilon_i \phi_i(1) \tag{3.5}$$

with

$$F(1) = H^N(1) + \sum_{j=1}^{n} \{2J_j(1) - K_j(1)\} \tag{3.6}$$

where the Coulomb and exchange operators $J_j(1)$ and $K_j(1)$ are defined by

$$J_j(1)\phi_i(1) = \int \phi_j^*(2) \frac{1}{r_{12}} \phi_j(2)\phi_i(1) \, d\tau_2 \tag{3.7}$$

$$K_j(1)\phi_i(1) = \int \phi_j^*(2) \frac{1}{r_{12}} \phi_i(2)\phi_j(1) \, d\tau_2 \tag{3.8}$$

The energy of the ground state is evaluated as

$$E_o = 2 \sum_{i=1}^{n} \varepsilon_i - \sum_{i,j=1}^{n} (2J_{ij} - K_{ij}) \tag{3.9}$$

With the Coulomb and exchange integrals J_{ij} and K_{ij} given by

$$J_{ij} = < \phi_i(1)\phi_j(2) \left| \frac{1}{r_{12}} \right| \phi_i(1)\phi_j(2) > \tag{3.10}$$

$$K_{ij} = < \phi_i(1)\phi_j(2) \left| \frac{1}{r_{12}} \right| \phi_j(1)\phi_i(2) > \tag{3.11}$$

Substituting relation (3.3) into equation (3.5), multiplication by ϕ_μ and integration over all space leads to

$$\sum_\nu F_{\mu\nu} c_{i\nu} = \varepsilon_i \sum_\nu S_{\mu\nu} c_{i\nu} \tag{3.12}$$

where

$$F_{\mu\nu} = < \phi_\mu(1) \left| F(1) \right| \phi_\nu(1) > \tag{3.13}$$

and the overlap integral

$$S_{\mu\nu} = < \phi_\mu | \phi_\nu > \tag{3.14}$$

The MO's are obtained by an iterative procedure for the sets of coefficients $c_{i\nu}$'s which define these MO's (3.3). Assuming starting values for these coefficients, the F matrix (3.13) is constructed from which new sets of coefficients are derived by applying the variation theorem. This procedure is repeated until self-consistency for the sets of coefficients is obtained. Especially the evaluation of three- and four-center repulsion integrals like

$$(\mu\nu|\rho\sigma) = \int \phi_\mu(1)\phi_\rho(2) \frac{1}{r_{12}} \phi_\nu(1)\phi_\sigma(2) \, d\tau_1 d\tau_2 \tag{3.15}$$

will complicate the calculations. Regarding the enormous amount of labour involved to calculate all these integrals, approximate MO methods have been developed which essentially consist in approximation or neglect of some of these integrals.

Details of the approximate MO methods – Neglect of Diatomic Differential Overlap (NDDO); Intermediate Neglect of Differential Overlap (INDO); Complete Neglect of Differential Overlap (CNDO); Extended Hückel method; π-Electron approximation – are described by several authors (Pople et al., 1970; Richards et al., 1970; Jug, 1969; Parr, 1964).

Despite the sophisticated approach provided by the SCF procedure differences with experimental energies can be expected. Depending on the

flexibility and magnitude of the chosen basis sets the Hartree-Fock
equations only approximately represent the reality of the molecular
situation. The difference between the experimental energy and the energy
resulting from the Hartree-Fock treatment is defined as the correlation
energy. The physical origin of the correlation energy lies in the in-
adequate picture of averaged-out interelectronic interaction which is
the basis of the Hartree-Fock approach.

3.3   π-ELECTRON APPROXIMATION

3.3.1   General

The π-electrons are treated independently of the σ-electrons
(σ-π separability condition). This means that the π-electrons move
around in the field of a fixed core containing the nuclei and the
σ-electrons. As a consequence the Hamiltonian for the π-electrons looks
like (3.2)

$$H(i) = \sum_i H^{core}(i) + \sum_{i>j} \frac{1}{r_{ij}} \qquad (3.16)$$

with $H^{core}(i) = -\frac{1}{2} \Delta(i) + V(i)$.

The semi-empirical theory which has been introduced by Pariser
and Parr (1953) and Pople (1953) is based on the following approxima-
tions:

i   Neglect of Overlap

The overlap of atomic orbitals $S_{\mu\nu}$ is taken zero for $\mu \neq \nu$

$$S_{\mu\nu} = <\phi_\mu \mid \phi_\nu> = \delta_{\mu\nu} \qquad (3.17)$$

ii   Zero Differential Overlap (ZDO)

Whenever the expression $\phi_\mu(i)\phi_\nu(i)$ with $\mu \neq \nu$ appears in a
repulsion integral, the integral is set equal to zero.

$$(\mu\nu \mid \rho\sigma) = (\mu\mu \mid \rho\rho) \, \delta_{\mu\nu} \, \delta_{\rho\sigma} \qquad (3.18)$$

iii   One-center repulsion integral

This quantity is commonly evaluated by the semi-empirical relation

$$\gamma_{\mu\mu} = (\mu\mu \mid \mu\mu) = I_\mu - A_\mu \qquad (3.19)$$

with I_μ = valence state ionization potential of atom μ
A_μ = electron affinity of atom μ.

The theoretical value of $\gamma_{\mu\mu}$ for carbon (16.93 eV), as calculated from Slater orbitals, is much too large since it ignores polarization of the core and correlation effects between π-electrons at one atom. In general the value of ~ 11 eV is used.

The two-center repulsion integrals $\gamma_{\mu\nu}$ are often scaled down compared with the theoretical values. Mataga and Nishimoto (1957) applied the following relation to evaluate the two-center repulsion integrals in the case of hydrocarbons

$$\gamma_{\mu\nu} = \frac{14.4}{a + r_{\mu\nu}} \text{ eV} \tag{3.20}$$

$$(a = 1.328 \text{ Å})$$

iv   The resonance and Coulomb integrals

In the case of nearest neighbours the resonance integral

$$\beta_{\mu\nu} = <\phi_\mu | H^{core} | \phi_\nu> \tag{3.21}$$

is regarded as a semi-empirical parameter. In general for non-nearest neighbours the resonance integral is set equal to zero. The Coulomb integral α_μ defined by the relation

$$\alpha_\mu = <\phi_\mu | -\tfrac{1}{2} \Delta + V_\mu | \phi_\mu> \tag{3.22}$$

is mostly approximated using the valence state ionization potential of atom μ (Hinze and Jaffé, 1962).

Applying these approximations to relation (3.12) the following equations result

$$\sum_\nu F_{\mu\nu} c_{i\nu} = \varepsilon_i c_{i\nu} \tag{3.23}$$

$$F_{\mu\mu} = \alpha_\mu + \tfrac{1}{2} P_{\mu\mu} \gamma_{\mu\mu} + \sum_{\sigma \neq \mu} (P_{\sigma\sigma} - n_\sigma)\gamma_{\mu\sigma} \tag{3.24}$$

$$F_{\mu\nu} = \beta_{\mu\nu} - \tfrac{1}{2} P_{\mu\nu} \gamma_{\mu\nu} \tag{3.25}$$

with $P_{\mu\nu} = 2 \sum_i c_{i\mu} c_{i\nu}$
    n_μ = number of π-electrons of atom μ participating
         in the π-electron system.

The last equations (3.24) and (3.25) define the elements of the SCF matrix.

TABLE 3.1

Parameter sets of benzene (energies in eV)

	$-\beta_{\mu\nu}$	γ_{00}	γ_{01}	γ_{02}	γ_{03}
Pariser-Parr I[a] (PP I)	2.39	10.53	7.30	5.46	4.90
Pariser-Parr II[b] (PP II)	2.805	10.53	7.30	5.46	4.90
Mataga-Nishimoto[c] (MN)	2.388	10.84	5.30	3.85	3.50

[a] Pariser and Parr (1953);   [b] Koutecky et al. (1964);   [c] Mataga and Nishimoto (1957).

TABLE 3.2

Configuration interaction of singly excited states of benzene
(energies in eV)

	Calculated values			Experimental data				
	PP I	PP II	MN	Electron impact			Photon impact	
S → S $^1B_{2u}$	4.9	5.73	4.90		5.0[b]	4.90[c]	4.98[d]	4.90[e]
$^1B_{1u}$	5.3	6.04	6.13	6.2[a]	6.2[b]	6.20[c]	6.26[d]	
$^1E_{1u}$	7.0	7.78	6.96	7.0[a]	6.9[b]	6.95[c]	6.96[d]	
S → T $^3B_{1u}$	4.0	4.45	3.17	3.88[a]	3.95[b]		3.82[f]	3.66[g]
$^3E_{1u}$	4.45	5.29	4.03	4.77[a]	4.75[b]			4.56[g]
$^3B_{2u}$	4.9	5.73	4.90	~5.4[a]	5.60[b]			

[a] This research (chapter V)   [e] Callomon et al. (1966)
[b] Doering (1969)   [f] Burland et al. (1970)
[c] Lassettre et al. (1968)   [g] Colson et al. (1965).
[d] Wilkinson (1956)

3.3.2 Configuration Interaction of singly excited configurations

By the SCF procedure, as outlined above, a satisfactory approximation of the MO's of the ground state may be obtained. Then properties of the ground state are easily calculated from these wave functions. However, our primary interest is the prediction of excitation energies. A first approximation of an excited state is obtained by the promotion of one electron from an occupied MO to a virtual MO. The virtual orbitals are also eigenfunctions of the SCF Hamiltonian for the ground state. Such an excited configuration is described as the sum of two Slater determinants (electron jump from occupied MO(i) – virtual MO(p)). In the case of an excited singlet state

$$\Psi_{i \to p}^{SCF} = \frac{1}{\sqrt{2}} \{ |\phi_1 \bar{\phi}_1 \cdots \phi_i \bar{\phi}_p \cdots \phi_n \bar{\phi}_n| + |\phi_1 \bar{\phi}_1 \cdots \phi_p \bar{\phi}_i \cdots \phi_n \bar{\phi}_n| \} \tag{3.26}$$

A better approximation of the wave function of the excited state is obtained if we take a linear combination of the available excited configurations, a treatment known as Configuration Interaction (CI). Using only singly excited configurations as a basis set the resulting state after CI is described by

$$\Psi_r^{CI} = \sum_{k,l} C_{r,k,l} \, \Psi_{k \to l}^{SCF} \tag{3.27}$$

k = index occupied MO's

l = index virtual MO's.

The energies of the resulting excited states E_r^{CI} and the sets of coefficients $C_{r,k,l}$'s are obtained by solving the secular equations

$$\sum_{k,l} C_{r,k,l} \, (H_{j \to q; k \to l} - E_r^{CI} \, \delta_{jk} \delta_{ql}) = 0 \tag{3.28}$$

where

$$H_{j \to q; k \to l} = < \Psi_{j \to q}^{SCF} | H | \Psi_{k \to l}^{SCF} > \tag{3.29}$$

The oscillator strength for an electronic transition between the ground state Ψ_o and an excited singlet level Ψ_r^{CI} is given by

$$f = 1.085 \times 10^{11} \, \nu \, \vec{M}_{r,o}^2 \tag{3.30}$$

with

$$\vec{M}_{r,o} = < \Psi_r^{CI} | \sum_j \vec{r}(j) | \Psi_o > \tag{3.31}$$

TABLE 3.3

Complete Configuration Interaction

Benzene (excitation energies in eV)

	Koutecky et al. (1965)[a]	Visscher and Falicov (1970)[b]	This research[c]	Experimental data[*]
$S \rightarrow S$ $^1B_{2u}$	5.21	4.49	4.66	4.90
$^1B_{1u}$	6.31	5.99	6.21	6.20
$^1E_{1u}$	7.47	6.79	7.04	6.95
$^1E_{2g}$	8.29	7.18	7.45	
$S \rightarrow T$ $^3B_{1u}$		3.80	3.93	3.90
$^3E_{1u}$		4.50	4.67	4.75
$^3B_{2u}$		5.50	5.76	5.60
$^3E_{2g}$		6.34	6.56	
Maximum deviation[**]	0.52	0.41	0.24	
Standard deviation	0.31	0.20	0.10	

[*] The most accurate experimental data are taken from Table 3.2.

[**] The deviations were obtained using the experimental values as reference.

[a] $\beta_{\mu\nu} = -2.805$ eV; $\gamma_{00} = 10.53$ eV; $\gamma_{01} = 7.30$ eV; $\gamma_{02} = 5.46$ eV; $\gamma_{03} = 4.90$ eV.

[b] $\beta_{\mu\nu} = -2.50$ eV; $\gamma_{00} = 10.72$ eV; $\gamma_{01} = 7.36$ eV; $\gamma_{02} = 5.68$ eV; $\gamma_{03} = 4.98$ eV.

[c] $\beta_{\mu\nu} = -2.60$ eV; $\gamma_{00} = 10.92$ eV; $\gamma_{01} = 7.35$ eV; $\gamma_{02} = 5.64$ eV; $\gamma_{03} = 5.02$ eV.

$\vec{M}_{r,o}$ is the transition moment (cm) between the ground state and Ψ_r^{CI} while ν is the frequency of the transition (cm^{-1}). The summation j includes all π-electrons while $\vec{r}(j)$ is the position vector of electron j.

Calculations on singlet excited states with partial or complete inclusion of singly excited configurations are abundant. It appears that nearly every theoretical chemist has his own set of parameters within the frame-work of the PPP (Pariser, Parr and Pople) method.

For hydrocarbons the variable parameters are the one- and two-center repulsion integrals ($\gamma_{\mu\nu}$) and the resonance integral $\beta_{\mu\nu}$. By means of the parameter sets as listed in Table 3.1 Pariser and Parr (1953), Koutecky et al. (1965) and Mataga and Nishimoto (1957) calculated singlet and triplet excitation energies of benzene (Table 3.2). Triplet energies as calculated with the PP II parameter set, which were not given by Koutecky (1965), have been added.

The energies of the singlet state of benzene as predicted by Mataga and Nishimoto are in fairly good agreement with the experimental values. All three sets of parameters give a rather bad estimate of triplet excitation energies. The presented experimental values correspond to the Franck-Condon maxima of the transitions.

In this context it may be useful to raise the following questions:

i   To what extent are triplet and singlet excitation energies predicted correctly by calculations in which also doubly excited configurations or all possible configurations are included?

ii   Can we use the same set of parameters such that for both treatments the best fit with experimental data is obtained?

iii Can we find a suitable criterion which allows to truncate the large number of included excited configurations without affecting too much the accuracy of the calculations?

In the next sections we will try to give a satisfactory answer to these questions.

All the relevant information concerning the derivations of spinfunctions, the evaluation of matrix elements in the CI matrix and details of the constructed computer programs are given in an appendix (3.3.6).

From now on inclusion of singly excited configurations in the calculations will be indicated by "singly CI". Inclusion of singly and doubly excited configurations by "doubly CI".

3.3.3 Complete Configuration Interaction (π-system)

Koutecky et al. (1965) performed a complete CI calculation for
the singlet states of benzene using two different sets of parameters.
The results they obtained for the five lowest transitions with one of
these sets (PP II) are presented in Table 3.3. The main objective of
their study was to evaluate the influence of triply and higher excited
configurations on the calculated singlet excitation energies. This
effect turns out to be rather small.

Recently Visscher and Falicov (1970) calculated the energies of
singlet and triplet transitions in benzene performing complete CI
(Table 3.3). Their aim was to find a suitable set of parameters in
order to obtain an optimal agreement with experimental excitation ener-
gies. The parameter set for the repulsion integrals which they con-
sidered to give the best fit is very similar to the one used by
Pariser and Parr (1953). We also studied the influence of the variation
of the repulsion integrals on the energies of the excited states. We
concluded that the repulsion integrals used by Visscher and Falicov
will give the best results. In order to extend this result to other
molecules we approximate the one-center repulsion integrals with the
formula (Van der Lugt, 1968)

$$\gamma_{\mu\mu} = 3.36 \; \{Z_\mu - 0.35 \; (P_{\mu\mu} - n_\mu)\} \; eV \tag{3.32}$$

Z_μ = effective nuclear charge as calculated from the
well known Slater rules.

and the two-center repulsion integrals were evaluated by

$$\gamma_{\mu\nu} = \frac{14.4}{\dfrac{a_{\gamma 1}}{Z_\mu + Z_\nu} \; \{a_{\gamma 2} - 0.025 \; (Z_\mu + Z_\nu)\}^{-r_{\mu\nu}} + r_{\mu\nu}} \; eV \tag{3.33}$$

Using these formula repulsion integrals are obtained ($a_{\gamma 1}$ = 24.0;
$a_{\gamma 2}$ = 4.0) which are quite similar to those used by Visscher and Falicov
or Pariser and Parr (Table 3.3). The magnitude of the two-center repul-
sion integrals are much higher compared with the values used by Mataga
and Nishimoto performing singly CI (Table 3.1). By lowering the
resonance integral $\beta_{\mu\nu}$ from -2.50 eV (Visscher and Falicov, 1970) to
-2.60 eV a better agreement with the experimental data is obtained. The
average deviation from the experimental excitation energies decreases
from 0.20 eV to 0.10 eV (Table 3.3). This value for the resonance

TABLE 3.4
Comparison of complete and doubly CI
A) Benzene (excitation energies in eV)

	Complete CI $k_\beta = 10.5$	Doubly CI $k_\beta = 10.5$	Doubly CI $k_\beta = 9.8$	Experimental values
$S \rightarrow S$ $^1B_{2u}$	4.66	4.84	4.52	4.90
$^1B_{1u}$	6.21	6.28	6.01	6.20
$^1E_{1u}$	7.04	7.33 (1.72)[a]	7.04 (1.62)[a]	6.95 (5.0)[b,c]
$S \rightarrow T$ $^3B_{1u}$	3.93	4.31	4.03	3.90
$^3E_{1u}$	4.67	4.83	4.53	4.75
$^3B_{2u}$	5.76	5.86	5.59	5.60
Energy shift of ground state[*]	−0.627	−0.604	−0.636	
Maximum deviation[**]		0.38	0.20	
Standard deviation		0.20	0.12	

B) 1,3,5-Trans-hexatriene (excitation energies in eV)

	Complete CI $k_\beta = 10.5$	Doubly CI $k_\beta = 10.5$	Doubly CI $k_\beta = 9.8$	Experimental values
$S \rightarrow S$ ^1A_g	4.85	5.10	4.76	
^1B_u	5.26	5.44 (1.10)[a]	5.29 (1.02)[a]	5.13 (4.7)[c,d]
^1B_u	5.80	6.02	5.59	
$S \rightarrow T$ ^3B_u	2.40	2.74	2.58	2.6[d,e,f]
^3A_g	3.87	4.26	3.97	~4.2[f]
^3B_u	4.76	5.21	4.84	
Energy shift of ground state[*]	−0.828	−0.793	−0.841	
Maximum deviation[**]		0.45	0.21	
Standard deviation		0.30	0.11	

[*] The SCF energy of the ground state is taken as zero level.

[**] The deviations were obtained using the complete CI values as reference.

[a] Oscillator strength,

[b] Jones et al. (1955),

[c] Logarithm of excitation coefficient.

[d] Minnaard (1970),

[e] Evans (1960),

[f] This research (chapter VII).

integral has also been used by Van der Lugt (1968) performing complete VB calculations of benzene. Using the same repulsion integrals as in the PP II set he calculated the three lowest transitions at 4.76 eV, 5.93 eV and 7.04 eV.

For hydrocarbons the resonance integral can be approximated by means of the relation

$$\beta_{\mu\nu} = - k_\beta S_\mu \qquad (3.34)$$

If we refer to benzene as a standard for calibration ($\beta_{\mu\nu} = -2.60$ eV) this leads to $k_\beta = 10.5$ for complete CI calculations.

As a next step we want to compare calculations performed with doubly CI and those performed with complete CI. For benzene and 1,3,5-trans-hexatriene the first (lowest) six transitions are predicted at higher energy in the doubly CI calculations, despite the decreased shift of the ground state energy. Consequently we can conclude that the inclusion of configurations higher than doubly will affect the excitation energies to a larger extent than the ground state energy. This result is in line with our expectations. Triply excited configurations are expected to interact more intensively with singly excited configurations than with the ground state. Koutecky et al. (1964) studying the effect of inclusion of triply excited configurations concluded that they can only be neglected in the case of the ground state. In a following paper (1965) he concluded: "The results presented allow us to draw the conclusion that for parametrization used in semi-empirical methods higher than doubly or eventually triply excited configurations are not essential".

From the results of our calculations we must conclude that higher than doubly excited configurations will affect too much the calculated excitation energies. Therefore in the doubly CI calculations we will change the resonance integral somewhat compared with complete CI calculations. Using $k_\beta = 9.8$ ($\beta_\mu = -2.45$ eV in the case of benzene) better values are obtained for benzene and trans-hexatriene.

The standard deviations of these calculations compared with the complete CI results is ~ 0.1 eV. The one- and two-center repulsion integrals are kept the same. Variation of these parameters does not improve the results.

3.3.4 Perturbation criterion

The choice of benzene and 1,3,5-trans-hexatriene has not been quite arbitrary. Complete CI calculations turn out to be manageable up to six electrons (singlet 175 configurations; triplet 189 configurations). Molecular symmetry will help us to decrease the order of matrices which have to be diagonalized. For an eight-electron problem we already have to restrict ourselves to doubly CI (singlet 153 configurations; triplet 172 configurations).

We have to find a criterion to select only the important states of all the singly and doubly excited configurations such that the results are consistent with the outcome of the calculations in which all these configurations are included.

A suitable criterion should meet the next requirements:

i   The consistency of the limited doubly CI calculations should be rather high (better than 0.1 eV).

ii   Computer facilities will set a maximum to the order of matrices which can be diagonalized. Therefore the selection of configurations must be very effective to allow treating molecules with a large number of π-electrons.

Using an energy criterion (energy of excited configurations with respect to the SCF ground state energy) Allinger and co-workers (1967) approached this problem. They reached the following conclusions:

i   The best general criterion for inclusion of a configuration should be its energy.

ii   It is necessary to include some triply excited configurations.

iii It is not necessary to include all of the doubly excited configurations.

iv   The cut-off point for 0.2 eV consistency is at approximately 20 eV.

We do not share their opinion. In a following paper (Stuart and Allinger, 1968) they concluded that the inclusion of triply excited states leads to an improvement which is not as dramatic as they expected. We do not think the energy criterion is suited to select the most prominent states. To reach a consistency of 0.25 eV compared with the calculations in which all doubly excited configurations are included they needed 239 of the 251 configurations for a transition in naphthalene and 109 of the 153 configurations in the case of a transition in

1,3,5,7 octatetraene. The cut-off point is that high (20 eV) that we must conclude that convergence is too low. We have to look for a better selection procedure. This can be found by using perturbation theory.

Assuming that the exact function can be expanded in the complete set of original states

$$\Psi_k = \Psi_k^o + \sum_{i \neq k} C_{ki} \Psi_i^o \tag{3.35}$$

The unperturbed wave function Ψ_k^o which we want to improve must be a fair approximation of the exact wave function Ψ_k. Then the C_{ki}'s are small as the perturbation is small.

The Hamiltonian for the new problem is written as

$$H = H^o + H' \tag{3.36}$$

H = exact Hamiltonian

H^o = Hamiltonian of unperturbed system

H' = perturbation on H^o.

This problem has been treated extensively in many textbooks. According to Schiff (1955) the improved wave function to first order in H' (non-degenerate case) is given by

$$\Psi_k \simeq \Psi_k^o + \sum_{i \neq k} \frac{H'_{ik}}{E_k^o - E_i^o} \Psi_i^o \tag{3.37}$$

with

$$H'_{ik} = < \Psi_i^o |H'| \Psi_k^o > \tag{3.38}$$

$$E_k^o = < \Psi_k^o |H^o| \Psi_k^o > \tag{3.39}$$

while the energy to second order in H' is derived as

$$E_k \simeq E_k^o + H'_{kk} + \sum_{i \neq k} \frac{|H'_{ki}|^2}{E_k^o - E_i^o} \tag{3.40}$$

Using $< \Psi_k^o |H^o| \Psi_i^o > = 0$, (3.40) will lead to

$$E_k \simeq < \Psi_k^o |H^o + H'| \Psi_k^o > + \sum_{i \neq k} \frac{|< \Psi_k^o | H^o + H'| \Psi_i^o >|^2}{< \Psi_k^o |H^o| \Psi_k^o > - < \Psi_i^o |H^o| \Psi_i^o >} \tag{3.41}$$

Changing to the notation as used in our calculations ($H^o = H^{SCF}$)

$$E_k^{CI} \simeq \, <\psi_k^{SCF} \,|H|\, \psi_k^{SCF}> + \sum_{i \neq k} \frac{|<\psi_k^{SCF}\,|H|\,\psi_i^{SCF}>|^2}{<\psi_k^{SCF}|H^{SCF}|\psi_k^{SCF}> - <\psi_i^{SCF}|H^{SCF}|\psi_i^{SCF}>} \tag{3.42}$$

In this context (configuration interaction treatment) H' must be re-garded as the difference between the exact Hamiltonian H and H^{SCF}. In the case of the SCF calculation for the ground state H equals H^{SCF} giving H' = 0.

In zero order the final wave function ψ_k^{CI}, resulting from con-figuration interaction including all singly and doubly excited states, might be approximated by a single wave function ψ_k^{SCF}. However, it often appears that the wave function ψ_k^{CI} is not approximated well enough in this way. The perturbation theory can only be applied if the perturba-tion H' is small which implies that the unperturbed zero order wave function must be a fair approximation of the wave function ψ_k^{CI}. This problem is easily solved by taking instead of a single wave function ψ_k^{SCF}, a linear combination of the most important wave functions ψ_p^{SCF}'s participating in the final state ψ_k^{CI}. For this small number of config-urations we perform a separate, limited CI calculation from which we obtain a zero-order wave function ψ_{ko}^{CI} defined as

$$\psi_{ko}^{CI} = \sum_{p=1}^{n} C_{kp}\, \psi_p^{SCF} \tag{3.43}$$

In general the number of n is low (1 - 4 configurations). The configura-tions involved in this procedure are chosen such that it can be anti-cipated that the final wave function is represented for 80% or more by ψ_{ko}^{CI}.

Substituting the new zero-order wave function ψ_{ko}^{CI} into relation (3.42) we obtain

$$E_k^{CI} \simeq \, <\psi_{ko}^{CI}\,|H|\,\psi_{ko}^{CI}> + \sum_{\substack{i \neq p \\ p=1\ldots n}} \frac{|<\psi_{ko}^{CI}\,|H|\,\psi_i^{SCF}>|^2}{<\psi_{ko}^{CI}|H|\psi_{ko}^{CI}> - E_i^{SCF}} \tag{3.44}$$

or

$$E_k^{CI} \simeq E_{ko}^{CI} + \sum_{\substack{i \neq p \\ p=1\ldots n}} \frac{|<\psi_{ko}^{CI}\,|H|\,\psi_i^{SCF}>|^2}{E_{ko}^{CI} - E_i^{SCF}} \tag{3.45}$$

From the set of available excited configurations which are not included in the expansion of ψ_{ko}^{CI} we will select those configurations ψ_i^{SCF} which

TABLE 3.5

Application of perturbation criterion in doubly CI calculations[*]

A) Benzene (excitation energies in eV)

		Doubly CI (all states)	Perturba-tion crite-rion (2-13) 0.01 eV [**]	Perturba-tion crite-rion (2-10) 0.03 eV [**]	Energy criterion 25 states	Energy criterion 15 states
S→S	$^1B_{2u}$	4.52	4.50	4.41	5.40	5.21
	$^1B_{1u}$	6.01	5.98	5.89	5.97	5.88
	$^1E_{1u}$	7.04	7.03	6.99	7.20	7.25
S→T	$^3B_{1u}$	4.03	4.00	3.91	3.88	3.79
	$^3E_{1u}$	4.53	4.53	4.49	4.69	4.72
	$^3B_{2u}$	5.59	5.59	5.50	5.38	5.21
Energy shift ground state		-0.636	-0.613	-0.519	-0.418	-0.232
Maximum deviation[***]			0.03	0.12	0.88	0.69
Standard deviation			0.02	0.09	0.27	0.31

B) 1,3,5-Trans-hexatriene (excitation energies in eV)

		Doubly CI (all states)	Perturba-tion crite-rion (5-20) 0.01 eV [**]	Perturba-tion crite-rion (3-12) 0.03 eV [**]	Energy criterion 25 states	Energy criterion 15 states
S→S	^1A_g	4.76	4.79	5.11	4.78	5.46
	^1B_u	5.29	5.28	5.10	4.80	4.78
	^1B_u	5.59	5.66	5.62	5.77	6.09
S→T	^3B_u	2.58	2.62	2.44	2.07	2.09
	^3A_g	3.97	4.01	3.85	3.50	3.42
	^3B_u	4.84	4.87	4.65	4.30	4.26
Energy shift ground state		-0.841	-0.792	-0.542	-0.257	-0.175
Maximum deviation[***]			0.07	0.35	0.49	0.70
Standard deviation			0.04	0.17	0.33	0.53

[*] k_β = 9.8

[**]   Numbers between parentheses give range of orders of matrices.

[***] The deviations were obtained using the (complete) doubly CI calcu-
       lations as reference.

meet the requirement[*]

$$\frac{|< \Psi^{CI}_{ko} |H| \Psi^{SCF}_{i} >|^2}{E^{CI}_{ko} - E^{SCF}_{i}} \geq A_{pc} \tag{3.46}$$

A_{pc} = perturbation criterion value.

Those states which fulfil this requirement are kept apart and are subjected to a configuration interaction treatment together with the already selected Ψ^{SCF}_{p}'s. The magnitude of the perturbation criterion will determine the number of excited configurations which are included in the CI and therefore also the quality of the resulting wave function Ψ_k and its energy E_k. This kind of process can be performed for each state we want to study.

In Table 3.5 calculations pertaining to benzene and 1,3,5-trans-hexatriene, based on this perturbation criterion are presented for values of 0.01 and 0.03 eV. The results with the energy criterion are also shown. It is clear that the energy criterion does not meet the requirements of consistency within 0.1 eV for the given orders of truncation. The value of 0.01 eV for the perturbation criterion turns out to give excellent agreement with the unlimited doubly CI calculations. This conclusion is supported by the results presented in Table 3.6 on

TABLE 3.6

Accuracy obtained with perturbation criterion

Perturbation criterion	Deviation[**] (eV)	Benzene	1,3,5-Trans-hexatriene	Pyridine	Borazole
0.01 eV	Maximum	0.03	0.07	0.07	0.06
	Standard	0.02	0.04	0.04	0.04
0.03 eV	Maximum	0.12	0.35	0.12	0.18
	Standard	0.09	0.17	0.06	0.15

[**] The deviations were obtained comparing the results of the limited double CI calculations with the outcome of calculations in which all singly and doubly excited configurations are included.

[*] A similar perturbation criterion has been developed by Whitten et al. (1969) independently of this work.

molecules as pyridine and borazole. The consistency obtained for a six-
electron system is ~ 0.05 eV. Another advantage of this perturbation
technique can be found in the relatively small order of matrices which
have to be diagonalized (Table 3.5).

Though we cannot predict whether the consistency for the value
of 0.01 eV of the perturbation criterion will change significantly by
extending this method to a larger problem with more than six electrons,
we are convinced that with this method convergence will remain high.

3.3.5 Applications

3.3.5.1 Parametrization of singly CI calculations

For the calculation of energies of singlet transitions using
singly CI we have also used a parameter set with scaled down repulsion
integrals. Using equation (3.33) with $a\gamma_1$ = 8.57 and $a\gamma_2$ = 1.4 we find
in the case of benzene the following values: γ_{00} = 10.92 eV; γ_{01} =
6.07 eV; γ_{02} = 4.50 eV; γ_{03} = 4.10 eV.

It seems worthwhile to look for a set of parameters predicting
triplet excitation energies using only singly CI. Fig. 3.2 shows the
variation of the calculated excitation energies of the first (lowest)
eight singlet and triplet levels of benzene in different stages of
Configuration Interaction. The singly CI values show excellent agree-
ment for the two lowest triplet states compared with complete CI calcu-
lations, while in the case of the other triplet states a difference of
~ 0.4 eV is observed. The deviations for the energies of the singlet
states are much larger. In these calculations the parametrization was
used according to complete CI ($\beta_{\mu\nu}$ = -2.60 eV; $a_{\gamma 1}$ = 24.0 and $a_{\gamma 2}$ = 4.0).

We have found that the calculated energies for the triplet and
singlet excited states of benzene using singly CI show excellent agree-
ment with experimental data. This was effected with different para-
metrization which will imply different energies of the ground state. An
explanation of these effects might be found in the functioning of the
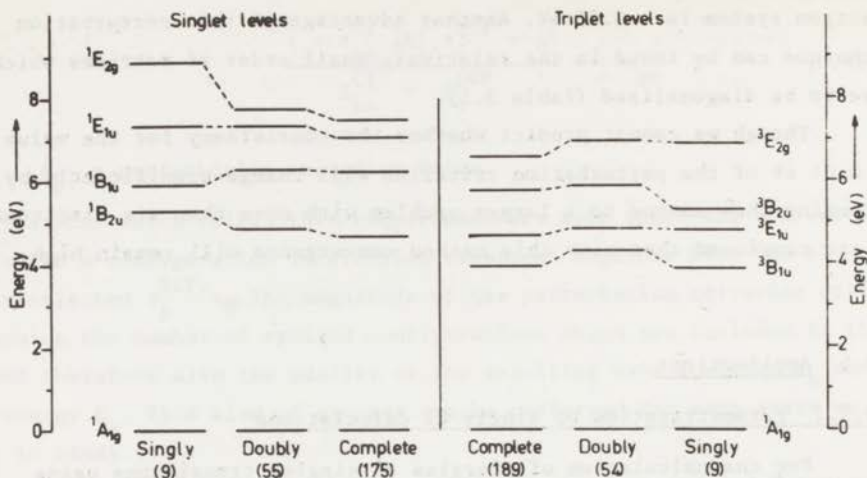$\sigma-\pi$ separability condition.

Benzene

Fig. 3.2 - The energies of the first (lowest) eight singlet and triplet states of benzene calculated in different stages of CI. The numbers between parentheses represent the number of included configurations.

We will summarize the parametrizations as used in the calculations of excited states for the different stages of CI:

i   Calculations with complete CI and singly CI (triplet levels).

Resonance integral: $\beta_{\mu\nu} = 10.5\ S_{\mu\nu}$

Repulsion integrals: One-center by equation (3.32)

Two-center by equation (3.33) with

$a_{\gamma1} = 24.0$ and $a_{\gamma2} = 4.0$.

ii   Doubly CI and restricted doubly CI (perturbation criterion) calculations:

Resonance integral: $\beta_{\mu\nu} = 9.8\ S_{\mu\nu}$

The repulsion integrals are evaluated similarly as in the complete CI calculations.

iii   Calculations including singly CI (singlet levels)

Resonance integral: $\beta_{\mu\nu} = 9.6\ S_{\mu\nu}$

Repulsion integrals: One-center by equation (3.32)

Two-center by equation (3.33) with

$a_{\gamma1} = 8.57$ and $a_{\gamma2} = 1.4$.

3.3.5.2 Benzene

Theoretical and experimental data are summarized in Table 3.7. For a discussion of the values see preceding sections.

TABLE 3.7

Benzene (excitation energies in eV)[*]

	Complete CI	Doubly CI	Doubly CI[**] 0.01	Singly CI	Experimental values[***]
S→S $^1B_{2u}$	4.66	4.52	4.50	4.91	4.90
$^1B_{1u}$	6.21	6.01	5.98	5.87	6.20
$^1E_{1u}$	7.04	7.04(1.62)	7.03(1.64)	6.96 (2.36)	6.95(5.0)
S→T $^3B_{1u}$	3.93	4.03	4.00	3.87	3.90
$^3E_{1u}$	4.67	4.53	4.53	4.79	4.75
$^3B_{2u}$	5.76	5.59	5.59	5.28	5.60

[*]   The values between parentheses correspond to oscillator strengths (calc.) or to the logarithm of extinction coefficients (exp.).

[**] Perturbation criterion 0.01 eV.

[***] The most accurate experimental data are taken from Table 3.2.

3.3.5.3 1,3,5-Trans-hexatriene

Theoretical and experimental data are presented in Table 3.8. The calculations based on singly CI give a wrong sequence for the first two singlet levels compared with the complete CI calculations. It appears that in the case of the excited state ^1A_g the doubly excited configuration, correlated with a two-electron jump from the highest occupied MO to the lowest unoccupied MO, will contribute largely (~ 30%) to the wave function of this state. For the triplet case (singly CI) the sequence is correct and the energies are rather well predicted. Intermolecular distances are taken from Haugen et al. (1966).

3.3.5.4 1,3-Trans-butadiene

Again the first two singlet levels are interchanged comparing the calculations with complete CI and the singly CI calculations (Table 3.9).

TABLE 3.8

1,3,5-Trans-hexatriene (excitation energies in eV)[*]

		Complete CI	Doubly CI	Doubly CI[**] 0.01	Singly CI	Experimental values
S→S	^1A_g	4.85	4.76	4.79	6.00	
	^1B_u	5.26	5.29(1.02)	5.28(1.03)	4.66(1.40)	5.13(4.7)[a]
	^1B_u	5.80	5.59	5.66	6.90	
S→T	^3B_u	2.40	2.58	2.62	2.21	2.6[a,b,c]
	^3A_g	3.87	3.97	4.01	3.65	~4.2[c]
	^3B_u	4.76	4.84	4.87	4.52	

[*] The values between parentheses correspond to oscillator strengths (calc.) or to the logarithm of extinction coefficients (exp.).

[**] Perturbation criterion 0.01 eV.

[a] Minnaard (1970) ; [b] Evans (1960); [c] This research (chapter VII).

TABLE 3.9

1,3-Trans-butadiene (excitation energies in eV)[*]

		Complete CI	Doubly CI	Doubly CI[**] 0.01	Singly CI	Experimental values	
S→S	^1A_g	5.98	5.51	5.63	6.96		
	^1B_u	6.16	6.00(0.70)	6.02(0.71)	5.65(1.00)	5.92(4.4)[a]	5.8-6.1[b]
	^1A_g	7.86	7.71	7.71	7.82		
S→T	^3B_u	3.05	2.97	2.98	2.83	3.3-3.8[b]	3.2[c]
	^3A_g	4.64	4.47	4.47	4.38	4.8[b]	3.9[c]
	^3B_u	7.39	6.85	6.84	8.89	(7.1[b])	

[*] The values between parentheses correspond to oscillator strengths (calc.) or to the logarithm of extinction coefficients (exp.).

[**] Perturbation criterion 0.01 eV.

[a] Allinger et al. (1967); [b] Brongersma (1968); [c] Evans (1960).

The prediction of triplet state energies is fairly correct in all types
of calculations. Intermolecular distances were taken from Haugen et al.
(1966). The molecule is assumed to be planar.

3.3.5.5 Naphthalene

In Table 3.10 the calculated energies of the first (lowest) six
triplet states and of the optically observed singlet states are pre-
sented, which can be compared with the experimental data. The agreement
is rather good. Hunziker (1972) measured the excitation energy of the
lowest triplet state $^3B_{2u}$ to the ^3A_g state at 2.25 eV. Meyer et al.
(1972) found an energy difference of 1.97 eV for these triplet states.
From our calculations (Table 3.10) the values of 2.06 eV (singly CI)
and 2.00 eV (doubly CI) can be derived as energy difference, thus
showing an excellent agreement with the experimental values. Bond
lengths in naphthalene were determined by Cruickshank (1960) using
X-ray crystallography. The calculations were performed using his values
and assuming planarity of the molecule.

3.3.5.6 Pyridine

Finally we will consider the heteromolecule pyridine. Not taking
into account the lone pair of the nitrogen atom we are left with a six-
electron problem (π-system). Applying the relation

$$\beta_{\mu\nu} = b_\beta S_{\mu\nu} (\alpha_\mu + \alpha_\nu) \tag{3.47}$$

with $\alpha_{N^+} = -12.55$ eV
$\alpha_{C^+} = -9.60$ eV,

the b_β are easily evaluated using the relation $b_\beta = -k_\beta/(\alpha_\mu + \alpha_\mu)$.

The calculated singlet excitation energies are in excellent
agreement with the experimental values (Table 3.11). Nearly no experi-
mental excitation energies are available of pyridine. The predicted
triplet energies of the singly CI calculations turn out to be in good
agreement with the results of the other types of calculation.
Intermolecular distances were used according to Bak et al. (1958).
Planarity of the molecule is assumed.

TABLE 3.10

Naphthalene (excitation energies in eV)[*]

		Doubly CI[**] 0.01	Singly CI	Experimental values
S → S	$^1B_{3u}$	4.15	4.21	4.11 (2.76)[a] 4.1[e]
	$^1B_{2u}$	4.97 (0.10)	4.64 (0.15)	4.61 (3.75)[a] 4.6[e]
	$^1B_{3u}$	6.31 (1.59)	5.86 (2.00)	5.88 (5.08)[a] 5.89[e]
	$^1B_{2u}$	6.48 (0.38)	6.21 (0.72)	
S → T	$^3B_{2u}$	3.25	3.05	3.2[b] 2.63[c] 3.0[e]
	$^3B_{3u}$	4.26	4.22	3.83[d]
	$^3B_{1g}$	4.44	4.18	
	$^3B_{2u}$	4.59	4.62	
	$^3B_{3u}$	4.91	4.58	
	^3A_g	5.25	5.11	(5.3[e])

[*] The values between paretheses correspond to oscillator strengths (calc.) or to the logarithm of extinction coefficients (exp.).

[**] Perturbation criterion 0.01 eV.

[a] Allinger et al. (1967); [b] Huebner (1968); [c] Evans (1957)(0-0 band); [d] Hansen et al. (1965)(0-0 band); [e] Aarts et al. (1972).

TABLE 3.11

Pyridine (excitation energies in eV)[*]

		Complete CI	Doubly CI	Doubly CI[**] 0.01	Singly CI	Experimental values
S→S	$^1B_1$	4.58	4.47(0.02)	4.45(0.02)	4.88(0.05)	4.90(3.2)[a]
	$^1A_1$	6.26	6.07	6.05	5.94(0.01)	6.17(3.7)[a]
	$^1B_1$	6.98	6.93(0.51)	7.00(0.72)	7.02(1.04)	6.94(4.8)[a] 7.22[b]
	$^1A_1$	7.16	7.14(0.53)	7.17(0.80)	7.12(1.18)	
S→T	$^3A_1$	3.90	4.04	3.99	3.84	(4.2)[c] 3.68[d]
	$^3B_1$	4.49	4.35	4.38	4.42	
	$^3A_1$	4.64	4.53	4.60	4.73	
	$^3B_1$	5.94	5.82	5.81	5.68	

[*] The values between parentheses correspond to oscillator strengths (calc.) or to the logarithm of extinction coefficients (exp.).

[**] Perturbation criterion 0.01 eV.

[a] Pickett et al. (1953); [b] El-Sayed (1962); [c] Brongersma (1968); [d] Evans (1957).

3.3.5.7 Summary

From the calculations which have been performed we may draw the conclusion that for hydrocarbons (planar system) the predicted energies resulting from limited CI calculations (doubly excited configurations) using the perturbation criterion will be accurate within 0.2 - 0.3 eV as compared with experimental values. The accuracy of the complete CI calculations is of the same order.

The calculations based on configuration interaction with only singly excited configurations in general predict reasonable triplet and singlet excitation energies. However, we observe that sometimes optically forbidden transitions (symmetry excited state ^1A_g) are calculated at much higher energy compared with values resulting from calculations with a larger amount of CI (1,3-trans-butadiene; 1,3,5-trans-hexatriene). For this kind of transitions inclusion of doubly excited configurations (especially closed shell configurations) might be essential.

3.3.6 Appendix

3.3.6.1 Construction of spin functions

In the space of spin functions for a system of N electrons we have 2^N linearly independent spin functions. For a given eigenvalue M of operator S_z the number of linearly independent functions will be reduced to

$$\binom{N}{\frac{1}{2}N + M} .$$

We are interested in spin functions being simultaneously eigenfunctions of $\vec{S}^2$ and S_z. For a given set of eigenvalues $S(S + 1)$ and M the number of f_S^N functions is obtained alike

$$\Theta_{S,M,k}^N \quad \text{with } k = 1,2 \ldots f_S^N$$

The choice of f_S^N independent functions is quite arbitrary. Usually a genealogical construction of spin functions is performed. The fundamental idea of this method is to add the spins of single electrons one by one and to determine the resultant spins according to the vector coupling formulae.
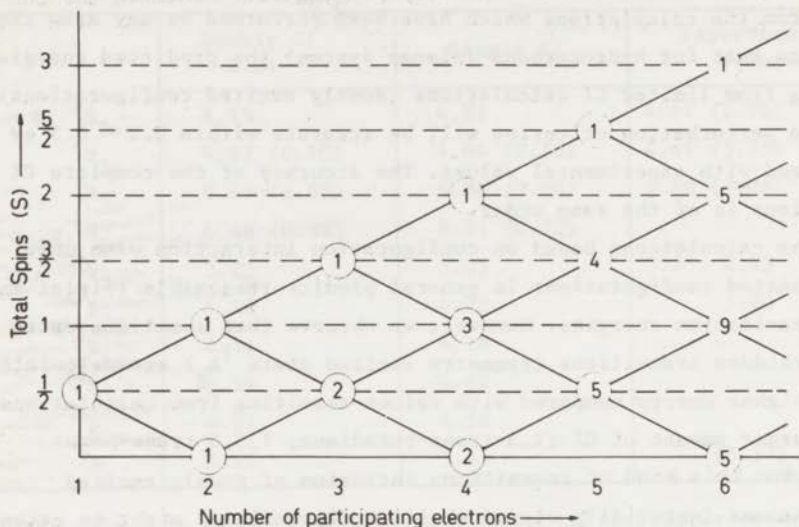
Branching Diagram

Fig. 3.3 - The branching diagram visualizing the construction of spin functions.

From spin functions with one electron less the following functions are obtained by means of a "step up" and "step down" procedure for S

"step up"

$$\theta^N_{S,M;S_1..S_{N-2},S-\frac{1}{2}} = \sqrt{\frac{S+M}{2S}} \; \theta^{N-1}_{S-\frac{1}{2},M-\frac{1}{2};S_1..S_{N-2}} \cdot \alpha$$

$$+ \sqrt{\frac{S-M}{2S}} \; \theta^{N-1}_{S-\frac{1}{2},M+\frac{1}{2};S_1..S_{N-2}} \cdot \beta \quad (3.48)$$

"step down"

$$\theta^N_{S,M;S_1..S_{N-2},S+\frac{1}{2}} = -\sqrt{\frac{S-M+1}{2S+2}} \; \theta^{N-1}_{S+\frac{1}{2},M-\frac{1}{2};S_1..S_{N-2}} \cdot \alpha$$

$$+ \sqrt{\frac{S+M+1}{2S+2}} \; \theta^{N-1}_{S+\frac{1}{2},M+\frac{1}{2};S_1..S_{N-2}} \cdot \beta \quad (3.49)$$

The suffix $S_1..S_{N-2},S+\frac{1}{2}$ of the function $\Theta^N_{S,M;S_1..S_{N-2},S+\frac{1}{2}}$ indicates the way of formation of this function having the final value of S.

The totality of spin functions built in this way can be clarified with the so-called "branching diagram" (Fig. 3.3). The number in each circle, which is the number of spin functions at given N and S, can be found by taking the sum of the numbers in the neighbouring circles, with N-1 electrons, which are directly connected with the original circle. Starting from a one-electron system with spin functions α or β we can easily find the spin functions for a 2-electron system using (3.48) and (3.49).

<u>2-electron system</u>

Singlet (1) $\Theta^2_{0,0;\frac{1}{2}} = \dfrac{1}{\sqrt{2}} (\alpha\beta - \beta\alpha)$ (3.50)

Triplet (1) $\Theta^2_{1,1;\frac{1}{2}} = \alpha\alpha$

$\Theta^2_{1,0;\frac{1}{2}} = \dfrac{1}{\sqrt{2}} (\alpha\beta + \beta\alpha)$ (3.51)

$\Theta^2_{1,-1;\frac{1}{2}} = \beta\beta$

From these spin functions we can derive the functions for the 3-electron system which we can use to evaluate the spin functions for four electrons.

<u>4-electron system</u>

Singlet (2) $\Theta^4_{0,0;\frac{1}{2},0,\frac{1}{2}} = \dfrac{1}{2} (\beta\alpha\beta\alpha - \alpha\beta\beta\alpha + \alpha\beta\alpha\beta - \beta\alpha\alpha\beta)$

(3.52)

$\Theta^4_{0,0;\frac{1}{2},1,\frac{1}{2}} = \dfrac{1}{\sqrt{3}} (\beta\beta\alpha\alpha + \alpha\alpha\beta\beta) - \dfrac{1}{2\sqrt{3}} (\alpha\beta\beta\alpha + \beta\alpha\beta\alpha + \alpha\beta\alpha\beta + \beta\alpha\alpha\beta)$

Triplet (3)

(M = 0) $\Theta^4_{1,0;\frac{1}{2},1,3/2} = -\dfrac{1}{\sqrt{6}} (\beta\beta\alpha\alpha + \alpha\beta\beta\alpha + \beta\alpha\beta\alpha - \alpha\beta\alpha\beta - \beta\alpha\alpha\beta - \alpha\alpha\beta\beta)$

(3.53)

$\Theta^4_{1,0;\frac{1}{2},1,\frac{1}{2}} = \dfrac{1}{\sqrt{3}} (\alpha\alpha\beta\beta - \beta\beta\alpha\alpha) + \dfrac{1}{2\sqrt{3}} (\alpha\beta\beta\alpha + \beta\alpha\beta\alpha - \alpha\beta\alpha\beta - \beta\alpha\alpha\beta)$

$\Theta^4_{1,0;\frac{1}{2},0,\frac{1}{2}} = \dfrac{1}{2} (\alpha\beta\beta\alpha - \beta\alpha\beta\alpha + \alpha\beta\alpha\beta - \beta\alpha\alpha\beta)$

The spin functions for 6 electrons, which are more complicated, are easily derived along the same lines.

The configurations which are used in the CI treatment of our cal-
culations are strongly related to these spin functions.

A closed shell configuration like the ground state has no un-
paired electrons and therefore can be described as a single determinantal
wave function (3.4).

A singly excited configuration which has two unpaired electrons
is given by (3.26) after using (3.50) and (3.51).

A doubly excited configuration with four unpaired electrons is
described as a linear combination of determinantal wave functions derived
from (3.52) and (3.53). Triply excited configurations with six unpaired
electrons are obtained in a similar way.

3.3.6.2 Computer programs

Mulder and Van der Lugt constructed a computer program to calcu-
late singlet excitation energies, which consists of an SCF procedure
(Pariser, Parr and Pople formalism – sections (3.2) and (3.3)) and
Configuration Interaction of singly excited states. This program was
easily adapted for the calculation of triplet excitation energies in the
singly CI scheme. The inclusion of doubly excited configurations,
initiated by Mulder, was carried out for both the singlet and triplet
case. The procedure to calculate oscillator strengths is somewhat more
complicated than in the case of singly CI (3.30) as now the final ground
state is described as a linear combination of the original ground state
configuration and the excited state configurations.

The diagonal elements of the CI matrix, energies of the configu-
rations, were calculated from programmed formulae. The non-diagonal
elements were evaluated from the programmed expressions for the spin
functions. Moreover, in the case of doubly CI for singlet states every
type of non-diagonal element was also programmed. The results from these
different methods of calculation were found to be identical.

It seems worthwhile to indicate the method of calculation for the
matrix elements of doubly CI. In general each configuration consists of
a linear combination of determinantal wave functions. We will describe
the way in which the interaction between two determinants like e.g.

$$< |....i\bar{j}p\bar{q}.... \mid H \mid ....k\bar{l}r\bar{s}....|> \qquad (3.54)$$

is evaluated.

The symbols i, j, k and l refer to the occupied MO's ϕ_i, ϕ_j, ϕ_k and ϕ_l while p, q, r and s refer to the virtual MO's ϕ_p, ϕ_q, ϕ_r and ϕ_s.

The expression $(ij \mid pq)$ is defined as

$$(ij \mid pq) = \int \phi_i(1) \phi_p(2) \frac{1}{r_{12}} \phi_j(1) \phi_q(2) \, d\tau_1 d\tau_2 \qquad (3.55)$$

The energy of the ground state (3.9) is also given by

$$E_o = 2 \sum_{k=1}^{n} \varepsilon_k^{core} + \sum_{k,l=1}^{n} (2J_{kl} - K_{kl}) \qquad (3.56)$$

where $\varepsilon_k^{core} = \langle \phi_k \mid H^{core} \mid \phi_k \rangle$

While the MO energy ε_k is defined as

$$\varepsilon_k = \varepsilon_k^{core} + \sum_{l=1}^{n} (2J_{kl} - K_{kl}) \qquad (3.57)$$

it can easily be shown that

$$\langle \phi_p \mid H^{core} + \sum_{i=1}^{n} (2J_i - K_i) \mid \phi_j \rangle = \varepsilon_j \langle \phi_p \mid \phi_j \rangle = 0 \qquad (3.58)$$

for $p \neq j$

will lead to

$$F_{pj} = \varepsilon_{pj}^{core} + \sum_{i=1}^{n} \{2(ii \mid jp) - (ij \mid ip)\} = 0 \qquad (3.59)$$

Thus all matrix elements between the ground state configuration and the singly excited configurations will be zero (Brillouin theorem).

Using relations (3.56), (3.57) and (3.59) the matrix elements are easily derived.

For the calculation of expressions like (3.54) we will consider the following possibilities:

i   All spin orbitals in both determinants are exactly the same;

ii   The determinants differ in one spin orbital;

iii   The determinants differ in two spin orbitals;

iv   The determinants differ in more than two spin orbitals.

i   Determinantal wave functions being the same for both sides of (3.54) will occur only in the calculation of the energies of the excited state configurations (diagonal elements CI matrix).

Suppose we want to evaluate the following expression

$$< |....i\bar{p}...n\bar{n} \; |H| \; ....i\bar{p}...n\bar{n} \; | > \qquad (3.60)$$

Writing out all possible interactions we obtain as result

$$= \{ 2 \sum_{k \neq i}^{n} \varepsilon_k^{core} + \varepsilon_i^{core} + \varepsilon_p^{core} \} +$$

$$\{ \sum_{k,l=1}^{n} (2J_{kl} - K_{kl}) - J_{ii} - \sum_{k \neq i}^{n} (2J_{ki} - K_{ki}) \} + \qquad (3.61)$$

$$\{ J_{ip} + \sum_{k \neq i}^{n} (2J_{kp} - K_{kp}) \}$$

The second part of expression (3.61) arises from all possible inter-actions (only repulsion terms) leaving out spin orbital $\bar{\phi}_i$. The last part corresponds to the possible interactions of spin orbital $\bar{\phi}_p$ with the other spin orbitals.

As a result for (3.60), using (3.57), we find

$$= 2 \sum_{k=1}^{n} \varepsilon_k^{core} - \varepsilon_i + \varepsilon_p + \sum_{k,l=1}^{n} (2J_{kl} - K_{kl}) + K_{ip} - J_{ip}$$

$$= E_o - \varepsilon_i + \varepsilon_p + (ip \,|\, pi) - (ii \,|\, pp) \qquad (3.62)$$

ii   Expression (3.54) with one different spin orbital in the deter-minants will lead to complicated expressions if all possibilities of interaction of the electrons are taken into account. However, using relation (3.59) we can facilitate the calculations. Suppose we want to calculate

$$< | \; ....i\bar{p}.... \; |H| \; ....i\bar{s}.... \; | > = \qquad (3.63)$$

(new notation):

$$< i\bar{p} \; |H| \; i\bar{s} > = \varepsilon_{ps}^{core} + \sum_{k \neq i}^{n} \{2(kk \,|\, sp) - (ks \,|\, kp)\} + (ii \,|\, sp)$$

$$= \varepsilon_{ps}^{core} + \sum_{k=1}^{n} \{2(kk \,|\, sp) - (ks \,|\, kp)\} - (ii \,|\, sp) + (ip \,|\, is)$$

$$= F_{ps} - (ii \,|\, sp) + (ip \,|\, is)$$

with F_{ps} being zero according to (3.59).

Summarizing the possible types which might occur in our calculations

Between singly excited configurations only:

$$\langle i\bar{p}\,|H|\,i\bar{s}\rangle = (ip\,|\,is) - (ii\,|\,ps)$$

$$\langle i\bar{p}\,|H|\,j\bar{p}\rangle = (jp\,|\,ip) - (ij\,|\,pp) \tag{3.64}$$

Between singly and doubly excited configurations:

$$\langle p\bar{p}\,|H|\,i\bar{p}\rangle = (pi\,|\,pp) - (pi\,|\,ii) \qquad\qquad (i \to p)$$

$$\langle s\bar{p}\,|H|\,i\bar{p}\rangle = (is\,|\,pp) - (is\,|\,ii) \qquad\qquad (i \to s,p) \tag{3.65}$$

$$\langle i\bar{j}s\bar{p}\,|H|\,i\bar{j}j\bar{p}\rangle = (sj\,|\,pp) - (sj\,|\,ii)$$

Between doubly excited configurations only:

$$\langle p\bar{q}\,|H|\,p\bar{p}\rangle = (pp\,|\,pq) - (pq\,|\,ii) - (pq\,|\,ii) + (pi\,|\,qi)$$

$$\langle i\bar{j}p\bar{p}\,|H|\,j\bar{j}p\bar{p}\rangle = (ij\,|\,pp) + (ij\,|\,pp) - (ip\,|\,jp) - (ij\,|\,ii)$$

$$\langle p\bar{q}\,|H|\,p\bar{s}\rangle = (pp\,|\,sq) - (sq\,|\,ii) - (sq\,|\,ii) + (si\,|\,qi)$$

$$\langle i\bar{j}p\bar{p}\,|H|\,i\bar{l}p\bar{p}\rangle = (lp\,|\,jp) + (lj\,|\,ii) - (lj\,|\,pp) - (lj\,|\,pp)$$

$$\langle i\bar{j}p\bar{q}\,|H|\,i\bar{j}p\bar{p}\rangle = (pq\,|\,pp) - (pq\,|\,ii) + (pi\,|\,qi) - (pq\,|\,jj)$$

$$\langle i\bar{j}p\bar{q}\,|H|\,j\bar{j}p\bar{q}\rangle = (ij\,|\,pp) + (ij\,|\,qq) - (ip\,|\,jp) - (ij\,|\,ii) \tag{3.66}$$

$$\langle i\bar{j}p\bar{q}\,|H|\,i\bar{j}p\bar{s}\rangle = (qs\,|\,pp) - (qs\,|\,ii) + (qi\,|\,si) - (qs\,|\,jj)$$

$$\langle i\bar{j}p\bar{q}\,|H|\,i\bar{l}p\bar{q}\rangle = (jp\,|\,lp) + (jl\,|\,ii) - (jl\,|\,pp) - (jl\,|\,qq)$$

$$\langle i\bar{p}j\bar{q}\,|H|\,i\bar{p}j\bar{s}\rangle = (pp\,|\,qs) - (qp\,|\,sp) - (qs\,|\,ii) - (qs\,|\,jj)$$
$$\qquad\qquad\qquad + (qi\,|\,si) + (qj\,|\,sj)$$

$$\langle i\bar{p}j\bar{q}\,|H|\,k\bar{p}j\bar{q}\rangle = (kp\,|\,ip) + (kq\,|\,iq) - (ki\,|\,pp) - (ki\,|\,qq)$$
$$\qquad\qquad\qquad + (ki\,|\,jj) - (kj\,|\,ij)$$

iii   If two spin orbitals are different (3.54) there are two possibilities

$$\text{same spins} \quad \langle s\bar{l}r\bar{k}\,|H|\,p\bar{l}q\bar{k}\rangle = (ps\,|\,rq) - (qs\,|\,pr)$$

$$\text{different spins} \quad \langle i\bar{j}p\bar{q}\,|H|\,i\bar{k}s\bar{q}\rangle = (kj\,|\,ps) \tag{3.67}$$

iv   A difference of more than two spin orbitals will give zero.

In the calculations with doubly CI (singlet and triplet) the non-diagonal elements of the CI matrix were obtained using only the programmed expressions of the spin functions and the different possibilities as given by (3.64) - (3.67). In the case of complete CI for four- and six-electron systems all elements of the CI matrix were evaluated using only the programmed expressions for the spin functions. Every interaction element was derived by writing out all possible combinations without using (3.59).

The calculations performed by Van der Lugt (1968) on 1,3-trans-butadiene (4 electrons) and those by Koutecky et al. (1965) and Visscher and Falicov (1970) on benzene (6 electrons) are consistent within 0.01 eV with the results of our calculations using the same parameters.

The most lengthy calculation was performed for the complete CI treatment of a six-electron system in the triplet case. Despite the application of a symmetry plane which splits up the matrix of order 189 into two parts, this calculation took about 2 hours on an IBM computer type 360-50 and 25 minutes on an IBM computer type 360-65. As computer language Fortran IV was used.

C H A P T E R   IV

E X P E R I M E N T A L

4.1   GENERAL

A schematic cross section of the electron spectrometer is shown in Fig. 4.1. The electrons produced by the directly or indirectly heated cathode are energy selected by electrodes 1 - 4. After crossing the interaction region they will finally end up at the electron collector C if no inelastic collisions with the target gas take place. The inelastically scattered electrons are collected after appropriate energy selection (electrodes 5 - 7) at the mantle M. The target gas is kept at a low pressure such that the mean free path of the electrons is large in comparison with the collision chamber dimensions.
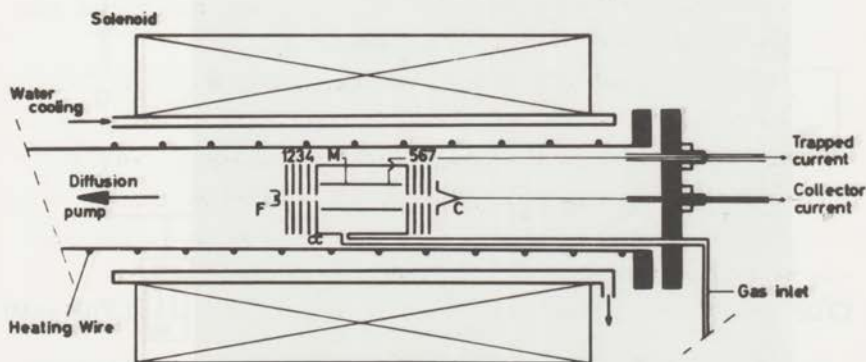

Fig. 4.1 - Cross section of the electron spectrometer.
F is the filament; 1, 2, 3 and 4 are electrodes defining the kinetic energy and the energy spread of the primary beam; M is the cylindrical electron collector (Mantle), positively charged with respect to the collision chamber CC; 5, 6 and 7 are electrodes which energy analyse the scattered electrons; C is the primary beam collector.

The magnetic field created by the solenoid (maximum 800 gauss) aligns
the primary beam along the axis of the system and additionally it will
regulate the diffusion process in which the inelastically scattered
electrons are energy analysed.

The vacuum system consists of three parts. A system containing the
electron spectrometer, a double inlet system for gases and liquids and
a high temperature inlet system permitting measurements of low vola-
tile compounds.

The use of low intensity primary beams (10^{-8} A) will require a highly
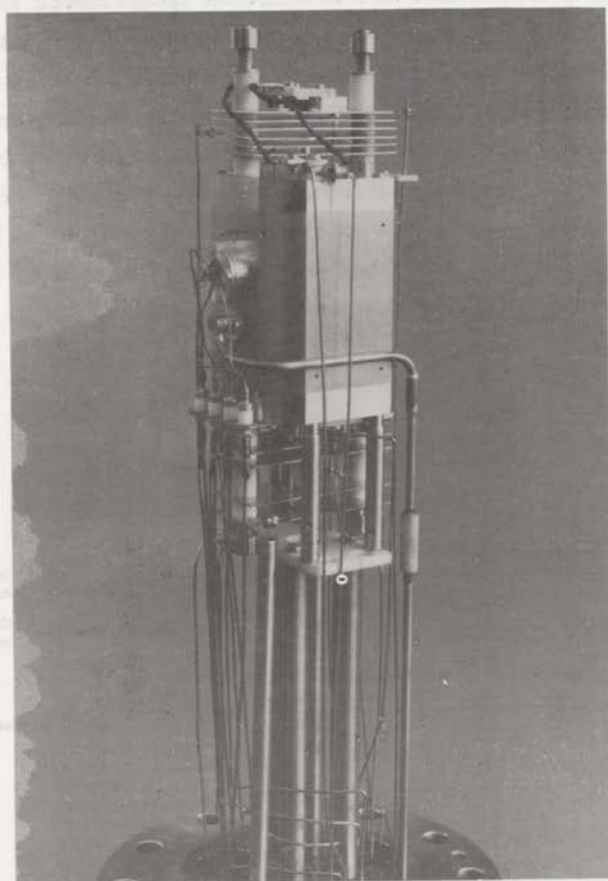sensitive detection system. In the present instrument the detected

Fig. 4.2 - A picture of the source configuration. The indirectly heated
cathode is clearly visible in the upper part of the system.

electron current is of the order $10^{-12} - 10^{-16}$ A.
Continuously heating and differentially pumping will minimize the con-
tamination of the electrodes.

Part of the measurements presented in this work were obtained using
the apparatus as constructed by Brongersma (1968), which will not be
described here. The introduction of a new technique (Knoop et al.,
1970) and some refinements lead to the construction of the apparatus
presented here. In Fig. 4.2 a picture of the source configuration is
shown.

4.2 VACUUM SYSTEM

A schematic diagram of the total vacuum system is presented in
Fig. 4.3. This essentially consists of three parts. The source system,
the double inlet system (maximum 150° C) and the high temperature inlet
system (maximum 350° C). The source system, sealed by silver and golden
gaskets, is pumped by a 350 l/sec oil diffusion pump (Edwards type EO4).
This pump is separated from the source region by a water cooled Pel-
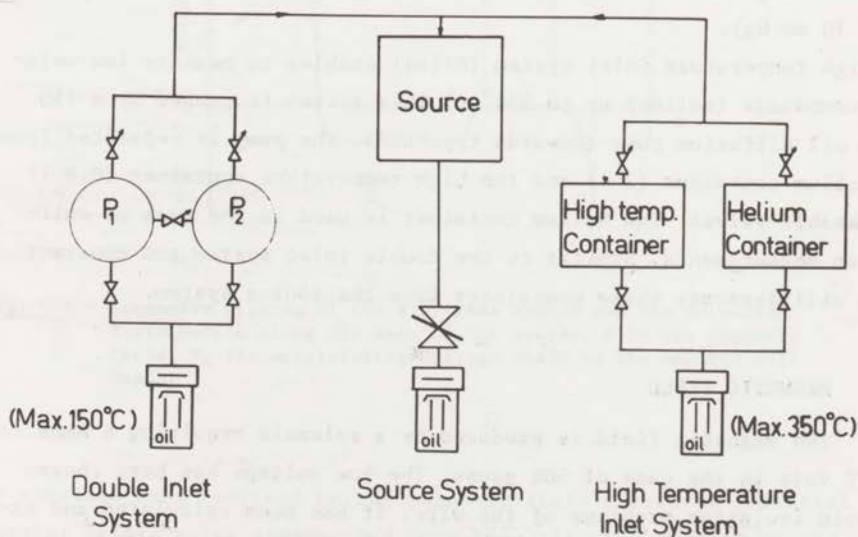tier baffle and a bakeable valve. The bakeout temperature of the system

Fig. 4.3 - A schematic diagram of the total vacuum system.

is limited at 350° C. Continuously heating and the application of stain-
less steel, vacromium (Ni-Cr alloy), silver, gold, and degussit will
ensure a clean vacuum system with background pressures lower than 10^{-8}
torr. An ionization gauge of very small dimensions and of very low heat
input (Politiek et al., 1968) is present near the interaction region.
This gauge allows direct measurement of the pressure of the target gas.
During measurements this pressure will range from 10^{-5} - 10^{-3} torr
depending on the gas used.

The double inlet system enables to introduce simultaneously two differ-
ent gas samples into the interaction region. A detailed description of
this system can be found elsewhere (Brongersma, 1968).

The two leak valves separating the spheres, at pressures P_1 and P_2, from
the source region will maintain a continuous and molecular gas flow
(Fig. 4.3). An additional variable leak valve (Edwards type LB2B) is
placed between the spheres providing a configuration allowing for long
time measurements. Applying a pressure P_1 being several times higher
than pressure P_2, a nearly constant pressure P_2 can be maintained by
adjusting the variable leak valve. Then a continuous and constant gas
flow to the interaction region results. The pressure at which the gas
is stored in the spheres is rather high (0.001 - 10 torr). This wide
pressure range is controlled using two membrane gauges (Lion DC 303,
1 and 10 mm Hg).

The high temperature inlet system (Atlas) enables to measure low vola-
tile compounds (solids) up to 350° C. This system is pumped by a 150
1/sec oil diffusion pump (Edwards type E02). The pump is separated from
the helium container (2 1) and the high temperature container (0.8 1)
by bakeable valves. The helium container is used in the case of cali-
bration measurements. Similar to the double inlet system two constant
leaks will separate these containers from the source system.

4.3   MAGNETIC FIELD

The magnetic field is produced by a solenoid requiring 6 Amps
and 39 Volt in the case of 500 gauss. The low voltage has been chosen
to avoid isolation problems of the wire. It has been calculated and ex-
perimentally confirmed that the contribution of the field components
perpendicular to the axial direction is less than 1 percent of the
total field in the essential part of the electron spectrometer.

The magnetic field serves a double purpose. It takes care of the confinement of the electron beam in the axis of the system and moreover it is essential for the energy selection of the inelastically scattered electrons.

4.4 DETAILS OF APPLIED METHODS

4.4.1 Retarding Potential Difference technique
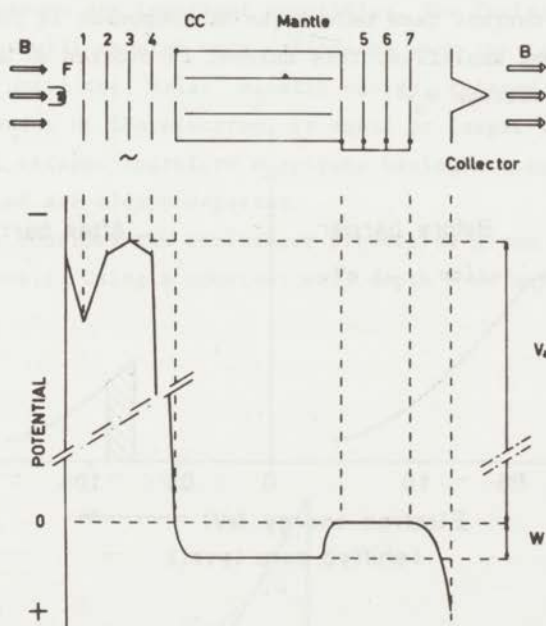
Fig. 4.4 - Schematic diagram of the electrode system and the potential distribution along the axis of the system. B is the magnetic field, V_a the accelerating voltage and W is the applied well depth.

An electron beam confined by the magnetic field crosses a potential barrier before being accelerated into the collision chamber CC and finally will reach the collector C (Fig. 4.4). A beam of quasi-monoenergetic electrons is obtained operating the electron gun in the AC version of the "Retarding Potential Difference" (R.P.D.) mode (Fox et

al., 1955). Electrode 1 is used to extract the electrons from the fila-
ment region while electrodes 2 and 4 will shield electrode 3 from
neighbouring disturbing potentials. An appropriate potential barrier
applied at electrode 3 will partly reflect and partly transmit the
emitted current produced by the filament. By varying the height of the
barrier by means of a potential modulation the transmitted current is
varied with the same frequency. In this way an AC component in the
primary beam is obtained with an electron energy spread in the order of
magnitude of the applied modulation width. Fig. 4.5 shows the energy
distribution of the electrons before and after the barrier. From the
Trapped Electron current (see below) the AC component is phase-sensi-
tively detected and amplified. This current is plotted as a function of
the accelerating voltage V_a.
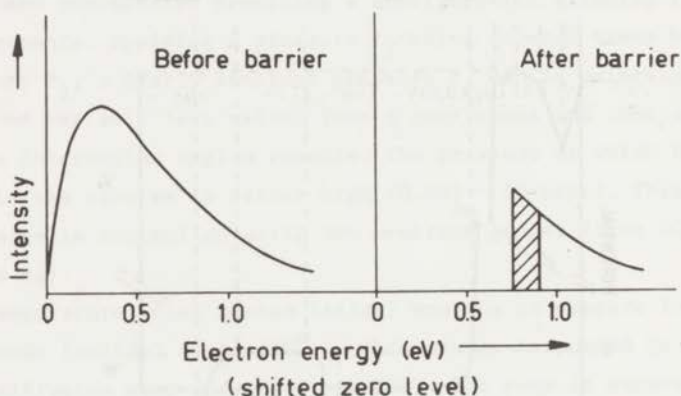
Fig. 4.5 - Schematic sketch of the energy distribution of the electron
beam before and after the barrier. The height of the barrier
is varied by means of a modulation resulting in an AC current
which is indicated by the shaded part.

4.4.2 Trapped Electron method

The Trapped Electron (T.E.) technique (Schulz, 1958) consists of
trapping low-energy electrons in a potential well. This potential well
is created by operating the cylindrical mantle M at a positive potential
(W) with respect to the collision chamber CC. Inelastically scattered
electrons which are left with a residual energy smaller than eW will be
collected at the mantle M.

$$e^- + \text{molecule} \rightarrow \text{molecule}^* + e^-$$

$$(E_i = e(V_a + W)) \qquad\qquad (E_f < eW) \qquad (4.1)$$
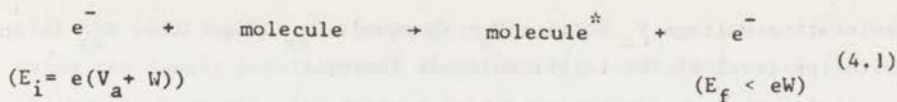
where

   E_i = initial energy of electrons

   E_f = final energy of electrons.

This process in which only the electrons with energy $E_f < eW$ are separated from higher energy electrons, essentially consists of a diffusion mechanism in which the magnitude of the axial magnetic field and the target gas pressure are important quantities. The inelastically scattered electrons will undergo many collisions with the target gas molecules (atoms) until the "axial" kinetic energy, related to the axial velocity component of the electron, is equal or larger than eW in which case they will escape. Therefore electrons having a total kinetic energy lower than eW are always detected.

Let us consider the excitation process as given by formula (4.1) more closely. Using a constant well depth W we may increase the
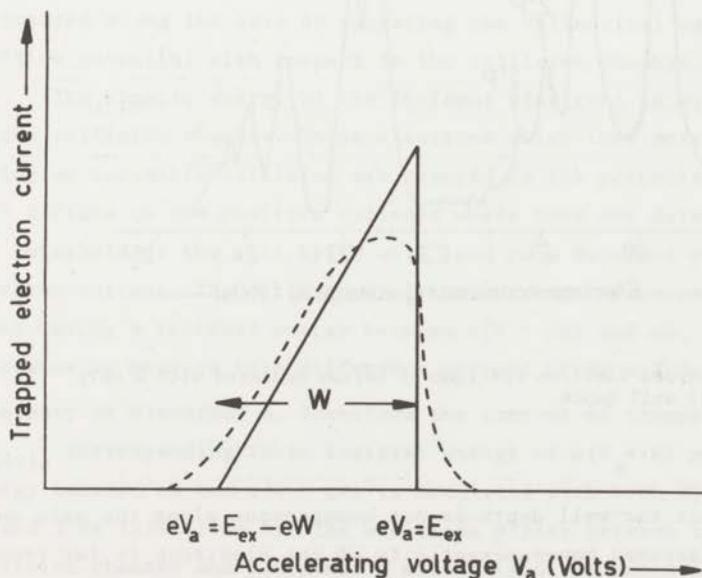

Fig. 4.6 - The theoretical peak shape for collection of slow, mono-
energetic electrons resulting from an excitation process is
shown. The dotted line presents a peak shape in which an
energy spread of the incident electrons is assumed.

accelerating voltage V_a until $e(V_a + W)$ equals E_{ex} (Fig. 4.6). E_{ex} is an excitation level of the target molecule (atom).

Assuming an excitation function which is a linear function of electron energy above the excitation energy E_{ex} for a range larger than W, the behaviour of the T.E. curve as a function of V_a will result as presented in Fig. 4.6. Since we collect only the electrons at the mantle M which are trapped by the potential well the curve will fall to zero for $eV_a = E_{ex}$. This is true as the inelastically scattered electrons at this energy are now left with an energy of eW and are capable to escape out of the potential well.
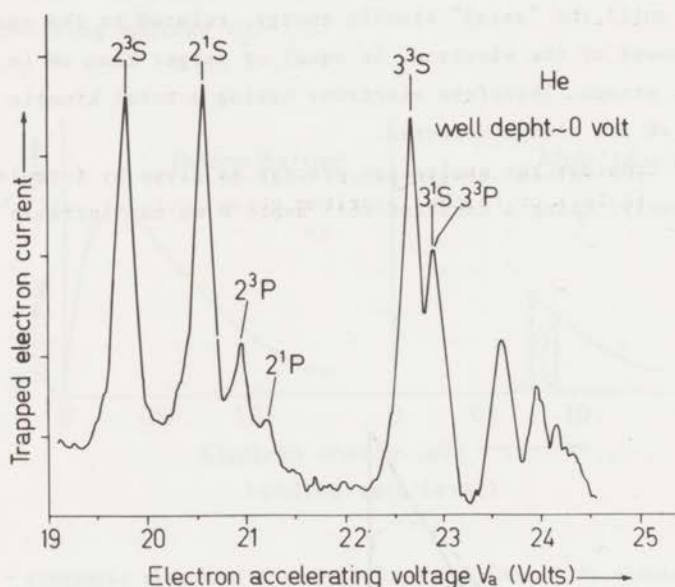

Fig. 4.7 - A Trapped Electron spectrum of helium measured with a very small well depth.

In fact the well depth is not homogeneous along the axis and moreover the assumed mono-energeticity of the electrons is far from true. The dotted line (Fig. 4.6) indicates a shape which we might expect in this experiment.

From the curves shown in Fig. 4.6 we can conclude that the Full Width at Half Maximum (FWHM) of the peak is directly correlated

with the well depth W. In general the best T.E. spectra are recorded
using the lowest possible well depth. In Fig. 4.7 a T.E. spectrum of
helium is shown measured very close to the threshold of excitation
(W $\simeq$ 0 Volt).

4.4.3 The Double Retarding Potential Difference method

The resolution of the excitation spectra obtained with the T.E.
method decreases rapidly when the energy above threshold (well depth)
is increased. In general this makes it impossible to obtain sensible
excitation spectra at energies higher than 0.5 eV above threshold.
Brongersma suggested a method to overcome this resolution problem. A
Double Retarding Potential Difference (D.R.P.D.) technique is applied
to energy analyse the incident as well as the scattered electrons.

In Fig. 4.8 a schematic picture of the electrode system and the
potential along the path of the primary beam are shown. The primary beam
is modulated at electrode 3 (frequency 30 Hz) to generate a quasi mono-
energetic beam (R.P.D.; Fox et al., 1955). The beam aligned by a magne-
tic field of 500 gauss traverses the collision chamber. A potential well
is created along the axis by operating the cylindrical mantle at a
positive potential with respect to the collision chamber.

The kinetic energy of the incident electrons is equal to $e(V_a + W)$
in the collision chamber. Those electrons which lose more than eV_a
during an inelastic collision are trapped in the potential well. They
will diffuse to the positive cylinder where they are detected. Lowering
the threshold of the well by ΔW will lead to a decrease of the trapped
electron current. The difference of the currents corresponds to elec-
trons having a residual energy between $e(W - \Delta W)$ and eW. In the present
apparatus we measure this difference current using a 3 Hz modulation
frequency at electrode 6. Therefore the current of trapped electrons
I_{mantle} corresponding to an incident energy of $e(V_a + W)$ and a scattered
energy between eW and $e(W - \Delta W)$ is modulated with both 30 Hz (electrode
3) and 3 Hz (electrode 6). The electrode plates between the grounded
collision chamber and electrode 6 will shield the potential well W from
the second modulation and vice versa.

The effect of the inhomogeneity of the well depth will be dis-
cussed later.
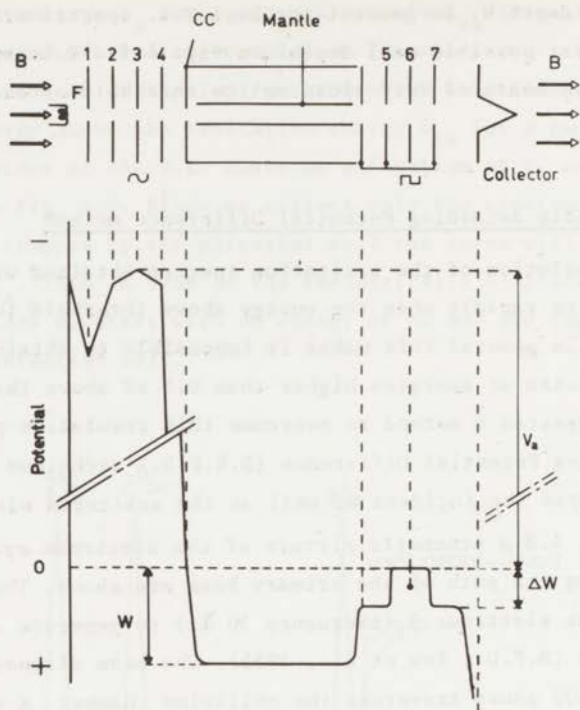
Fig. 4.8 - Schematic diagram of the electrode configuration and the potential distribution along the axis of the system. B is the magnetic field, CC the collision chamber, W the well depth and ΔW the amplitude of the second modulation.

In Fig. 4.9 a sketch is presented of the movement of a packet of electrons of a given energy distribution passing through the modulation region by increasing the accelerating voltage V_a. Every packet of electrons is directly correlated to an excitation process or any other energy loss process. The energy spread of the resulting packet of electrons is always larger than the applied modulation width or the energy distribution of the initial packet.

The D.R.P.D. method can be operated in two different ways.

The well depth can be fixed as the accelerating voltage V_a is varied. Energy loss spectra are produced in which the residual energy of the scattered electrons ΔE (eW) is kept constant (see Fig. 4.10).
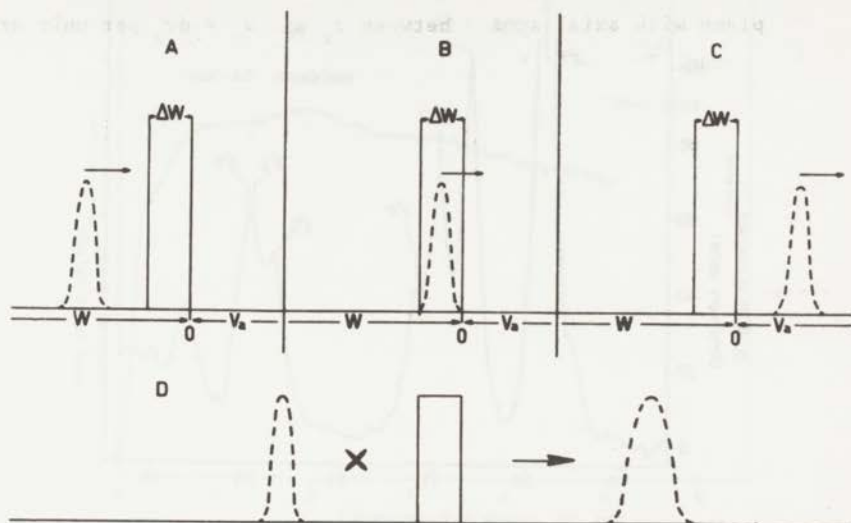
Fig. 4.9 - The upper part illustrates the movement of a packet of elec-
trons of given energy distribution along the potential axis
by gradually increasing the accelerating voltage V_a.
   A) The packet of electrons will always be collected at the
      cylindrical detector. However, as it is located below the
      modulation width it will not contribute to the D.R.P.D.
      current.
   B) Electrons will be collected depending on the height of
      the applied modulation. In this case all the electrons
      will contribute to the D.R.P.D. signal. The vertical
      lines indicate the two extreme positions of the modula-
      tion.
   C) The packet of electrons is now above the modulation
      region. These electrons will not be collected as they
      always will escape from the potential well W.
   D) The functioning of the modulation width, through which
      the packet of electrons passes, is sketched. Finally an
      energy distribution results which is always larger than
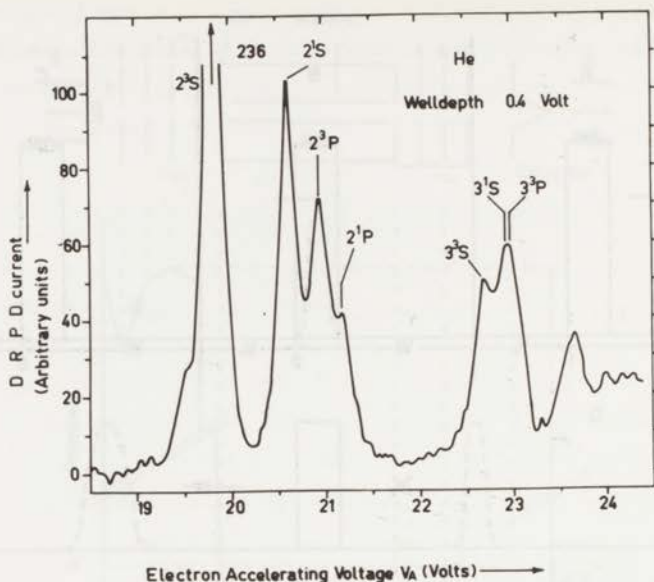   the modulation width or the initial energy distribution.

Fig. 4.10 - Energy loss spectrum of helium with the D.R.P.D. method. The well depth W is fixed at 0.4 Volt.

Moreover the energy loss E ($E = eV_a$) can be fixed taking E equal to the excitation energy of a given process. Varying the well depth a plot results of the cross section behaviour of the excitation process against excess energy of the electrons ΔE (see Fig. 4.11).

4.4.4 Diffusion mechanism and relation to resolution

The movement of the scattered electrons, mainly regulated by the axial magnetic field and the target gas, consists of a helical path parallel with the axis of the system. The helical path can be changed when collisions with target gas molecules (atoms) take place. The same collisions often cause a change in the direction of the velocity vector of the electron, which is the basis of the selection mechanism. Again and again the electron will be energy selected at the ends of the chamber whether it has sufficient "axial" (defined from axial velocity
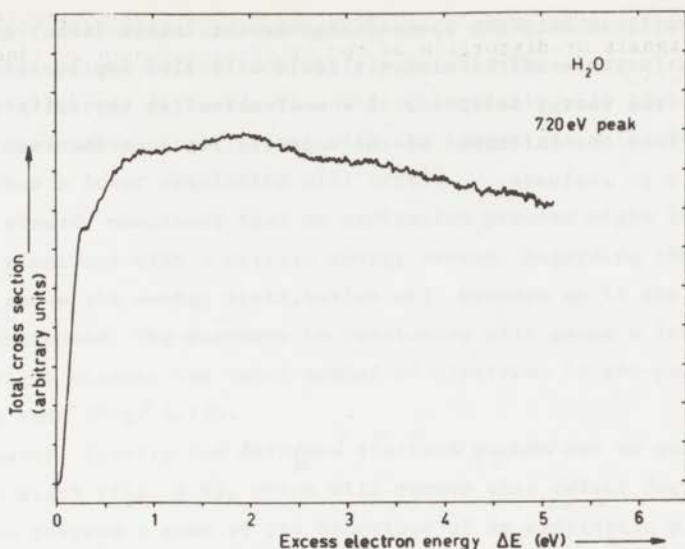
Fig. 4.11 - The total cross section behaviour of the 7.2 eV triplet excitation process of water against excess energy of the electrons ΔE (eW).

component) energy to escape from the potential well. In the case of the T.E. technique Schulz (1958) approximated the time τ for a slow electron to reach the mantle M:

$$\tau = 0.26 \, \frac{e \, B^2 \, R^2}{mV \, \nu_{coll.}} \tag{4.2}$$

where

R = radius cylinder M

$\nu_{coll.}$ = collision frequency

B = magnetic field

m = electron mass

eV = kinetic energy of electron

e = electron charge.

In the present experiment τ will be in the order of 10^{-3}- 10^{-2} seconds. It should be noted that the frequencies used in the modulation techniques are limited in magnitude by this diffusion time.

An increase of the magnetic field will increase the diffusion
time which will enhance the space charge in the interaction region.
However, an increase of the magnetic field will also improve the effec-
tiveness of the energy selection of the electrons as the diffusion time
increases. Thus the influence of the magnetic field on the resolution
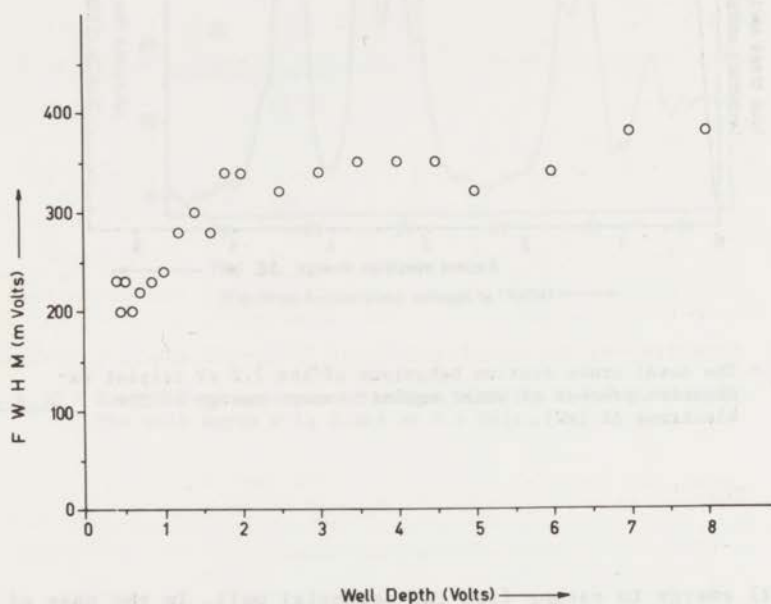is difficult to evaluate.

Fig. 4.12 - The Full Width at Half Maximum of the $1^1S \to 2^3S$ transition
of helium is plotted against the well depth.

Fig. 4.12 presents the behaviour of the Full Width at Half Maxi-
mum (FWHM) of the $1^1S \to 2^3S$ excitation peak of helium measured with the
D.R.P.D. technique against well depth. A clear decrease of resolution
is observed with increasing excess energy of the electron. This beha-
viour is in agreement with our expectations.

The energy selection mechanism of the scattered electrons cannot
be perfect due to the limited number of collisions with the target gas
molecules (atoms). This imperfection will affect the resolution more if
the energy is higher.

Moreover, by increasing the energy of the scattered electron in general the radial velocity component is also enhanced resulting in a larger radius of the helical motion (r = mv/eB). This larger radius will imply a shorter diffusion time and consequently will give a decrease of the number of collisions with the target gas molecules (atoms). Thus a lower resolution will result.

We already mentioned that an excitation process might induce a packet of electrons with a certain energy spread. Regarding the facts mentioned above the energy distribution will broaden up if the well depth is increased. The decrease in resolution will cause a lowering of peak height because the total number of electrons in the packet will remain the same (Fig. 4.13).

However, finally the deformed electron packet has to pass the modulation width (Fig. 4.9), which will remove this defect for a great part. If we perform a scan of the behaviour of an excitation process versus energy (well depth) we have to adapt the modulation width such

Small well depth   **Large well depth**

Intensity

0   0

Electron energy ⟶
(shifted zero level)
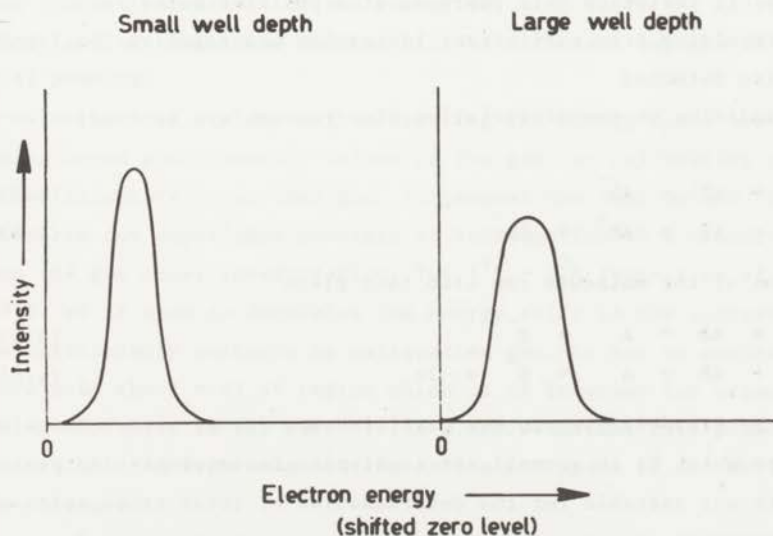
Fig. 4.13 - In the case of equal transition probabilities at different well depths a decrease of peak height will result for the initial peak if the resolution is lowered.

that the final resolution is slowly varying or such that the modulation
width is more than the largest FWHM of the initial energy distributions.
The last condition is hard to fulfil as we cannot measure this quantity
directly.

The results of such measurements on helium turn out to agree
very nicely with other work (chapter 5). Though the above mentioned
defect cannot be removed completely it can be kept very small.

If the modulation width is smaller than the basis spread of the
initial energy distribution and the resolution is decreased by increa-
sing the well depth, an immediate consequence will be a peak shift to
higher energy. This behaviour is confirmed experimentally. For well
depths of 0.5 Volt to 8 Volt the shift increases up to 0.10 Volt.

4.4.5 Collection of ions

The formation of positive or negative ions can be measured with
the T.E. technique by operating the collector M at a negative or posi-
tive potential. However, the collection of these ions does not depend
only on the potential of the collector M but also on the kinetic energy
of the ions. If collector M is operated at a positive potential
electrons resulting from excitation, ionization and negative ion forma-
tion are also detected.

In addition to non-dissociative electron capture or ionization
like

$$e^- + AB \rightarrow AB^- \qquad (4.3)$$
$$e^- + AB \rightarrow AB^+ + 2e^- \qquad (4.4)$$
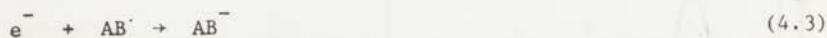
dissociation of the molecule can also take place

$$e^- + AB \rightarrow A + B^- \qquad (4.5)$$
$$e^- + AB \rightarrow A + B^+ + 2e^- \qquad (4.6)$$
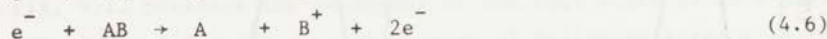
In the dissociation process particles are formed with an angular
distribution which is in general not isotropic. Consequently the present
apparatus is not suitable for the determination of total cross sections
of these processes.

Equation 4.3 describes a process which is the basis of the so-
called scavenger method. Excitation spectra are obtained using molecules
which easily attach electrons of a specific energy. For threshold

measurements the molecule SF_6 is used which only "collects" zero-energy electrons. The SF_6^- is detected by means of a mass spectrometer.

$$e^- \quad + \quad SF_6 \quad \rightarrow \quad SF_6^- \tag{4.7}$$

$$(E_f \simeq 0)$$
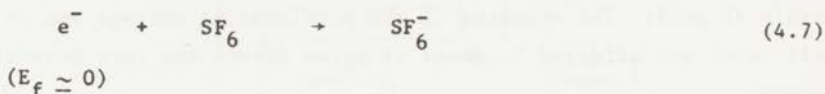
Using the mantle M to detect the SF_6^- ions we can also produce scavenger excitation spectra (Brongersma, 1968).

With the T.E.-method electrons and ions are collected. Applying the D.R.P.D. technique only electrons are detected. Thus the character of the particles is easily established.

4.4.6 Energy calibration

In general the kinetic energy of the electrons reaching the grounded collision chamber CC will differ from the energy eV_a (V_a is the accelerating voltage). This difference is mainly due to the variation of contact potentials (work functions) depending on the nature and pressure of the introduced gas and the temperature. Consequently the contact potentials of the energy defining electrode (first modulation) and the collision chamber will be different because of differential pumping.

The possible ways of calibrating the energy scale are either using known spectroscopic values of the gas, or calibrating against known structure in another gas. In general the last method is applied which in our experiment consists of introduction of a mixture of helium and the gas under investigation. The $1^1S \rightarrow 2^3S$ transition of helium at 19.82 eV is used to determine the energy shift in the mixture. Helium is particularly suitable as calibrating gas. It has no excitation levels in the 1 - 11 eV region which is of interest for organic molecules. Moreover in the case of the D.R.P.D. method this peak remains quite isolated from neighbouring excitation peaks if the well depth is enlarged.

Despite small primary beam currents, gold plating of the source and continuously heating the shift in contact potentials (work functions) can reach values up to 0.3 eV.

4.5   DETECTION SYSTEM

A schematic diagram of the control and measuring system is presented in Fig. 4.14. All the potentials in the apparatus are stable within 10 mVolt. The scanning of the accelerating voltage and of the well depth are effected by means of motor driven ten turn potentiometers.

The current of trapped electrons to the detector M is very small (10^{-12} - 10^{-16} A). To detect such currents electrometer circuits are needed using measuring resistances of the order of 10^{11} Ω.

It is very important to keep the input capacitance as low as possible in order to achieve an acceptable frequency band width compared with the modulation frequencies used. As the time constant, formed by the capacitance of the mantle times the measuring resistance used, is of the order of 10 sec ($C_{mantle} \simeq 100$ pF) band width improvement is badly needed.

This is effected in two ways:

i)   by negative current feedback from the output resulting in a so-called "virtual earth" of the collector;

ii)   by positive capacitive feedback reducing the effect of the parasitic capacitance across the measuring resistor to a large extent.

By keeping the actual amplifier band width reasonably wide an overall time constant of a millisecond can be obtained without undue noise or parasitic oscillations.

For very low level signals a time-averaging computer is available. A measuring consisting of N runs will result in a signal – noise improvement proportional to $\sqrt{N}$.

The D.R.P.D. signal is established as follows. After the first modulation (frequency f_1) the primary beam consists of a DC and AC part

$$A \; + \; B \sin 2\pi f_1 \, t \qquad\qquad\qquad (4.8)$$

If excitation takes place and the second modulation ($f_2 \ll f_1$) is applied the current reaching the collector will be composed of

$$A_1 + B_1 \sin 2\pi f_1 t + (A_2 + B_2 \sin 2\pi f_1 \, t) \sin 2\pi f_2 \, t \qquad (4.9)$$

$$(A = A_1 + A_2; \; B = B_1 + B_2)$$

or

$$A_1 + B_1 \sin 2\pi f_1 \, t + A_2 \sin 2\pi f_2 \, t + B_2 \sin 2\pi f_1 t \sin 2\pi f_2 \, t$$
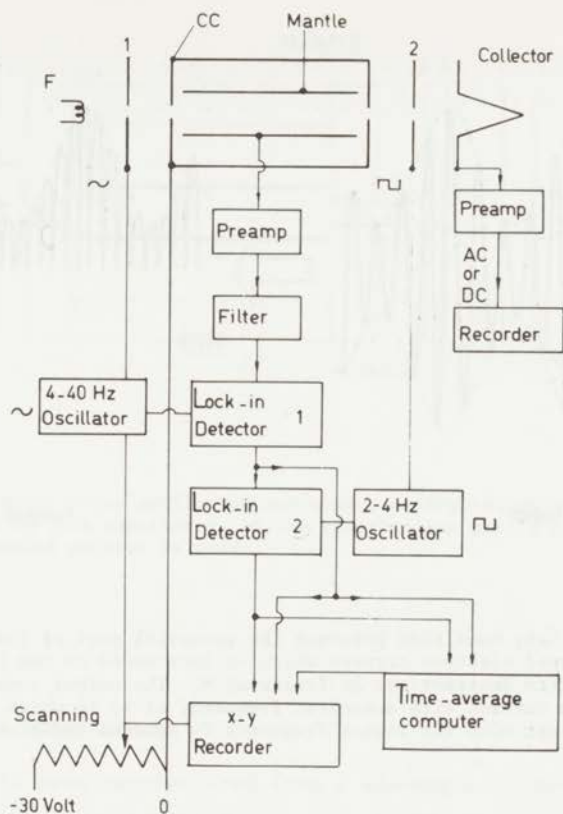
$$(4.10)$$

Fig. 4.14 - Schematic diagram of the detection system (see also Fig.
4.8).

The current corresponding to the last part of formula (4.10) is
of interest. With this electron current both the mono-energeticity of
the electrons (first modulation) and the energy of the scattered elec-
trons eW (second modulation) are directly represented. For detection two
lock-in detectors are used after each other (Fig. 4.14). The first one
is locked at the higher frequency (30 Hz) using no integration time. The
ouput consists of a current in which the part with the second frequency
($\sim$ 3 Hz) is undisturbed (Fig. 4.15). This output is introduced to the
second phase sensitive detector locked at f_2. Of course now high inte-
gration times must be used (10 - 30 - 100 seconds), to minimize noise

| Input | Output |
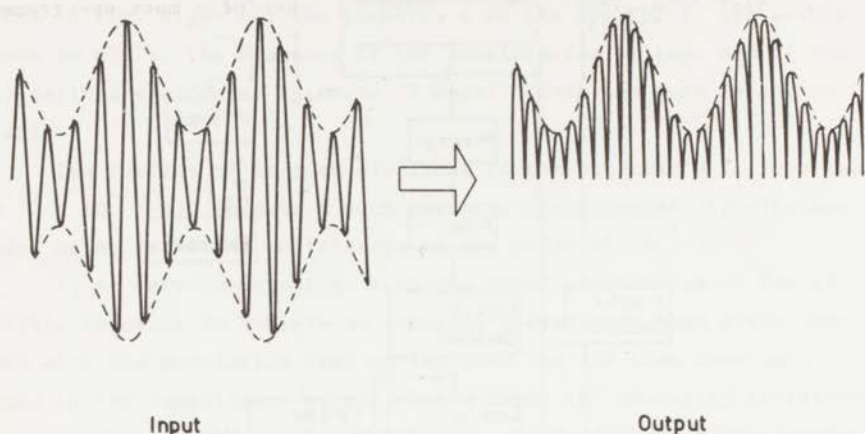
<u>Fig. 4.15</u> – The left hand side presents the essential part of the
trapped electron current which is introduced to the first
lock-in detector set at frequency f_1. The output consists
of a current with a doublet frequency of f_1 in which the
current with the lowest frequency f_2 remains undisturbed.

in the final current which is fed to the XY-recorder.

The velocity of scanning must be low as low frequencies and
high integration times are applied. The frequencies must be sufficient-
ly separated (30 and ~ 3 Hz) and well selected to avoid that higher
orders of the lowest frequency will interfere with the second frequen-
cy. Moreover both frequencies should be chosen very low otherwise the
diffusion mechanism will be disturbed.

$$f_2 \ll f_1 \ll \frac{1}{\tau} \qquad\qquad (\tau = \text{diffusion time}) \qquad (4.11)$$

In the present apparatus the second modulation consists of a
square wave. This will not essentially change the method of operation.

The last part of equation (4.10) can be developed as

$$(B_2/2) \cos 2\pi(f_1 - f_2)t - (B_2/2) \cos 2\pi(f_1 + f_2)t \qquad (4.12)$$

This means that the D.R.P.D. technique can also be operated
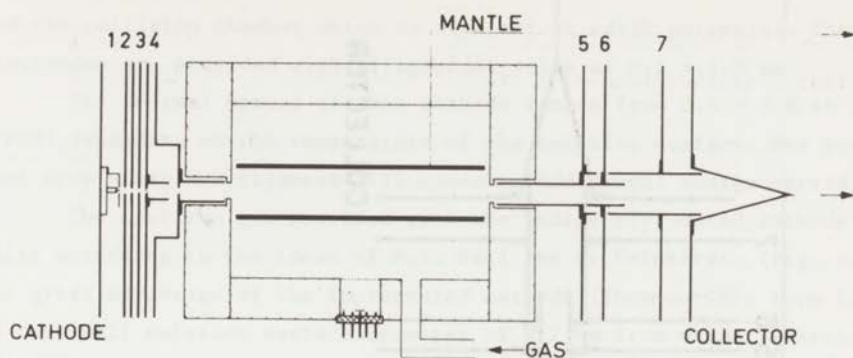using only one lock-in detector set at the difference or sum frequency.

Fig. 4.16 - Schematic cross section of one source configuration as is
used in this experiment. In the electron gun part a direct-
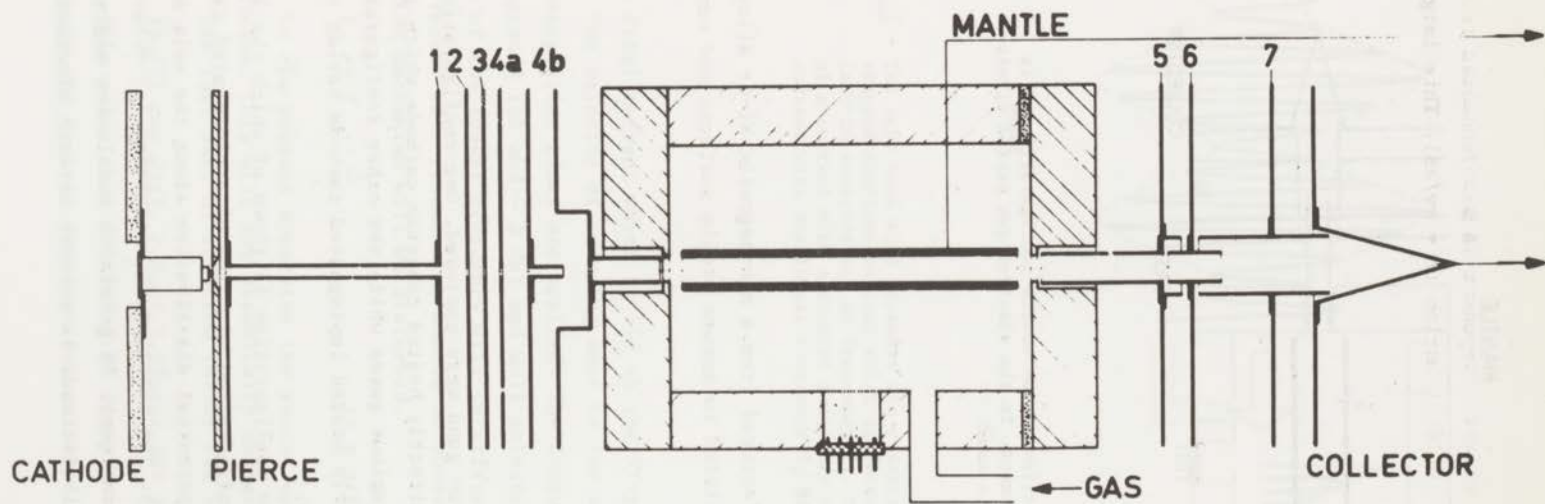ly heated cathode is used.

4.6   ELECTRON SPECTROMETER

All parts were manufactured from a non-magnetic Ni-Cr alloy
(vacromium) which are goldplated to ensure stable surfaces and contact
potentials.

4.6.1 Electron guns

4.6.1.1 Details

Two different electron guns were employed. One configuration
essentially consists of a directly heated tungsten cathode which is
rather insensitive for contagious gases while the other configuration
is provided with an indirectly heated impregnated cathode having a
lower thermal energy spread.

In Fig. 4.16 a source configuration is shown of which the left
hand side represents the configuration with the directly heated cathode.
A schematic diagram of the potential distribution along the axis of the
gun is presented in Fig. 4.4. The function of electrodes 1 - 4 has been
described before (R.P.D. technique). In general a modulation width of 20
mVolt is used. An additional electrode is present between electrode 4

Fig. 4.17 - Schematic cross section of a source configuration provided with an indirectly heated cathode gun.

and the collision chamber which is also set at earth potential. The electrodes are provided with ellipsoidal slits of 0.5 × 1.5 mm.

The thermal spread of this cathode ranges from 0.5 - 0.8 eV (FWHM) depending on the temperature of the emissive surface. The potential drop along the filament will cause an additional energy spread.

The electron gun provided with the indirectly heated cathode was built according to the ideas of R.I. Hall and J. Reinhardt[*] (Fig. 4.17). The great advantage of the impregnated cathode (Thomson-CSF, type CI-10) is the small emission surface diameter of 0.2 mm from which nevertheless high emission currents are obtained (up to 10 A/cm^2).

The electrodes are accurately aligned. The Pierce geometry electrode (aperture 0.8 mm) will produce a parallel beam. The function of electrode 1 (length 34 mm, aperture 1.5 mm) will be discussed later. The retarding electrode 3 is shielded by electrodes 2, 4a and 4b from potential disturbances. The potentials of electrodes 1-4 are essentially the same. Only the potential of electrode 3 is somewhat higher (more negative) depending on the modulation width (10 - 20 mVolt). Electrodes 1 - 4 are provided with 1.2 mm apertures.

4.6.1.2 Resolution of electron gun

The resolution of the electron gun with the directly heated cathode (tungsten filament) is rather low due to the large thermal energy spread (~ 2300 K). We will restrict ourselves to the discussion of the resolution limiting factors in the case of the indirectly heated cathode. Most of the mentioned factors are also true for the other gun.

Variable contact potentials (work functions) will give rise to a decrease of energy resolution. However, as the electron gun is differentially pumped this effect is estimated to be small even if gases like benzene or pyridine are measured.

Space charge effects will become important if large primary currents are used. Marmet (1964) has shown that the relaxation of the energy distribution may lead to deformed peak shapes. Using low intensity beams (~ 10^{-8} A) these effects will be circumvented.

The widths of the apertures ($\geq$ 1.2 mm) are that large that scattering of the electrons against the electrodes will not take place.

[*] Private communication.

Scattering might induce all kind of disturbing effects like negative signals or distortion of the excitation functions (Anderson et al., 1967).

The function of electrode 1 (Fig. 4.17) is to separate the electron region with its space charge from the energy defining process at the retarding electrode. It has been observed by Hall (1971) that lower resolution and a deformed R.P.D. distribution will result if this distance is too short.

The most important factor limiting the energy resolution arises from the radial momentum of the electrons perpendicular to the magnetic field. Due to the magnetic field the radial momentum will be transformed into a tangential motion with a radius which is small compared with the dimensions of the slits. The R.P.D. technique only takes into account the axial (longitudinal) velocity component and leaves the radial component undisturbed. Thus the radial momentum spread will entirely contribute to the final energy spread of the detected electrons.

Suppose the electrons are released isotropically from the cathode at temperature T. Then in velocity space the Maxwellian velocity distribution can be written as

$$f(\vec{v}) = A \ e^{-\frac{1}{2} \ mv^2/kT} \qquad (4.13)$$

where

k = Boltzman factor

$A = (\frac{m}{2\pi kT})^{\frac{1}{2}}$

Considering the number of electrons with velocity components between $\vec{v}$ and $\vec{v} + d\vec{v}$

$$f(\vec{v}) \ d\vec{v} = A \ e^{-\frac{1}{2} \ mv^2/kT} \ d\vec{v} \qquad (4.14)$$

Changing to cylindrical coordinates $(dv_x dv_y dv_z \cdot v_r dv_r dv_z d\phi)$ we obtain

$$f(v_r, v_z, \phi)v_r dv_r dv_z d\phi = A \ e^{-\frac{1}{2} \ m(v_r^2 + v_z^2)/kT} v_r dv_r dv_z d\phi \qquad (4.15)$$
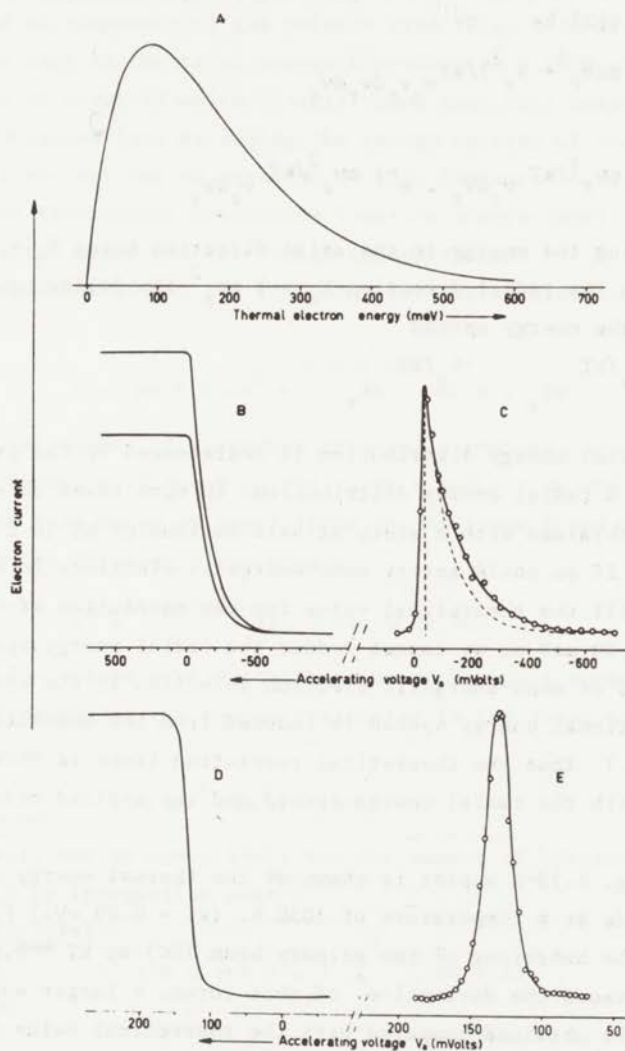
where

r = radial component

z = axial component

Integrating ϕ from $0 \rightarrow 2\pi$ leads to

$$= 2\pi \ A \ e^{-\frac{1}{2} \ m(v_r^2 + v_z^2)/kT} v_r dv_r dv_z \qquad (4.16)$$

Fig. 4.18 - A) Total energy distribution of thermally emitted electrons
from a cathode at temperature T = 1050 K.
B) Plots of primary beam (DC) against accelerating voltage.
The lower one is obtained with a cathode potential
50 mVolt more positive.
C) Derivative of primary beam (DC) giving the experimental
axial energy spread (~ 90 meV) which can be compared with
the theoretical curve (dotted line) which has a FWHM of
62 meV.
D) Plot of AC component of primary beam versus accelerating
voltage.
E) Derivative of the AC component of primary beam having an
energy spread at half maximum of 20 meV (modulation width
10 mVolt).

We want to calculate the number of electrons crossing a vertical plane with axial speeds between v_z and $v_z + dv_z$ per unit area and per second. This will be

$$\sim e^{-\frac{1}{2} m(v_r^2 + v_z^2)/kT} v_z v_r dv_r dv_z \qquad (4.17)$$

or

$$\sim e^{-\frac{1}{2} mv_r^2/kT} v_r dv_r \cdot e^{-\frac{1}{2} mv_z^2/kT} v_z dv_z \qquad (4.18)$$

Defining the energy in the axial direction being $E_z = \frac{1}{2} mv_z^2$ and the energy in the radial direction $E_r = \frac{1}{2} mv_r^2$ the following form is derived for the energy spread

$$\sim e^{-E_z/kT} dE_z \cdot e^{-E_r/kT} dE_r \qquad (4.19)$$

The total energy distribution is represented by the product of an axial and a radial energy distribution. In both cases an exponential decrease is obtained with a width at half maximum of $kT \ln 2$ (62 meV at $T = 1050$ K). If we could select mono-energetic electrons in the axial direction still the theoretical value for the resolution of our gun is limited at ~ 60 meV as we cannot reduce the radial energy spread. However, instead of mono-energetic electron selection in the axial direction an additional energy spread is induced from the modulation width (first R.P.D.). Thus the theoretical resolution limit is directly correlated with the radial energy spread and the applied modulation width.

In Fig. 4.18-A a plot is shown of the thermal energy distribution of the cathode at a temperature of 1050 K. (kT = 0.09 eV.) Fig. 4.18-B represents the behaviour of the primary beam (DC) at $kT \approx 0.09$ eV while Fig. 4.18-C shows the derivative* of this curve. A larger energy spread of ~ 90 meV is obtained compared with the theoretical value of 62 meV.

---

* Numerical differentiation was used according to the Lagrange approximation in the case of a six terms series:

$$\frac{d\, f(x)}{dx} \approx \frac{1}{5!\, h} \sum_{i=0}^{5} A_i\, f(x_i)$$

where

h = interval of neighbouring points x_i and x_{i+1}.

Applying a modulation width of 10 mVolt an energy spread of 20 meV is observed for the AC component (Fig. 4.18-E) which is obtained by differentiating the AC component of the primary beam (Fig. 4.18-D).

In the case of the total energy distribution a FWHM of $\sim$ 220 meV (Fig. 4.18-A) is involved which clearly shows that this energy spread will not be obtained just by adding the energy spreads of the two separate energy distributions of equation (4.19). However, it can be easily shown that the theoretical resolution limit is always lower than the sum of the modulation width and the radial energy spread:

From equation (4.14) the following form is obtained in spherical coordinates

$$f(v) \; dv = 4 \pi v^2 \; e^{-\frac{1}{2} m v^2/kT} \; dv \qquad (4.20)$$

The total number of electrons crossing a vertical plane per unit area and per second with speed in the range v and v + dv and a direction of motion that makes an angle lying in the range Θ and Θ + dΘ with the normal to the vertical plane equals

$$\sim v^3 \; e^{-\frac{1}{2} mv^2/kT} \; \sin \Theta \cos \Theta \; dv \; d\Theta \qquad (4.21)$$

If we now assume a potential barrier of V_1, only those electrons will pass having sufficient energy (velocity) in the axial direction which means that

$$\frac{1}{2} mv^2 \cos^2\Theta \geq eV_1 \qquad (4.22)$$

This will set an upper limit for the number of electrons within the angle of Θ by integration over Θ

$$\sim \{ \int_{\Theta=0}^{\Theta=\Theta_{max}(v)} v^3 \sin \Theta \cos \Theta \; e^{-\frac{1}{2} mv^2/kT} \; d\Theta \} \; dv \qquad (4.23)$$

or

$$\sim v^3 \; e^{-\frac{1}{2} mv^2/kT} \; dv \int_{1}^{\cos \Theta_{max}} \cos \Theta \; d \cos \Theta \qquad (4.24)$$

where

$$\cos \Theta_{max} = \sqrt{\frac{2eV_1}{mv^2}}$$

leading to

$$\sim v^3 \; e^{-\frac{1}{2} mv^2/kT} \; (1 - \frac{2eV_1}{mv^2}) \; dv \qquad (4.25)$$

This form will only be different from zero if $v > \sqrt{\dfrac{2eV_1}{m}}$. Equation (4.25) will give

$$\sim \{ v^3 \, e^{-\frac{1}{2} mv^2/kT} \, dv - \frac{2eV_1}{m} v \, e^{-\frac{1}{2} mv^2/kT} \, dv \} \tag{4.26}$$

or

$$\sim \{ E \, e^{-E/kT} \, dE - eV_1 \cdot e^{-E/kT} \, dE \} \tag{4.27}$$

The first part represents the energy distribution if no barrier is present. The second part gives the deviation due to the potential barrier V_1. For a second potential barrier V_2, somewhat higher than V_1, a similar form of (4.27) is obtained. The difference current derived from the currents corresponding to barriers V_1 and V_2 (equation (4.27)) can be written in the following way
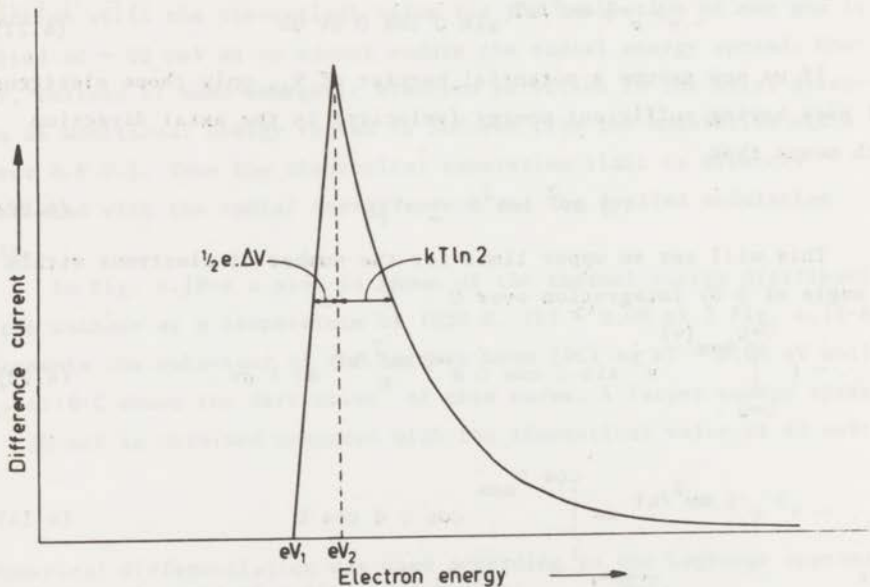
Fig. 4.19 - The theoretical energy distribution of the difference current is presented. The width at half maximum is directly related with the modulation width ΔV and the radial energy spread kT ln 2.

$$\Delta I \ (E, V_1, V_2) \ dE \sim e^{-E/kT} \ (eV_2 - eV_1) \ dE \qquad (4.28)$$

$$E \geq eV_2 > eV_1$$

$$\Delta I \ (E, \ V_1) \ dE \quad \sim e^{-E/kT} \ (E - eV_1) \ dE \qquad (4.29)$$

$$eV_2 \geq E \geq eV_1$$

$$\Delta I \ (E) \ dE \qquad = 0 \qquad (4.30)$$

$$eV_1 \geq E$$

Equations (4.28), (4.29) and (4.30) will fully describe the actual situation in which the potential barrier is varied by means of a modulation technique (1° R.P.D.). In Fig. 4.19 the energy distribution of the difference current is presented. Between potentials V_1 and V_2, equation (4.29) will describe the situation.

If a very small modulation width ($\Delta V = V_2 - V_1$) is applied a nearly linear onset is obtained giving an energy width of $\frac{1}{2}$ e . ΔV for the first part of the curve. In any case this part of the FWHM is always smaller than e . ΔV. As for the second part an exponential decrease is found (equation (4.28)) with a width at half maximum of kT ln 2. Then the FWHM (theoretical) is given by

$$C_{\Delta V}(e \ . \ \Delta V) + kT \ ln \ 2 \qquad (4.31)$$

in which $C_{\Delta V}$ is a variable such that $\frac{1}{2} \leq C_{\Delta V} < 1$. The value of $C_{\Delta V}$ depends on the behaviour of the onset of the difference current (equation (4.29)).

We have shown that the theoretical limit of the FWHM in the R.P.D. technique is always lower than the sum of the modulation width and the radial energy spread. For a cathode temperature of 1050 K and a modulation width of 10 mVolt a FWHM of $\sim$ 70 meV will result. This is much less than the experimentally observed lowest value of $\sim$ 160 meV. A discussion to explain this difference will be given later (see section 4.6.4).

Using the indirectly heated cathode an improvement in resolution of about 40 meV is obtained compared with the directly heated cathode.

4.6.2 Trapped electron collector (mantle) and collision chamber

The beam enters the grounded collision chamber through a 3.5 mm
diameter aperture and leaves through a 4 mm diameter aperture. Schema-
tic cross sections of the different configurations are presented in
Fig. 4.16 and Fig. 4.17. In the case of the cylindrical mantle two
different sizes of diameter are used, 10 mm and 4 mm. The last size is
particularly suited for plots of the excitation cross section against
the energy because the contribution of well depth potentials different
from zero or from the applied voltage of the mantle V_W is relatively
small[*]. This case is illustrated in Fig. 4.20.
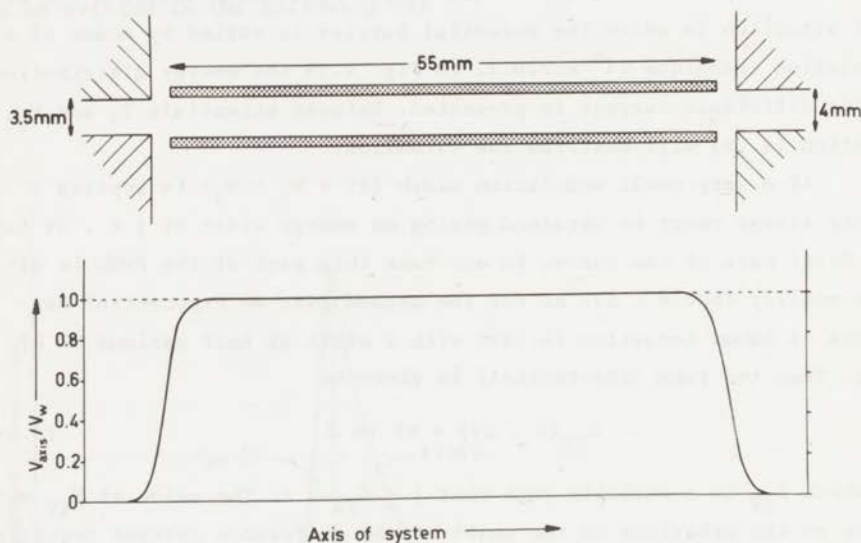
Fig. 4.20 – The variation of potential along the axis of the inter-
action region. The contribution of potentials different
from V_W appears to be relatively small. The collision
chamber was taken at zero potential.

---

[*] The calculation of the potential along the axis of the system was per-
formed by Brongersma following the method of Weber (1967). Numerical
solution of the Laplace equation for a system of rotational symmetry
with adequate boundary conditions is obtained by means of iteration.

In other work (Schulz et al., 1959; Bowman and Miller, 1965; Brongersma, 1968) the well depth was effected in a different way. Between the cylindrical mantle and the axis of the system one or more grids, at earth potential, were placed. A small fraction of the potential of the cylindrical mantle penetrates through this grid into the centre of the tube. It can be anticipated that the well depth obtained in this way will possess a certain degree of variation.

Using no grids no disadvantageous effects were observed. Negative signals due to metastable atom impact (helium) were not observed. At energies above the threshold of ionization positive ions will also reach the mantle using this configuration. With grids these ions will partially or totally be prevented in reaching the mantle. The rising of background current with increasing energy, which is often observed in T.E. spectra using grid(s), is no longer present with our set-up.

4.6.3   Second modulation electrodes and electron collector

The back side of the source configurations (Fig. 4.16, Fig. 4.17), defining the cathode region as the front side, consists of the second modulation electrodes and the primary beam collector.

Electrode 5, length 18 mm - internal diameter 4 mm, will shield the interaction region from the energy selection region and vice versa. The length of electrode 6, $2\frac{1}{2}$ times the internal diameter (4 mm), is large enough to guarantee the correct functioning of the potential modulation. Electrode 7, length 20 mm - diameter 8 mm, will shield the modulation region from the electron collector which is kept at + 6 Volt. Electrons of the primary beam before collection will collide several times with the surface of the electron collector due to the oblique shape of this electrode. This configuration will prevent the electrons to scatter back into the interaction region.

Electrodes 5 and 7 are set at a positive potential ΔW (Fig. 4.8). ΔW is the width of the second modulation as effected at electrode 6.

In the source configuration of Fig. 4.16 the back flange of the collision chamber is at earth potential. This will cause a varying efficiency of the energy selection process of the scattered electrons depending on the ratio of W and ΔW. Excitation spectra at a specific well depth are produced correctly. However, the relative intensity of the scattered electrons versus energy (variation of well depth) will be

largely affected, especially at low energies. This defect is circumvented using a cylindrical mantle of 4 mm (Fig. 4.17) and applying the same potential at the back flange as is used at electrode 5 and 7 (ΔW). Then total efficiency is assured for every well depth.

One might expect loss of trapped electron signal due to collection at the back flange and electrode 5. We performed measurements in a configuration in which electrode 5 is modulated similar as electrode 6. Hardly any intensity changes were observed which indicate a negligable loss of electrons.

The cross section measurements versus energy essentially consists in varying the well depth. It has been confirmed experimentally that decrease of well depth will give identical results as obtained by lowering the threshold of the well by adding a positive potential to the back flange and electrodes 5, 6 and 7.

4.6.4 Present limitations of the resolution

We will resume the more important phenomena which restrict the resolving power of the present apparatus (minimum 150 - 160 meV with T.E. method).

a) Radial energy spread.

The FWHM of the energy distribution of the primary beam in the axial direction has been determined being ~ 90 meV (see section 4.6.1). Theoretically a value of 62 meV is predicted. The difference might be explained on the basis of space charge and contact potentials. Thus for the radial energy spread a larger value than the theoretical value of 62 meV can be expected.

b) R.P.D. technique.

Using a modulation width of 10 mVolt an energy spread of the AC component of the primary beam is observed of 20 meV. This is much more than the theoretical value of 5 meV (half of the modulation width, see section 4.6.1). Probably the same reasons as mentioned in section a) are responsible for this difference, though part of it might be caused by imperfectly chopping of the primary beam.

c) Influence of contact potentials.

The preparation of the electrons, the selection procedure of the trapped electrons suggests that contact potentials might play an important role concerning the resolution. When using a target gas of "clean" atoms/molecules like helium or nitrogen the lowering of resolution should be less. However, "dirty" molecules like H_2O, benzene or pyridine will, despite continuously heating, cause contact potentials which will decrease the resolution of the system.

The present apparatus was built with the main objective to measure organic molecules. Therefore, oil diffusion pumps can be used. In the case of "clean" molecules mercury diffusion pumps are preferable in order to minimize contamination of the source surface.

The source is gold plated to minimize charging of surfaces. However, we have observed that the resolution is slowly decreasing in the course of time despite renewed gold plating. It looks promising to change to molybdenum as source material, which has a reputation of very stable surfaces and contact potentials (Zecca[*]: Hall, 1971).

d) Space charge.

It is difficult to evaluate its contribution to the energy spread of the electrons.

e) Selection procedure of scattered electrons.

There always will be an additional energy spread due to the imperfection of the selection mechanism. Using the D.R.P.D. method a continuous decrease of resolution is observed with increasing well depth.

With the T.E. technique the resolution is directly related to the magnitude of the well depth (section 4.6.1).

[*] private communication.

C H A P T E R   V

H E L I U M   A N D   B E N Z E N E

5.1 HELIUM[*]

5.1.1 Singly excited states

5.1.1.1 Introduction

Resonances in the cross section near inelastic threshold form an important feature of electron-atom scattering. The occurrence of these phenomena has been clearly demonstrated both in differential (Chamberlain et al., 1965; Ehrhardt et al., 1968) and in total cross sections (Pichanick and Simpson, 1968) for the electron-helium case. Up to now total cross sections were hard to obtain. In principle the production of metastables may yield this information. High resolution spectra have been reported by Pichanick and Simpson (1968). However, this method has the drawback that in exciting 2^1S states, 2^3S metastables will also be formed so that both species are detected simultaneously. Moreover, at higher incident energies cascading from higher excited levels to these metastable states will take place. Total cross sections determined by means of Penning ionization (Cermak, 1966) and other techniques for the detection of metastables (Holt and Krotkov, 1966) will also be affected by cascade processes.

Differential (angular) methods (Chamberlain et al., 1965) often suffer from difficulties in obtaining absolute values for the total cross sections. These difficulties especially arise from the fact that

---

[*] Part of this work has already been published (Brongersma, Knoop and Backx, 1972).
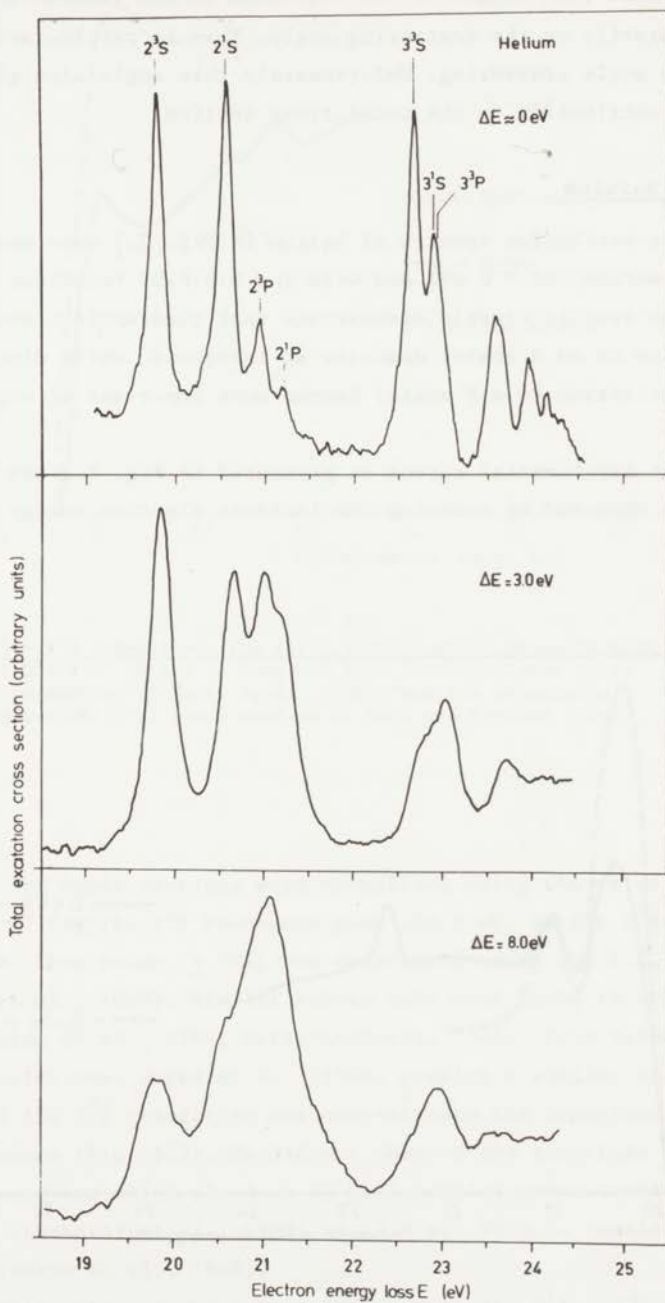
Fig. 5.1 - Excitation spectra of helium measured with the T.E. method
         ($\Delta E \approx 0$ eV) and with the D.R.P.D. technique ($\Delta E = 3$ eV,
         $\Delta E = 8$ eV).

the effective path length of the electrons in the interaction region
depends heavily on the scattering angle. This is particularly true for
near zero angle scattering. Unfortunately this angle also gives the
largest contribution to the total cross section.

5.1.1.2 Results

The excitation spectra of helium in Fig. 5.1 were measured with
the T.E. method ($\Delta E \approx 0$ eV) and with the D.R.P.D. technique ($\Delta E = 3$ eV,
8 eV). The spectra clearly demonstrate that quadrupole transitions
(excitation to an S state) dominate at threshold, while dipole transi-
tions (excitation to a P state) become more important at higher
energies.

The experimental curves as presented in Fig. 5.2 and Fig. 5.3
have been obtained by scanning the incident electron energy for a fixed
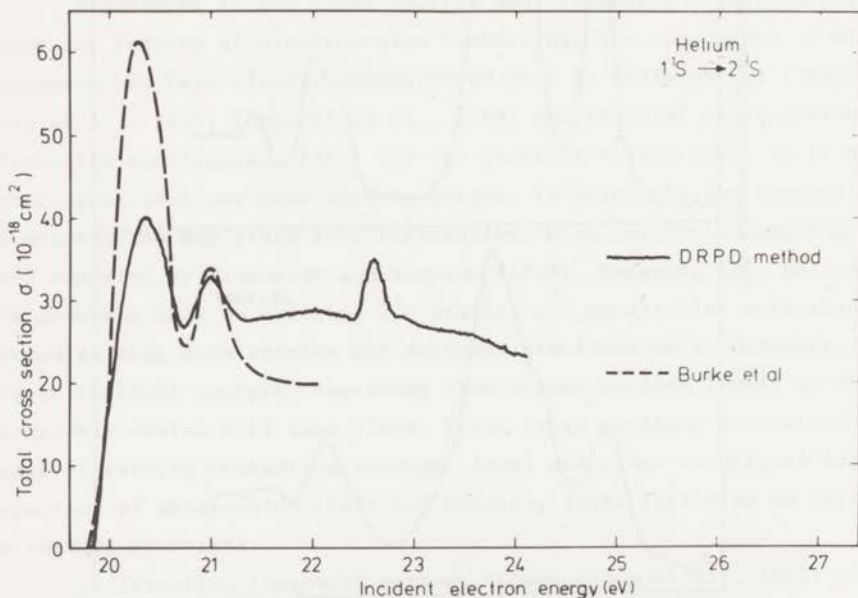
Fig. 5.2 - $1^1S \rightarrow 2^3S$ transition. The total cross section measured with
the D.R.P.D. method is compared with the calculated total
cross section of Burke et al. (1969). The experimental curve
was normalized using the value 4.0×10^{-18} cm^2 (Brongersma
et al., 1969) for the 2^2P resonance peak at 20.3 eV.
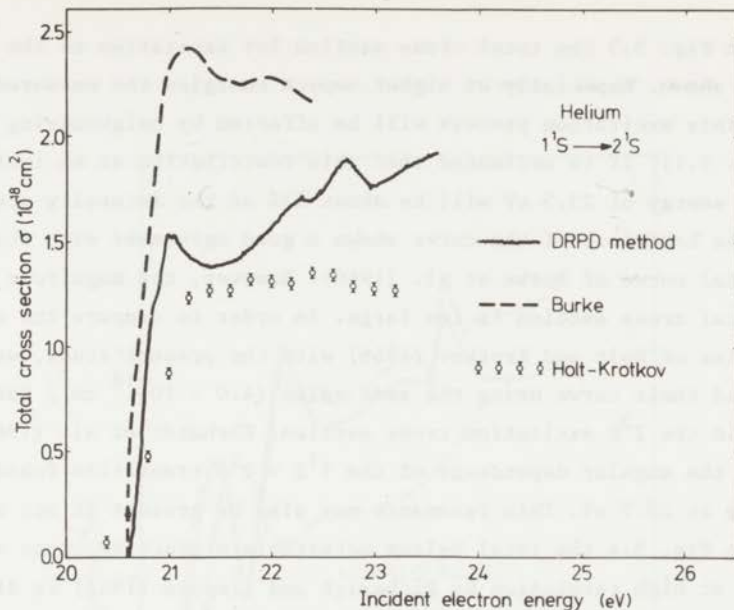
Fig. 5.3 - $1^1S \rightarrow 2^1S$ transition. The total cross section measured with the D.R.P.D. method is compared with the calculated total cross section of Burke et al. (1969) and the metastable production (2^1S) cross section of Holt and Krotkov (1966).

energy loss. The cross sections were normalized using the value 4.0×10^{-18} cm^2 for the 2^2P resonance peak (20.3 eV) in the 2^3S excitation process. This value ($\pm$ 30%) was determined using the T.E. method (Brongersma et al., 1969). Similar values have been found in other studies (Fleming et al., 1964; Maier-Leibnitz, 1935). From close-coupling calculations, Burke et al. (1969) predict a similar energy dependence of the 2^3S transition but overestimate the importance of the 2^2P resonance (Fig. 5.2). We did not observe any structure related to the 2^2S resonance which shows up in differential cross section measurements (Ehrhardt et al., 1968) at 19.9 eV. This is consistent with theory (Burke et al., 1969).

Neglecting the resonance contributions to the $1^1S \rightarrow 2^3S$ transition, the cross section reaches its maximum within 3 eV from the excitation threshold. This feature is characteristic for a singlet-triplet transition.

In Fig. 5.3 the total cross section for excitation to the 2^1S state is shown. Especially at higher impact energies the measured intensity of this excitation process will be affected by neighbouring peaks (see Fig. 5.1). It is estimated that this contribution at an incident electron energy of 23.5 eV will be about 25% of the intensity presented.

The behaviour of the curve shows a good agreement with the theoretical curve of Burke et al. (1969). However, the magnitude of the theoretical cross section is too large. In order to compare the work on metastables of Holt and Krotkov (1966) with the present study, we renormalized their curve using the same value (4.0×10^{-18} cm^2) for the maximum in the 2^3S excitation cross section. Ehrhardt et al. (1968) studying the angular dependence of the $1^1S \rightarrow 2^1S$ transition found a resonance at 20.7 eV. This resonance may also be present in our spectrum.

In Fig. 5.4 the total helium metastable production cross section obtained at high resolution by Pichanick and Simpson (1968) is displayed. This curve can be compared with the sum of the 2^3S and 2^1S D.R.P.D. total cross sections which is also presented. The energy scale of our curve has been calibrated using the 20.34 eV value for the 2^2P resonance. This value was obtained by Pichanick and Simpson (1968). The energy values of the other resonances now agree within 0.03 eV. The intensity of the metastable curve of Pichanick and Simpson has been normalized to our D.R.P.D. curve at 20.3 eV. Nevertheless, differences are found between the curves. These differences can be explained on basis of unequal efficiencies for the different metastables. Dunning et al. (1970) obtained a value of 0.73 ± 0.15 for the $2^1S/2^3S$ ratio in secondary electron ejection efficiency. From curves 1 and 2 (Fig. 5.4) a ratio of 0.85 ± 0.2 can be derived. Differences in the intensities (cf. curves 1 and 2) at higher energies will mainly be due to cascade processes which contribute to the metastable current.

Holt and Krotkov (1966) measured the metastable production cross section essentially consisting of 2^3S and 2^3P contributions (Fig. 5.4). The 2^2P resonance peak in the 2^3S excitation cross section is again used for normalization. In these experiments the 2^3P state has the same detection efficiency as the 2^3S state. This is true because atoms in the 2^3P state will decay to the 2^3S state long before they reach the detector. Therefore an estimate (curve 5 in Fig. 5.4) of the 2^3P total cross section is obtained by subtracting the 2^3S D.R.P.D. curve (Fig. 5.2) from this curve.
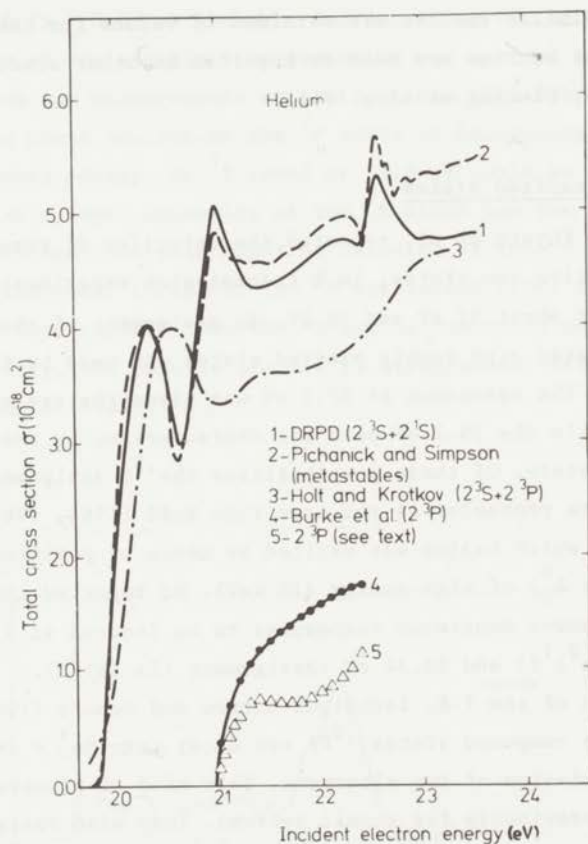
Fig. 5.4 - The sum of the 2^3S and 2^1S total excitation cross sections
obtained by means of the D.R.P.D. technique, curve 1; the
total helium metastable production cross section measured
by Pichanick and Simpson (1968), curve 2. Curves 1 and 2
are adapted to each other at the 2^2P resonance peak at
20.34 eV (see text); the metastable production cross section
from Holt and Krotkov (1966) due to 2^3S and 2^3P states,
curve 3; the calculated total cross section of the 2^3P state
of helium by Burke et al. (1969), curve 4; estimate of
2^3P total cross section obtained by subtracting the 2^3S
total cross section (D.R.P.D. method) from curve 3
$(2^3S + 2^3P)$, curve 5.

For the studied transitions the close-coupling calculations of Burke et al. predict cross sections which are in general too high. It is not likely that this is due to incorrect normalization of the experimental data. Similar results are obtained if values for the $2\,^2P$ resonance cross section are used as reported in other studies (Maier-Leibnitz, 1935; Fleming et al., 1964).

5.1.2 Doubly excited states

In 1965 Kuyatt et al. reported the detection of resonances, transient negative ion states, in a transmission experiment of helium at an energy of about 57 eV and 58 eV. An assignment of these resonances, associated with doubly excited states was made by Fano and Cooper (1965). The resonance at 57.1 eV was given the assignment of $(2s^2\,2p)\,^2P$, while the 58.2 eV peak was characterized by the $(2s\,2p^2)\,^2D$ or $(2s\,2p^2)\,^2S$ state. Of these possibilities the ^2D assignment was shown to be more probable. At the same time Rudd (1964, 1965) performed experiments in which helium was excited by means of positive ion bombardment (H^+ or H_2^+) of high energy (75 keV). He reported the parent states of the above mentioned resonances to be located at 57.82 eV (assignment $(2s^2)\,^1S$) and 58.34 eV (assignment $(2s\,2p)\,^3P$).

By means of the T.E. technique Burrow and Schulz (1969) observed that one of the compound states (^2P) can decay into $He^+ + 2e^-$ by simultaneous emission of two electrons. This kind of process has not been observed previously for atomic systems. They also observed close to threshold the doubly excited states $(2s^2)\,^1S$ and $(2s\,2p)\,^3P$. The measured higher intensity of the ^1S state compared with the intensity of the ^3P state is somewhat surprising. Grissom et al. (1970) also studied helium with the T.E. technique. They measured in the same energy range only one prominent peak at 58.38 eV which is due to the ^3P state. In their spectra a weak shoulder is observed at the energy where the ^1S state should appear.

Using the T.E. method in our apparatus both electrons resulting from excitation and ionization and positive ions are collected. The ions will also be detected as no grids are present to prevent these particles reaching the mantle. As a consequence no information could be obtained with this method.

With the D.R.P.D. technique only electrons are collected.
In Fig. 5.5 D.R.P.D. spectra are presented measured at excess energies
of the electrons of 0.5 eV and 2 eV. In both spectra only one peak is
observed at 58.35 $\pm$ 0.05 eV probably corresponding to the $(2s\ 2p)^3P$
state. Because of low signals time averaging was applied (100 runs -
30 hours). From our measurements we can conclude that near threshold
the excitation cross section of the ^3P state is increasing with
increasing excess energy. No ^1S level at 57.8 eV could be observed.
Due to a probably lower intensity of the ^1S state and the rather low
resolution involved this peak might be obscured by the ^3P state. As we
might assume that near threshold the ^3P excitation cross section will
increase much more rapidly than the ^1S excitation cross section with
increasing energy, our results are not in disagreement with the work of
Burrow and Schulz (1969).
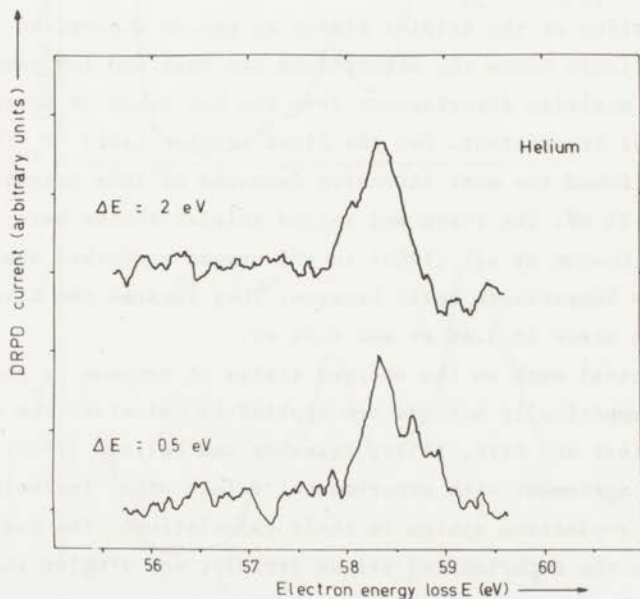
Fig. 5.5 - Excitation spectra of helium measured at ΔE = 0.5 eV and
2 eV. One peak can easily be distinguished located at
58.35 eV (^3P). For the production of these spectra time
averaging was applied.

5.2 BENZENE

5.2.1 Introduction

The excited electronic states of benzene have been the subject of many theoretical and experimental studies. Experimental data prior to 1965 have been summarized by Herzberg (1966). The excitation energies of the lowest three singlet levels $^1B_{2u}$, $^1B_{1u}$ and $^1E_{1u}$ are well known to be 4.98 eV, 6.26 eV and 6.96 eV. These values correspond to maxima in the absorption curves obtained with photon impact (Wilkinson, 1956). With electron impact spectroscopy the singlet states are observed at nearly the same energies (Lassettre et al., 1968; Doering, 1969). The required energies for excitation to the first three (lowest) triplet levels of benzene $^3B_{1u}$, $^3E_{1u}$ and $^3B_{2u}$ are 3.95 eV, 4.75 eV and 5.60 eV.

Observation of the triplet states by photon absorption is extremely difficult since the absorptions are weak and low temperatures are needed to minimize interference from the hot bands of nearby singlet-singlet transitions. For the first triplet level $^3B_{1u}$ Burland et al. (1970) found the most intensive features of this transition at 3.71 eV and 3.82 eV. The first and second triplet states have been in-vestigated by Colson et al. (1965) in the oxygen perturbed absorption spectra of low temperature solid benzene. They located the first and second triplet state at 3.66 eV and 4.56 eV.

Theoretical work on the excited states of benzene is abundant. Usually semi-empirically methods are applied to calculate the excitation energies (Pariser and Parr, 1952). Visscher and Falicov (1970) obtained a rather good agreement with experimental values after inclusion of all states of the π-electron system in their calculations. The average deviation from the experimental values (triplet and singlet states) is about 0.2 eV.

Very recently ab-initio calculations (all electrons) on the excited states of benzene were reported by Peyerimhoff et al. (1970). Large differences are found between their calculated values and the ex-perimental data.
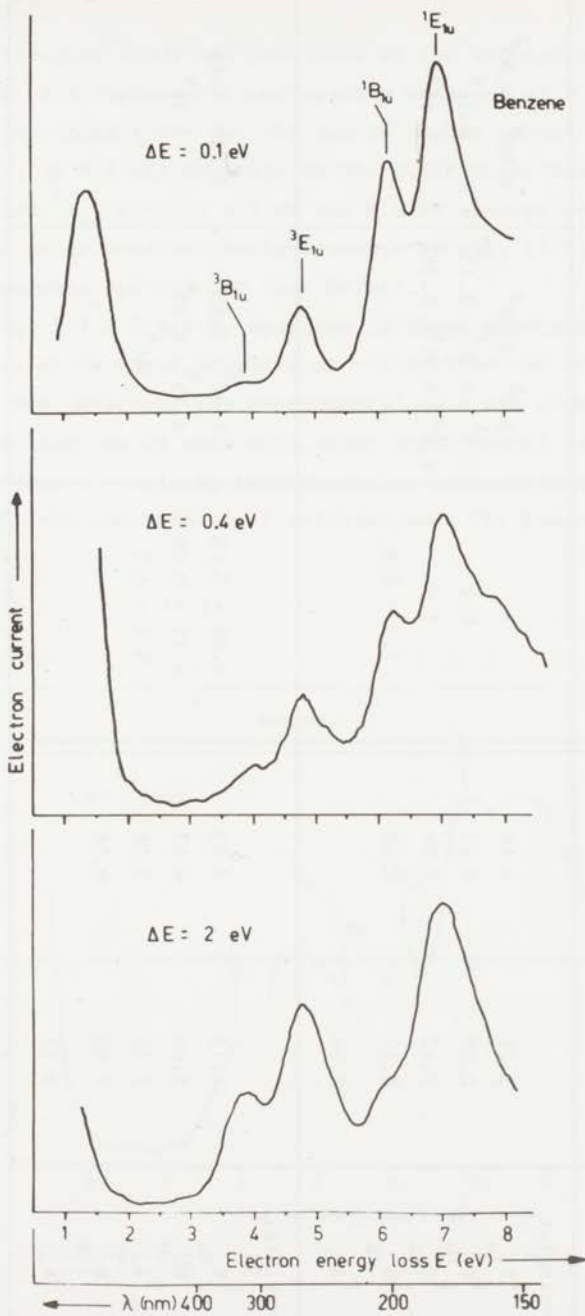
<u>Fig. 5.6</u> - Excitation spectra of benzene measured with the T.E. technique (ΔE = 0.1 eV) and with the D.R.P.D. method (ΔE = 0.4 eV; ΔE = 2 eV).

TABLE 5.1   Benzene

Excitation energies (eV)

Transitions	Calculated values		Experimental data		
	Ab-initio[a] calculations	This research*	Electron impact		Photon impact
			This research**	Other studies	
Singlet-singlet					
$\pi \rightarrow \pi^{*}$ $^{1}B_{2u}$	5.21	4.66		5.0[b] 4.90[c]	4.98[d] 4.90[e]
$^{1}B_{1u}$	8.09	6.21	6.2	6.2[b] 6.20[c] 6.15[f]	6.26[d]
$^{1}E_{1u}$	9.42	7.04	7.0	6.9[b] 6.95[c] 6.96[f]	6.96[d]
$^{1}E_{2g}$	8.57	7.45	7.7 - 7.9		
$\sigma \rightarrow \pi^{*}$ $^{1}A_{2u}$	10.06				
Singlet-triplet					
$\pi \rightarrow \pi^{*}$ $^{3}B_{1u}$	4.13	3.93	3.88 $\pm$ 0.05	3.95[b] 3.85[f]	3.82[g] 3.66[h]
$^{3}E_{1u}$	5.20	4.67	4.77 $\pm$ 0.05	4.75[b] 4.75[f]	4.56[h]
$^{3}B_{2u}$	7.35	5.76	5.3 - 5.5	5.60[b]	
$^{3}E_{2g}$	7.60	6.56			
$\sigma \rightarrow \pi^{*}$ $^{3}A_{2u}$	9.72				

*   Semi-empirical calculations (chapter III) in which all configurations of the π-electrons are included. The resonance integral β was given the value of -2.60 eV. The repulsion integrals were used as evaluated in chapter III.

**   Collected data from T.E.- and D.R.P.D. measurements.

a = Peyerimhoff et al. (1970); b = Doering (1969); c = Lassettre et al. (1968); d = Wilkinson (1956); e = Callomon et al. (1966); f = Hubin-Franskin et al. (1970). The transition at 4.75 eV has been reassigned; g = Burland et al. (1965); h = Colson et al. (1970).

5.2.2 Results

An extensive study has been made of the excitation spectrum of benzene. Fig. 5.6 represents some spectra measured with the T.E. technique near threshold ($\Delta E = 0.1$ eV) and at higher excess energies ($\Delta E = 0.4$ eV; $\Delta E = 2$ eV) by means of the D.R.P.D. method. The assignments $^1B_{2u}$ and $^1B_{1u}$ for the 4.8 eV and 6.2 eV absorptions as has been suggested in other studies (Hubin-Franskin et al., 1970; Compton et al., 1968) are somewhat speculative (see below).

In Fig. 5.7 a D.R.P.D. spectrum is shown measured at an excess energy of 0.9 eV. A vague shoulder at ~ 5.4 eV and an additional peak at ~ 7.8 eV are observed. The experimental data are summarized in Table 5.1. A comparison can be made with other experimental data and with theoretical values resulting from ab-initio calculations (Peyerimhoff et al., 1970) and semi-empirical calculations. The semi-empirical
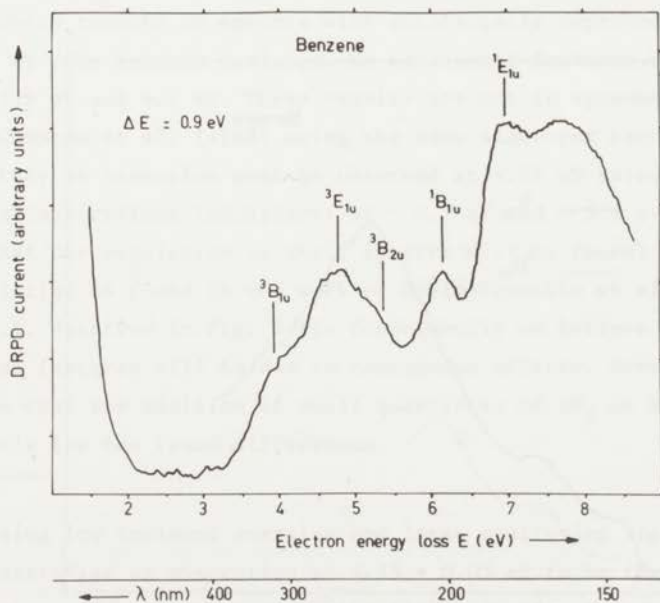
Fig. 5.7 - D.R.P.D. spectrum of benzene measured at an excess energy of 0.9 eV. A shoulder can be observed at ~ 5.4 eV probably due to the excitation of the third triplet level of benzene ($^3B_{2u}$).

calculations were performed with inclusion of all states of the
π-electron system using nearly the same parametrization as applied by
Visscher and Falicov (1970). An average deviation of 0.1 eV is obtained
compared with the experimental excitation energies.

We will now discuss the absorptions which show up in our spectra
(Fig. 5.6 and Fig. 5.7) more extensively.

<u>3.88 eV absorption</u>

This absorption peaking at 3.88 $\pm$ 0.05 eV is characterized as a
transition to the $^3B_{1u}$ state. This assignment which is also given in
many other studies (Brongersma, 1968; Doering, 1969; Hubin-Franskin et
al., 1970) seems to be correct beyond any doubt. Additional support for
this assignment can be obtained by scanning the energy dependence of
the total cross section by means of the D.R.P.D. method. A plot of this
dependence shows a maximum at $\Delta E \sim 2$ eV (Fig. 5.8). The first part of
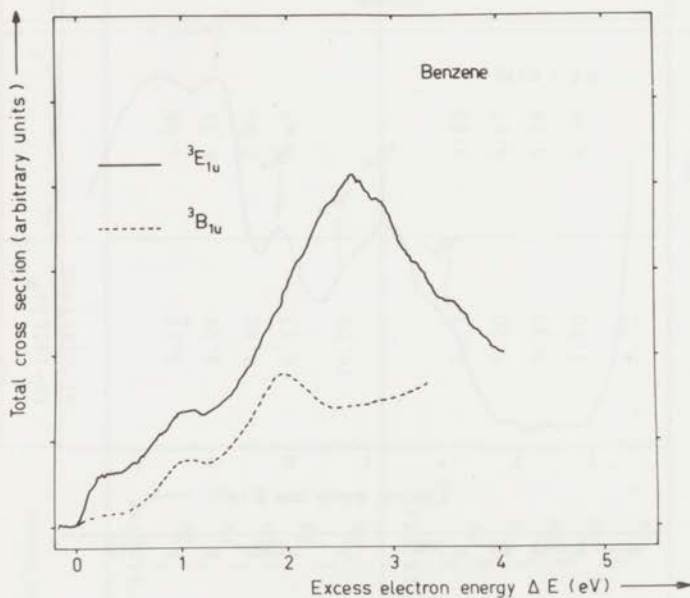
Fig. 5.8 - The behaviour of the total cross sections of the first
triplet state $^3B_{1u}$ at 3.88 eV (dotted line) and the second
peak at 4.77 eV   (probably $^3E_{1u}$) against increasing excess
energy.

the curve shows a similar behaviour as the curve for the 4.8 eV absorp-
tion. This is due to the large natural absorption widths and the low
resolution of the apparatus which cause a large overlap of the two ab-
sorptions (e.g. see Fig. 5.7). The contribution of the elastically
scattered electrons, peaking around zero energy, to the intensity of
the 3.9 eV absorption will grow in importance with increasing excess
energy ΔE. This explains the increase in intensity of the last part of
the dotted curve (Fig. 5.8).

4.77 eV absorption

In our spectra an intensive absorption is observed at 4.77 $\pm$
0.05 eV. Using the so-called scavenger technique (SF_6) threshold excit-
ation spectra of benzene were obtained by Hubin-Franskin et al. (1970)
finding a similar peak at 4.75 eV. They characterized this absorption
as due to the first singlet state $^1B_{2u}$.

Hubin-Franskin et al. also applied deconvolution of the measured
spectra which results in spectra with artificially improved resolution.
The 4.75 eV peak remains isolated. No additional features were found
between 3.9 eV and 6.2 eV. These results are not in agreement with the
work of Compton et al. (1968) using the same scavenger technique. In the
latter study an intensive peak is observed at 4.88 eV surrounded by two
additional absorptions (shoulders) at $\sim$ 4.7 eV and $\sim$ 5.4 eV. It is not
likely that the resolution in their spectra will be (much) better than
the resolution as found in the work of Hubin-Franskin et al. or in this
study (T.E. spectrum in Fig. 5.6). Consequently we believe that their
additional features will be due to contageous effects. Brongersma (1968)
suggested that the addition of small quantities of SF_6 or HCl might be
responsible for the found differences.

Using low incident energies and large scattering angles Doering
(1969) identified an absorption at 4.75 $\pm$ 0.05 eV to be the second
triplet state ($^3E_{1u}$). He measured the first singlet state at 5.0 eV
which is in good agreement with light absorption data (Table 5.1).
Based on maximum agreement with these data we find an assignment of a
triplet state $^3E_{1u}$ to be more justified than an assignment of a singlet
state $^1B_{2u}$ for our 4.77 eV absorption. This assignment is supported by

studying the energy dependence of the total cross section of this tran-
sition (Fig. 5.8). The observed behaviour which consists of an increase
up to $\Delta E \sim 2.6$ eV followed by a sharp decrease, is characteristic for a
triplet excitation. Two peculiar shapes are found in this curve at
~ 0.4 eV and ~ 1.2 eV. These features might be explained by shape
resonances[*] (excited negative ion states, $(Bz^-)^*$ at ~ 5.2 eV and
~ 6.0 eV).

In our spectra no sign is found of the first singlet state $^1B_{2u}$
located at 5.0 eV (Doering, 1969). However, our resolution does not
permit an observation of this state, with probably weak intensity, due
to the small energy separation with the second triplet state at 4.77 eV.

5.3 - 5.5 eV absorption

Doering (1969) observed the third triplet state of benzene at
5.6 eV. The triplet state assignment was based on the relative inten-
sity of this transition compared with other transitions at various
scattering angles. Only near an excess energy of 0.9 eV (see Fig. 5.7)
we can observe a weak shoulder with a probable maximum in the range of
5.3 - 5.5 eV. This is probably the same transition as found by Doering
at 5.6 eV.

6.2 eV absorption

Lassettre et al. (1968) have noticed a change in the relative
intensities of the vibrational bands of the second singlet transition
at 6.2 eV with varying scattering angles (angles less than 8°; incident
energy 50 eV). They concluded that two electronic states are involved
which are located at 6.20 eV ($^1B_{1u}$) and at 6.31 eV.

Doering (1969) has shown that with incident electron energies
of 13.6 eV and 20 eV the ratio of the intensities of the 6.2 eV peak
and the 6.95 eV (optically allowed) third singlet transition is constant
over a wide range of scattering angles ($9^o - 80^o$). Moreover the ratio
is also the same for the two different energies. The angular behaviour
and energy dependence of the ratio give evidence that the nature of the

---

[*] An explanation based on a defect of the experimental procedure should
also be considered. However, the excellent agreement of the measured
excitation functions of helium (2^3S and 2^1S - section (5.1)) with
other data does not support such a view.

6.2 eV transition is also optically allowed like the third singlet state $^1E_{1u}$ at 6.95 eV. This implies an analogy with photon impact experiments despite the low incident energy of the electrons.

Nevertheless we believe that the change in the relative intensities of the vibrational bands with varying angle as observed by Lassettre et al. (1968) might be induced by an optically forbidden process, the direct excitation of the $^1B_{1u}$ state (octupole transition)[*].

In our spectra we observe a strange behaviour for the ratio of the 6.2 eV peak and the 7.0 eV peak if we increase the energy. At threshold the two peaks have comparable intensity (see also Hubin-Franskin, 1970) whereas with increasing excess energy a decrease of the intensity of the 6.2 eV absorption is observed. The high intensity near threshold might be explained by a resonance in the excitation function of the 6.2 eV transition (Knoop et al., 1970). Consequently an excited state of the negative ion of benzene might lie close to 6.2 eV. This nicely agrees with the value of ~ 6.0 eV derived from the resonance at ~ 1.2 eV observed in the excitation function of the $^3E_{1u}$ state (4.77 eV). The behaviour of the 6.2 eV absorption might also be explained by direct excitation to the $^1B_{1u}$ state. Another explanation based on the existence of a triplet state at 6.2 eV or very close to that value can not be excluded. Then the $^3E_{2g}$ level calculated at 6.56 eV (Table 5.1) will be a principal candidate for assignment.

7.0 eV absorption

The overall behaviour of the total cross section of the 7.0 eV absorption against excess energy (0 - 4 eV) shows a continuous increase of intensity. This behaviour is in agreement with what we would expect for an optically allowed transition.

7.7 - 7.9 eV absorption

At increasing excess energies between 0.4 eV and 1.2 eV we observe a sudden rise and decrease of one or more transitions near 7.8 eV (Fig. 5.6 and 5.7). Triplet character for the transition(s) or resonances in the excitation functions of the transition(s) involved might explain this behaviour.

[*] J.A. v.d. Hart-v.d. Hoek, private communication.

5.2.3 Summary

From our study we must conclude that in the case of benzene singlet-triplet excitation processes are very intensive near threshold. The 4.8 eV peak firstly been identified as the first singlet transition $^1B_{2u}$ in other studies, turns out to be due to excitation of the second triplet state $^3E_{1u}$. The third triplet state $^3B_{2u}$ is possibly detected as a vague shoulder at ~ 5.4 eV. Thus we find a sequence of relative intensities (total cross sections) near threshold for the first three triplet states

$$I(^3E_{1u}) > I(^3B_{1u}) \gg I(^3B_{2u})$$

This relation has already been predicted by Matsuzawa (1969) using the Ochkur and Ochkur-Rudge approximations for incident electron energies of 10 - 100 eV. Despite the approximations involved in his calculations the resulting qualitative picture fits our experimental outcome.

From the excitation function of the second triplet state $^3E_{1u}$ we found evidence of two excited negative ion states of benzene at energies of ~ 5.2 eV and ~ 6.0 eV. The behaviour of the excitation function of the 6.2 eV absorption near threshold suggests a negative ion state at ~ 6.2 eV.

C H A P T E R   V I

W A T E R   A N D   R E L A T E D   C O M P O U N D S

6.1   WATER (H_2O)

6.1.1   Introduction

        In recent years a good deal of attention has been given to the
excitation of water vapour by electron impact. At small scattering
angle and high electron energy optically allowed transitions are obser-
ved (Skerbele et al., 1968). Studies at low electron energy, including
excitation near threshold, reveal additional absorptions (Trajmar et
al., 1971; Knoop et al., 1972; Schulz, 1960; Compton et al., 1968), of
which most of them were characterized as triplet states. It is well
known that the low energy region is very favourable for triplet excit-
ation.

        Calculations of the electronic ground state of water are abun-
dant (e.g. Ellison and Shull, 1955). However, up to now the excited
states of water have not met the interest they deserve. A large discrep-
ancy exists between the available theoretical values and the experi-
mentally determined excitation energies of the low lying excited states.

        The formation about triplet states in water is important for
the radiation chemistry of aqueous solutions.

6.1.2   Molecular Orbital description of water

        Fig. 6.1 presents a schematic picture of the molecular orbitals
in water and of their symmetry (Herzberg, 1966). For convenience the
M.O. energies as calculated by Ellison and Shull (1955) are given be-
tween parentheses. These values are in fairly good agreement with the

results of Al-Joboury and Turner (1967) as obtained from photoelectron spectroscopy.

The sequence of the unoccupied molecular orbitals is still somewhat speculative. Up to now it has been assumed that the $2b_2$ orbital is lying higher in energy than the $4a_1$ orbital. This means that excitation of an electron from the lone pair orbital $1b_1$ to the $2b_2$ orbital

$$(1a_1)^2(2a_1)^2(1b_2)^2(3a_1)^2(1b_1)^2 \rightarrow (1a_1)^2(2a_1)^2(1b_2)^2(3a_1)^2(1b_1)(2b_2)$$

$${}^1A_1 \qquad\qquad {}^{1,3}A_2$$
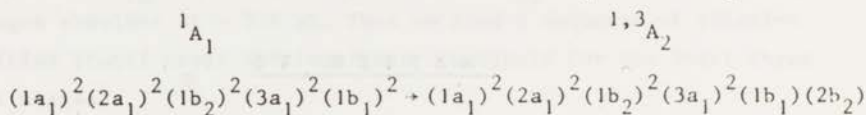
will require more energy than the electron jump $1b_1 \rightarrow 4a_1 ({}^1A_1 , {}^{1,3}B_1)$.

M.O. - scheme of H_2O
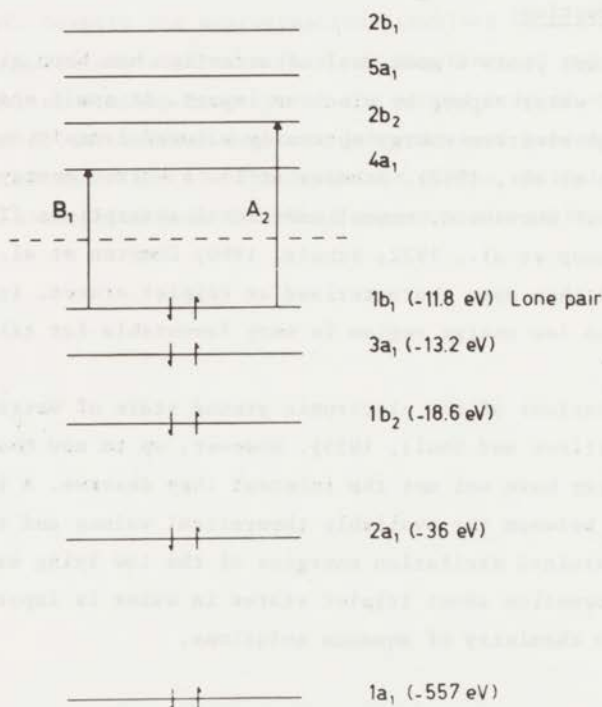
Fig. 6.1 - Schematic picture of the occupied and virtual molecular orbitals of H_2O. The M.O. energies of the occupied levels as calculated by Ellison and Shull (1955) are given between parentheses. The lowest lying transitions are also indicated (B_1 and A_2).

$^{1,3}A_1$ excitations can be generated in the following ways

$$1b_1 \rightarrow 2b_1$$
$$3a_1 \rightarrow 4a_1$$

In Table 6.1 some theoretical data of the lowest lying excited states of water ($^{1,3}B_1$, $^{1,3}A_2$ and $^{1,3}A_1$) are compared with experimental data.

Claydon et al. (1971) have studied the energies and potential surfaces of the first eight excited states of water using a semiempirical approach (I.N.D.O.). Though the errors in this kind of calculation might be quite large the authors claim to have achieved considerable success in the case of CO_2.

TABLE 6.1

Summary of theoretical data of the lower lying excited states in water.

	Energies in eV				
	Claydon (1971) I.N.D.O.	Hunt (1969) I.V.O.	Miller (1969)	Horsley (1969)	Experimental data
$^1B_1$	7.43	8.53	6.5	7.9	7.49[a] 7.44[b]
$^3B_1$	6.20	7.88	6.1	7.3	7.20 ± 0.05[c]
$\Delta_{S-T}(B_1)^*$	1.23	0.65	0.38	0.6	0.27
$^1A_2$	8.03	10.35			
$^3A_2$	7.49	9.98			(4.5[c,d] ?)
$\Delta_{S-T}(A_2)$	0.54	0.37			
$^1A_1^{**}$	10.85	10.75		9.95	9.67[d] 9.75[a]
$^3A_1$	8.67	9.82		9.00	(9.1[c] ?)
$\Delta_{S-T}(A_1)$	2.18	0.93		0.95	

*   Singlet-triplet separation energy
** $(3a_1 \rightarrow 4a_1)$

a   Watanabe (1953)   c   This work
b   Skerbele et al. (1968)   d   Trajmar et al. (1971).

Hunt et al. (1969) evaluated the excitation energies of H_2O using a S.C.F. method with certain restrictions. In the so-called I.V.O. (Improved Virtual Orbital) method the self Coulomb and exchange terms are removed in the Hartree Fock Hamiltonian. Moreover the core was assumed to be "frozen".

Miller et al. (1969) calculated the excitation energies for the $^1B_1$ and $^3B_1$ states using a fairly large Gaussian basis set. The singlet-triplet separation energy $\Delta_{S-T}(B_1)$ was found to be rather small (0.38 eV).

Horsley and Fink (1969) examined the potential surfaces of the $^1A_1$, $^3A_1$, $^1B_1$ and $^3B_1$ excited states. S.C.F. calculations on open shell configurations were carried out using Nesbet's symmetry and equivalence restriction method. Contribution of the 3s orbital in the basis results in a rather good agreement with experimental data (see Table 6.1).
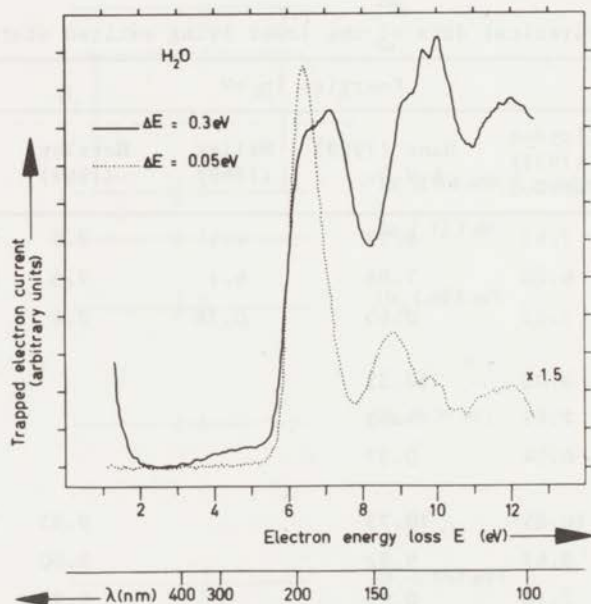
Fig. 6.2 – Excitation spectra of H_2O measured with the T.E. method at ΔE=0.3 eV and 0.05 eV (dotted line). In the 0.3 eV spectrum the 7.2 eV peak (triplet transition) is clearly resolved from the 6.5 eV peak (H^- ions, see Schulz, 1960). Using the T.E. method both electrons and negative ions are detected.

From these calculations no definite proof can be obtained that the sequence of the two lowest lying unoccupied orbitals ($4a_1$ and $2b_2$) will be as suggested by Herzberg (1966) (Fig. 6.1). Consequently it does not seem likely that the A_2 excitations will require less energy than the B_1 excitations.

More refined calculations on the A_2 system than performed by Claydon et al. (1971) or Hunt et al. (1969) are needed to settle this problem.

6.1.3 Experimental results

In our spectra (Fig. 6.2 and 6.3) the dominant transition is observed at 7.2 eV. This agrees with the 7.3 eV value found by Schulz (1960) using the T.E. method. However, it is known from electron impact studies at higher energy (Skerbele et al., 1968; Trajmar et al., 1971) and photon impact work (Watanabe et al., 1953) that the maximum

TABLE 6.2

Water vapour (energies in eV)

Electron impact		Photon[d] impact	Assignment
This research[*]	Other work		
4.4 – 4.6	4.5[a]		see text
	~ 6.2[b]		$^1A_2$ (?)
6.5	6.5[c]		H^- peak
7.2	7.3[c]		triplet state $^3B_1$ or $^3A_2$
	7.5[a] 7.44[b]	7.49	$^1B_1$
8.8	8.8[c]		H^- peak
9.1	9.2[c]		$^1A_2$ (?) or triplet state
9.7	9.67[a] 9.70[b]	9.75	$^1A_1$ or triplet state
	9.81[a]		
10.0	10.1[c] 10.00[a,b]	9.99	$^1B_1$ or triplet state
	10.17[a] 10.14[b]	10.15	$^1A_1$

[*] Collected data from T.E.- and D.R.P.D. measurements.

[a] Trajmar et al. (1971)   [c] Schulz (1960)

[b] Skerbele et al. (1968)   [d] Watanabe et al. (1953).
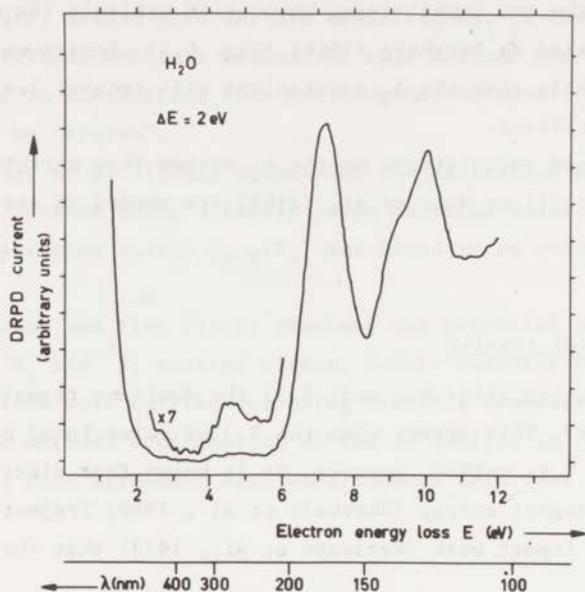
Fig. 6.3 - Excitation spectrum of H_2O measured with the D.R.P.D. method at an excess energy of the electrons of 2 eV.

of the absorption band of the lowest singlet state ($^1B_1$) lies in the range 7.44-7.49 eV (Table 6.2). It is unlikely that the difference between these values and our value of 7.2 eV is due to an error in energy calibration. The identification of the 7.2 eV transition as a triplet state ($^3A_2$ or $^3B_1$) seems more reasonable.

Up to now it has been assumed that the $^1B_1$ state (7.5 eV) will be the lowest excited singlet level. For this reason any excited state below this level has to be a triplet state.

Additional support for the assignment was obtained from the energy dependence of the total cross section studied with the D.R.P.D. method. A plot of this dependence (Fig. 6.4) shows a maximum at ~ 2 eV above threshold followed by a continuous decrease with increasing energy. Such a behaviour is characteristic for a triplet excitation process (see for instance Aarts et al., 1969; Smit et al., 1963).
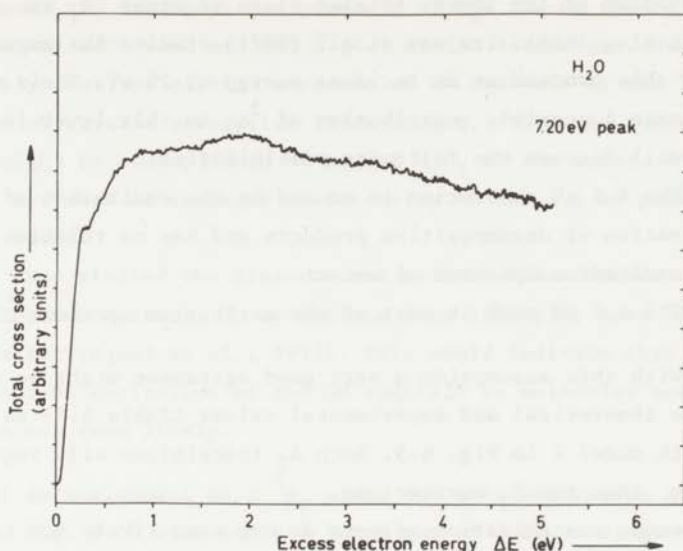
Fig. 6.4 - The behaviour of the total cross section of the 7.2 eV tran-
sition of H_2O with increasing excess electron energy (ΔE).

The rather rapid decrease could explain why Trajmar et al. (1971) did
not observe this process at an incident energy of 20 eV. Due to the
large natural width, low resolution of our apparatus and apparently
a relatively weak intensity of the lowest singlet transition, no peak
or shoulder could be observed at 7.5 eV. This is not surprising, be-
cause it is known that optically allowed singlet-singlet transitions
sometimes appear very weakly in threshold excitation spectra (Brongers-
ma and Oosterhoff, 1969).

An assignment of $^3B_1$ for this 7.2 eV absorption seems very likely.
Then the singlet-triplet separation energy $\Delta_{S-T}(B_1)$ of 0.27 eV is
in good agreement with most of the calculated values (Table 6.1).

A weak and broad peak at 4.4-4.6 eV is clearly observed in our
spectra (Fig. 6.2 and 6.3). This absorption cannot be due to the forma-
tion of negative ions, because such contributions are eliminated in the
D.R.P.D. method (see 4.4.5). In other threshold excitation experiments
a similar peak was observed (Schulz, 1960) to which a possible

characterization of the lowest triplet state of water $^3B_1$ was attributed (Compton et al., 1968). Trajmar et al. (1971) studied the angular behaviour of this process at an incident energy of 20 eV. Their measurements indicate a possible contribution of $^3A_2$ to this level (4.5 eV).

We will discuss the following possibilities:

i   The 4.5 eV absorption is caused by the excitation of contamination or decomposition products and has no relation with the excitation spectrum of water.

ii The 4.5 eV peak is part of the excitation spectrum of water.

i) With this assumption a very good agreement might be obtained between the theoretical and experimental values (Table 6.1) as is illustrated with model I in Fig. 6.5. Both A_2 transitions will require more energy than the B_1 excitations.

However, contamination effects do not seem likely but cannot be totally excluded. It can easily be checked from experimental data that possible contaminants like N_2, O_2 or CO do not have any excitation levels around 4.5 eV.

Assignments of the B_1 and A_2 transitions in H_2O
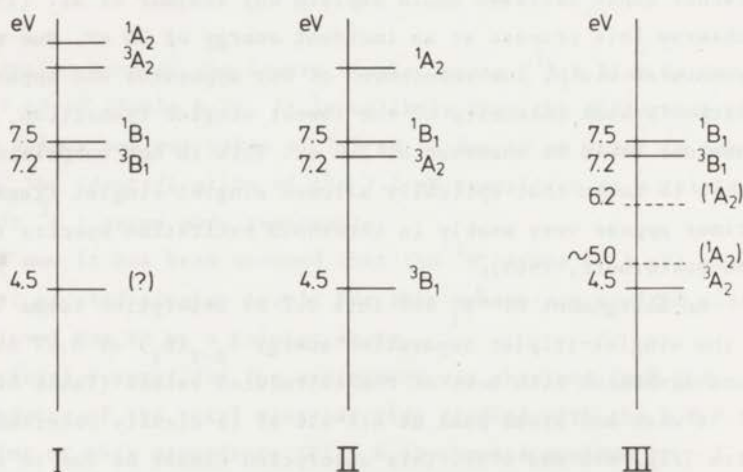
Fig. 6.5 - Possible models to explain the excitation spectrum of water for the B_1 and A_2 transitions.

One of the decomposition products of H_2O the OH radical is known to show an emission band at 3060 Å (4.1 eV) in discharges. However, it seems likely that the partial pressure of OH radicals is too low to furnish an observable absorption (Oldenburger, 1938). An increase of OH radicals might be accomplished by adding H_2O_2 to the water. A 10% mixture does not show an increase in intensity of the 4.5 eV peak compared with pure water.

We have studied the pressure and primary beam dependence of the trapped electron current. No deviations from linearity nave been observed (see also Trajmar et al., 1971). This would indicate that an explanation based on excitation of the OH radicals or molecular complexes of water does not seem likely.

ii) An assignment as a $^3B_1$ state for this absorption at 4.5 eV (model II, Fig. 6.5) will imply a large gap of 3 eV as singlet-triplet separation energy. This seems rather improbable but not impossible.

An alternative assignment of $^3A_2$ state for this absorption will be in agreement with the work of Trajmar et al. (1971). The weak absorption observed by Skerbele et al. (1968) at 6.2 eV might be characterized by the $^1A_2$ state (model III, Fig. 6.5).

In formaldehyde the singlet-triplet separation energy of the $n \to \pi^*$ transition is found to be small (0.4 eV – Henderson et al., 1965). From comparison of the electronic structure of this molecule and water we may expect small singlet-triplet separation energies (a few tenths of an eV) for the A_2 transition. Therefore the broad absorption at ~ 4.5 eV in water might consist of a triplet and a singlet transition of the same symmetry (A_2).

6.2   DEUTERATED WATER (D_2O)

The isotope effect is expected to change the potential energy function and configuration of the molecule in negligible amounts. Indeed the spectra look very similar with those obtained with H_2O. A small improvement of resolution is observed apparently due to a smaller natural width of the excitation peaks. This is easy to understand on basis of smaller vibrational spacings in the potential energy functions.

The broad absorption at ~ 4.5 eV is observed with the same relatively weak intensity as in H_2O.

6.3 HYDROGEN SULPHIDE (H₂S)

6.3.1 Introduction

In some respects the excitation spectra of H_2O and H_2S will show a large resemblance. The calculations of Moccia (1964) and Rauk et al. (1967) on the ground state of H_2S support this view. With regard to symmetry aspects the highest occupied molecular orbitals are quite similar to H_2O.
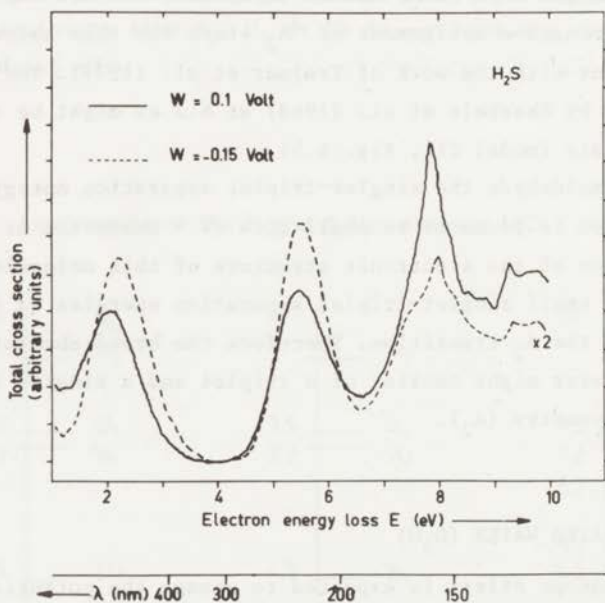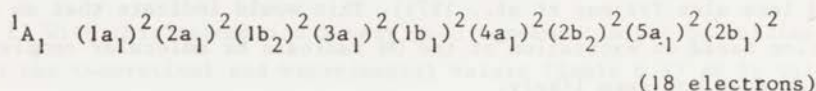
The ground state is described as

$$^1A_1 \quad (1a_1)^2(2a_1)^2(1b_2)^2(3a_1)^2(1b_1)^2(4a_1)^2(2b_2)^2(5a_1)^2(2b_1)^2$$

(18 electrons)

Fig. 6.6 - Spectra of H_2S measured with the T.E. technique at W=0.1 Volt (ΔE=0.1 eV) and at a negative mantle potential W= - 0.15 Volt. For negative mantle potentials only negative ions are measured (see also section 6.3.2).
At W=0.1 Volt (ΔE=0.1 eV) excitation peaks will appear on top of the negative ion peaks. Using the T.E. technique (W > 0 Volt) both electrons and negative ions are measured.

while for H_2O the ground state looks like

$$^1A_1 \quad (1a_1)^2(2a_1)^2(1b_2)^2(3a_1)^2(1b_1)^2 \qquad\qquad (10 \text{ electrons})$$
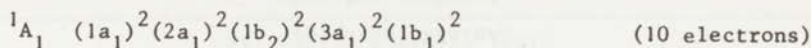
In analogy with water the lowest optically allowed state $^1B_1$ will result from excitation of a lone pair electron $(2b_1 \rightarrow 6a_1)$ as already suggested by Mulliken in 1935. Photoelectron spectroscopy (Al-Joboury et al., 1964) gave evidence that the highest molecular orbital (-10.42 eV) has a non-bonding character. Thus the lowest lying excited states in H_2S will be formed by excitation of an electron from the lone pair orbital.

Recently Hillier et al. (1970) performed ab-initio calculations on the excited singlet states of H_2S. They calculated the $^1B_1$ state at higher energy than the $^1A_2$ state.

6.3.2 Dissociative processes

Negative ion formation resulting from dissociative processes as induced by electron impact can easily be measured by using the T.E. technique with a negative mantle potential. Then only negative ions will reach the collector. The results obtained in this way are shown in Fig. 6.6 and summarized in Table 6.3. The energy axis of the spectrum presented in Fig. 6.6 (dotted line) is corrected for the shift due to the negative mantle potential.

Large differences are found between the experimental data of Jäger et al. (1966) and our values (Table 6.3). In our work three peaks are of comparable intensity 2.2 eV, 5.5 eV and 8.0 eV (see Fig. 6.6). This is in contrast with the work of Jäger et al., where only one intensive peak at 2.27 eV is observed. Moreover three additional peaks are observed in our work.

A tentative explanation of the differences might be found due to recombination or decomposition processes taking place during the time of flight of the negative ion before detection. This time is relatively large in the apparatus of Jäger due to mass analysis of the products. In our system the negative ion will be detected at the cylindrical mantle within a time which is less than 10^{-6} sec.

It is hard to evaluate whether angular dependent selection of the emitted ions will be present in the apparatus of Jäger thus possibly limiting the number and nature of the detected ions.

TABLE 6.3

Hydrogen sulphide

Dissociative processes involving negative ion formation induced by
electron impact (energies in eV)

This research	Other work	Formed products[a]
2.2	2.27 (234)[a] 2.2[b]	SH^- + H
	2.67 (3)[a]	S^- + H_2
5.5	5.9 (4)[a]	S^- + H_2
7.6		
8.0		
8.3		
9.2 - 9.8	9.2 (5)[a]	S^- + 2H

[a] Jäger et al. (1966); The relative intensities are presented between
parentheses.

[b] Fayard et al. (1971).

6.3.3 Excitation energies

In Fig. 6.6 a T.E. spectrum is shown measured at $\Delta E=0.1$ eV (W=
0.1 Volt). On top of the negative ion peaks (section 6.3.2) absorp-
tions due to excitation processes of H_2S can be observed.

A remarkable similarity is found between the T.E.- and the
D.R.P.D. spectra measured at the same excess energy of $\Delta E=0.3$ eV (Fig.
6.7). As we know with the D.R.P.D. technique only electrons are detected.

In the D.R.P.D. spectrum, the 1.8-1.9 eV peak which shifts to
lower energy with increasing excess energy is probably due to the for-
mation of a transient negative ion state (H_2S^-):

$$e^- \quad + \quad H_2S \rightarrow (H_2S)^- \quad \rightarrow \quad H_2S^* \quad + \quad e^-$$

(E + ΔE)   vibrationally   (ΔE)
                                                    excited (E)
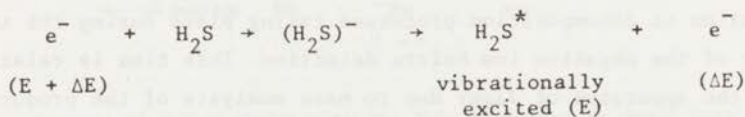
As the formation energy of this negative ion will hardly depend
on the incident energy of the electron E + ΔE the electron energy loss
E will decrease if we increase the excess energy of the detected elec-
tron ΔE (Schulz, 1959).

TABLE 6.4

Hydrogen sulphide

Excitation energies (eV)		
Electron impact This research	Photon impact[a,b]	Assignment
1.8 - 1.9		transient negative ion state
5.8		triplet state
	6.32	$^1B_1$
	7.85	
7.9	8.03	triplet or singlet state
	8.18	
8.5	Rydberg	triplet
8.8		or
9.3	states	singlet states

[a] Price (1936)

[b] Watanabe et al. (1964)

An intensive absorption peaking at 5.8 eV is found in the D.R.P.D. spectra. This process is obscured in the T.E. spectra by the 5.5 eV peak resulting from negative ion capture.

From photon impact studies (Price, 1936; Watanabe et al., 1964) the maximum of the optically allowed singlet level ($^1B_1$) is observed at 6.32 eV (Table 6.4).
Similar to water the difference between these values (0.5 eV) is not likely being due to an error in energy calibration. The assignment of a triplet state for the 5.8 eV absorption seems reasonable considering the analogy with the water spectra. Additional support for the triplet assignment is obtained from the energy dependence of the total cross section studied with the D.R.P.D. method. A plot of this dependence (Fig. 6.8) shows a maximum at 1.4 eV followed by a steep descent and then a slow decrease. The slow decrease might be due to an increasing contribution of the neighbouring singlet level $^1B_1$ (6.32 eV) with increasing excess energy. The peculiar shape of the first part of the curve (Fig. 6.8) might be explained in the following ways:
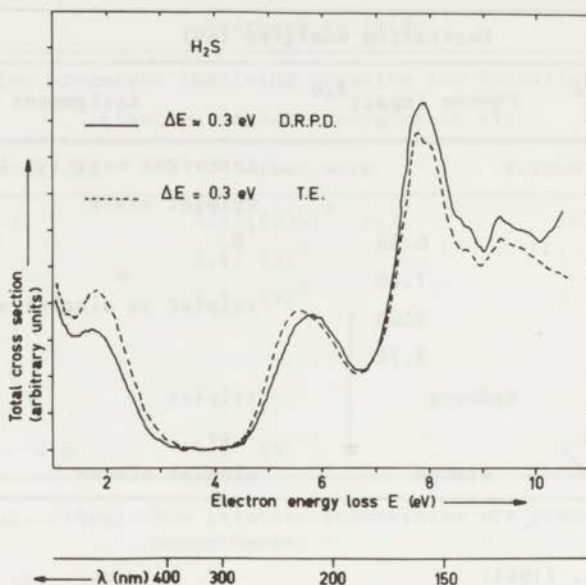
Fig. 6.7 - Excitation spectra of H_2S measured with the T.E. method
(dotted line) and with the D.R.P.D. method at an excess
energy $\Delta E=0.3$ eV. The relative intensities of the curves are
arbitrary.
Despite the fact that with the D.R.P.D. technique no nega-
tive ions are measured the spectra look very similar (see
text).

i   Occurrence(s) of a shape resonance (excited negative ion
    state, $(H_2S^-)^*$) at 0.8 eV and/or at 1.4 eV excess energy.

ii Nearby lying obscured excited state (at possibly lower ener-
    gy) which gives a large contribution of intensity up to 0.8
    eV excess energy.

Neglecting the possible resonant process at 1.4 eV excess energy
the cross section reaches its maximum within 3 eV from the excitation
threshold. The slow decrease of the curve is not in contradiction with
a triplet assignment (see helium 2^3S, chapter 5).

Considering the analogy of H_2S with H_2O especially for the 7.2
eV (H_2O) and 5.8 eV (H_2S) triplet states, an assignment of $^3B_1$ for the
5.8 eV peak seems very likely. Then a singlet-triplet separation energy
$\Delta_{S-T}(B_1)$ of 0.5 eV is obtained.
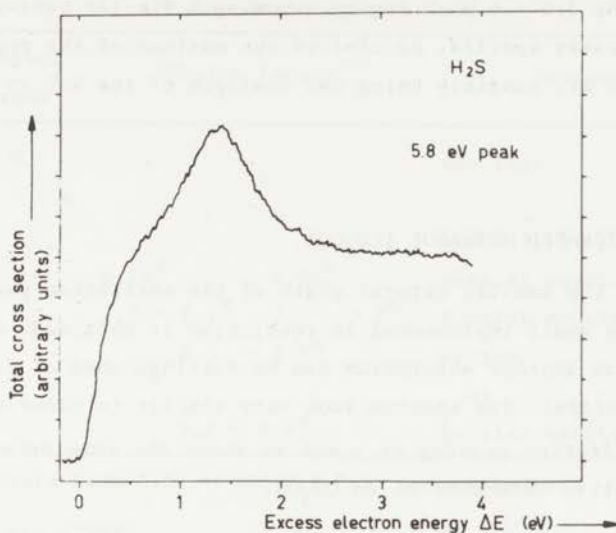
Fig. 6.8 - The behaviour of the total cross section of the 5.8 eV
transition of H_2S with increasing excess electron energy.

6.4   METHANOL (CH_3OH)

The methanol spectra (Fig. 6.9 and 6.10; Table 6.5) display a
great similarity to those of water. The first optical singlet level is
known to peak at 6.75 eV (Harrison et al., 1959; Hagège et al., 1968).
In our spectra, an intense transition is observed at 6.5 eV. Following
the analogy with water, a triplet assignment is probable. In any case
the analogy is true for the highest occupied molecular orbital. From a
photoelectron spectroscopy study on methanol, Al-Joboury et al. (1967)
concluded that the lowest ionization peak (10.83 eV) could be attri-
buted to the lone pair orbital of oxygen.

In contrast to water no H^- ions could be detected using the
T.E. technique. This could easily be established since no negative ion
signal was found applying a negative well depth.

For excess energies up to 3 eV a weak and broad absorption is observed in the 3.0 - 6.0 eV region, showing a similar behaviour as found in the water spectra. At $\Delta E=4$ eV the maximum of the peak can be found at ~ 4.4 eV, possibly being the analogue of the 4.5 eV absorption in water.

6.5   PERDEUTERATED METHANOL (CD_3OD)

Due to the smaller natural width of the excitation peaks (isotope effect) a small improvement in resolution is obtained. Close to the 8.3 eV peak another absorption can be distinguished at 8.0 eV (threshold spectra). The spectra look very similar to those of CH_3OH. The broad absorption peaking at ~ 4.4 eV shows the same behaviour with the same relative intensity as in CH_3OH.
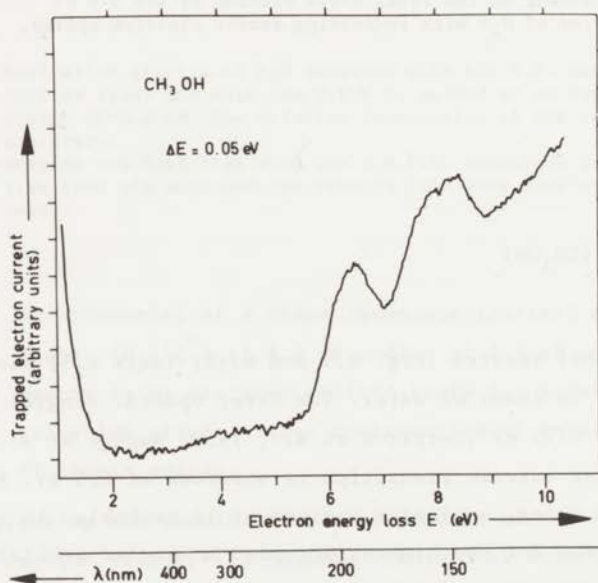
Fig. 6.9 - Excitation spectrum of methanol measured with the T.E. technique at $\Delta E=0.05$ eV.

TABLE 6.5

Methanol (energies in eV)

Electron impact This research[*]	Photon impact			Assignment
3.0 - 6.0 maximum at ∼ 4.4				see text
6.5				probably triplet state
	6.74[a]	6.76[b]		singlet excitation
7.9	7.7 - 8.1[a]	7.7[b]	7.8[b]	singlet excitation (?)
8.3		8.3 - 8.7[a]		singlet
				or
9.3		9.0 - 9.6[a]		triplet excitations

[*] Collected data from T.E. - and D.R.P.D. measurements.

[a] Hagège et al. (1968)

[b] Harrison et al. (1959)

TABLE 6.6

Di-methyl-ether

Excitation energies (eV)

Electron impact This research[*]	Photon impact		Assignment
4.5 - 4.8			see text
6.1			triplet state (?)
6.7	6.75[a]	6.73[b]	probably singlet state
7.3	7.29 -	7.37[b]	singlet
7.7	7.62[a,b]		or
8.5 - 9.5	8.4		triplet states
	Rydberg		
	series	↓	

[*] Collected data from T.E.- and D.R.P.D. measurements

[a] Harrison et al. (1959)

[b] Hernandez (1963).
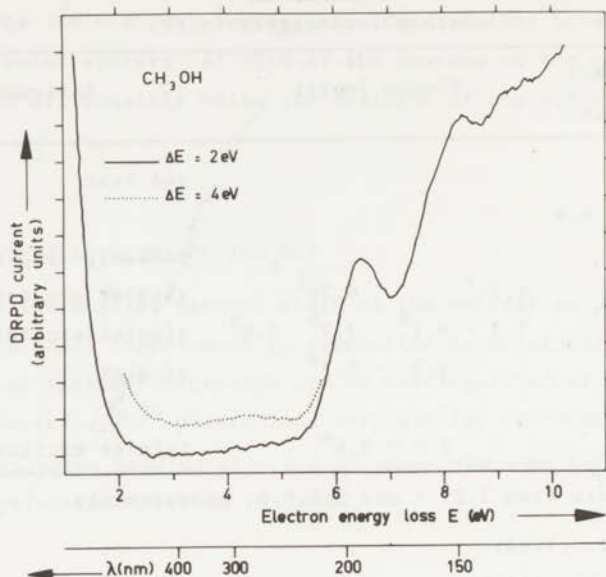
Fig. 6.10 – Excitation spectrum of methanol measured with the D.R.P.D.
method at ΔE=2 eV. The dotted line presents a part of the
D.R.P.D. spectrum measured at an excess energy of 4 eV.
A maximum can be observed peaking at ~ 4.4 eV.

6.6   DI-METHYL-ETHER (CH₃OCH₃)

In some respects the spectra of di-methyl-ether look somewhat
different compared with those of methanol (Fig. 6.11; Table 6.6). From
photon-impact work (Harrison et al., 1959; Hernandez, 1963) the first
optical singlet level is known to peak at 6.74 eV. Thus a singlet
character of our 6.7 eV peak seems more probable than a triplet assign-
ment. Therefore a triplet character might be attributed to the 6.1 eV
absorption which shows up weakly in the threshold spectra. Just like in
water and methanol a small increase in intensity can be observed in the
3-6 eV region. At ΔE=4 eV a maximum of this weak absorption is found at
4.5 - 4.8 eV.
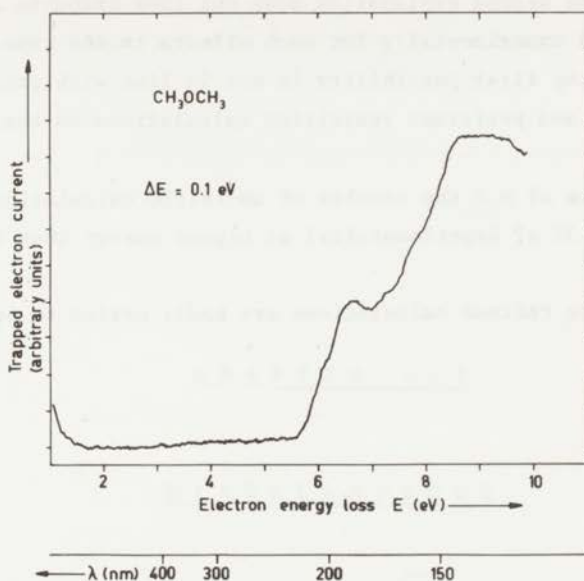
Fig. 6.11 - Excitation spectrum of di-methyl-ether measured with the
T.E. method at ΔE=0.1 eV.

6.7 SUMMARY

In the spectra of water a dominant peak is observed at 7.2 eV
which is characterized as the triplet state $^3B_1$. For H_2S and methanol
a similar absorption is found at 5.8 eV and 6.5 eV. Triplet assignments
seem likely. Scanning the behaviour of the total cross section of the
5.8 eV peak of H_2S versus excess energy, a shape resonance is possibly
observed at 1.4 eV. Consequently an excited negative ion state of H_2S
might exist at ~ 7.2 eV.

From our experimental data on H_2O, D_2O, CH_3OH, CD_3OD and di-
methyl-ether a very weak absorption with its maximum lying in the energy
range 4.4 - 4.8 eV is observed. For H_2S a similar process cannot be
found possibly obscured by the intensive triplet excitation at 5.8 eV.

As stated before this mystery band might be due to excitation
processes of the molecule itself (A_2 transitions in H_2O(?)) or is
caused by the excitation of contamination or decomposition products

(OH radicals). The second explanation does not look probable as no support was found experimentally for such effects in the case of water.

However, the first possibility is not in line with present theoretical thinking and performed restricted calculations on the excited states of water.

In the case of H_2S the results of ab-initio calculations predict the $^1B_1$ state (6.32 eV experimentally) at higher energy than the $^1A_2$ state.

Anyway more refined calculations are badly needed to settle this problem.

C H A P T E R   V I I

M I S C E L L A N E O U S

7.1   1,2 DIMETHYL-CYCLOHEXENE
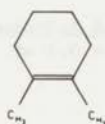
The excited states of ethylene and its derivates have been
studied intensively in recent years. The so-called "mystery band" which
shows up weakly in light absorption spectra ~ 6 eV (Potts, 1955) has
been of special interest. It has been proposed by Berry (1963) that
this absorption is due to a $\sigma(C-H) \rightarrow \pi^*$ transition. Robin et al. (1966)
are of the opinion that the assignment of a $\pi \rightarrow \sigma^*(C-H)$ transition
looks more probable.

The study of these olefins with low-energy electron spectroscopy
suggests that steric hindrance of the substituents might favour the
detection of the mystery band. Brongersma (1968), using the T.E. tech-
nique, observed mystery band absorptions at ~ 6.1 eV for cis-butene-2
and at ~ 5.5 eV for tetramethylethylene, but failed to measure similar
absorptions for ethylene, trans-butene-2 and 1,6 heptadiene.

In Fig. 7.1 a threshold spectrum (excess energy $\Delta E = 0.1$ eV) of
1,2 dimethyl-cyclohexene is presented which shows peculiar features.
Apart from the detection of the triplet state at 4.2 eV ($\pi \rightarrow \pi^*$) and
the singlet state at 7.9 eV ($\pi \rightarrow \pi^*$), two additional absorptions are
observed at ~ 5.4 eV and ~ 6.2 eV. A triplet assignment for one of
these peaks cannot be excluded.
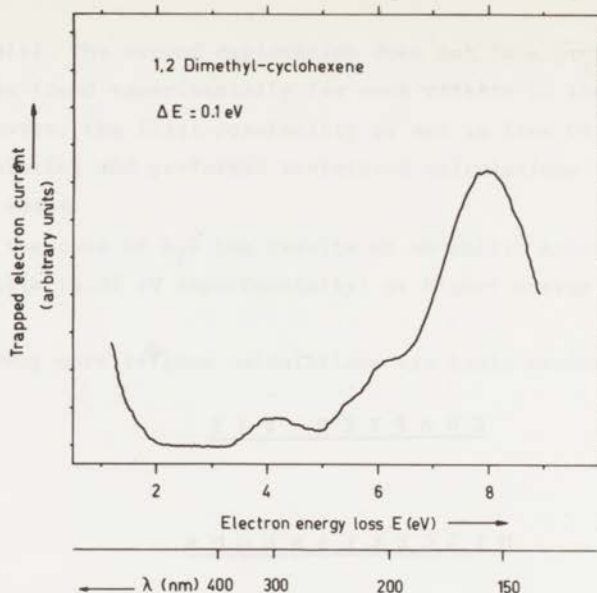
Fig. 7.1 – A T.E. spectrum of 1,2-dimethyl-cyclohexene measured at an excess energy ΔE = 0.1 eV.

As far as we know this is the first time that for olefins two mystery bands are observed below the optically allowed singlet state (7.9 eV). For ethylene Berthod (1966) calculated a symmetrically allowed singlet transition at 6.3 eV ($\pi \rightarrow \sigma^*$) with the corresponding triplet transition at 5.5 eV.

7.2   7-DEHYDRO-CHOLESTEROL
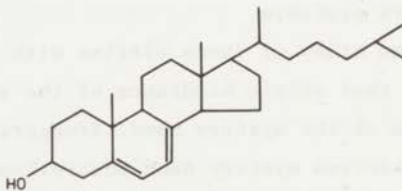
The information about excited states of 7-dehydro-cholesterol is important for the photochemistry of steroids. Because of low volatility of this compound the experiments were performed at elevated temperatures (175°C) while also the high-temperature inlet system was used. In Fig. 7.2 a T.E. spectrum of 7-dehydro-cholesterol is shown measured at an excess energy $\Delta E \sim$ 0.1 eV. Maxima of absorptions are observed at 3.8 eV (triplet level) and at 6.3 eV (probably singlet
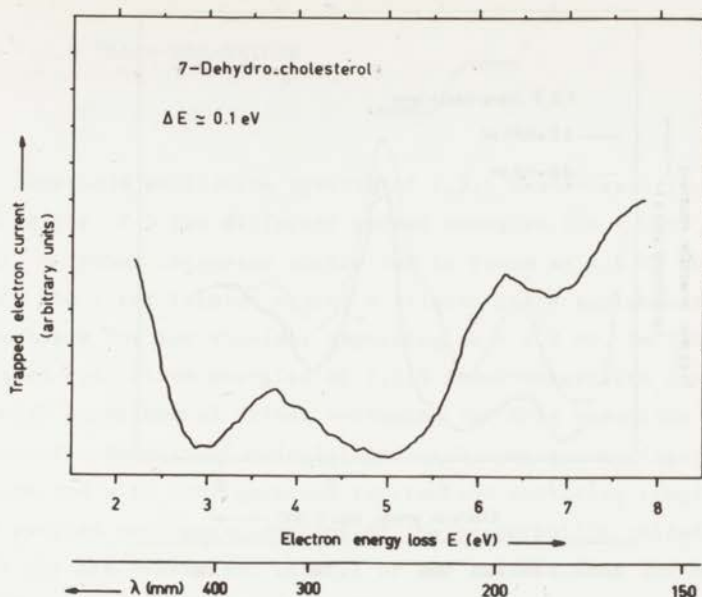
Fig. 7.2 – T.E. spectrum of 7-dehydro-cholesterol measured at an ex-
cess energy $\Delta E \sim 0.1$ eV.

level). The relatively high value of 3.8 eV compared with the value of
3.2 - 3.3 eV (Evans, 1960; Brongersma, 1968) for the lowest triplet
level in 1,3 trans-butadiene is somewhat surprising. If the double bonds
in this system (7-dehydro-cholesterol) would have little or no inter-
action with each other the triplet excitation energies will be of the
same order of magnitude as found in ethylene (4.4 eV, Brongersma (1968);
4.59 eV, Evans (1960)). Therefore a rotation around the middle (single)
bond of the conjugated system of 7-dehydro-cholesterol (90° rotation
gives two "separate" double bonds) might explain the higher value of
3.8 eV compared with the value of ~ 3.3 eV for 1,3 trans-butadiene.
This implies a non-planarity of the conjugated part of this steroid.
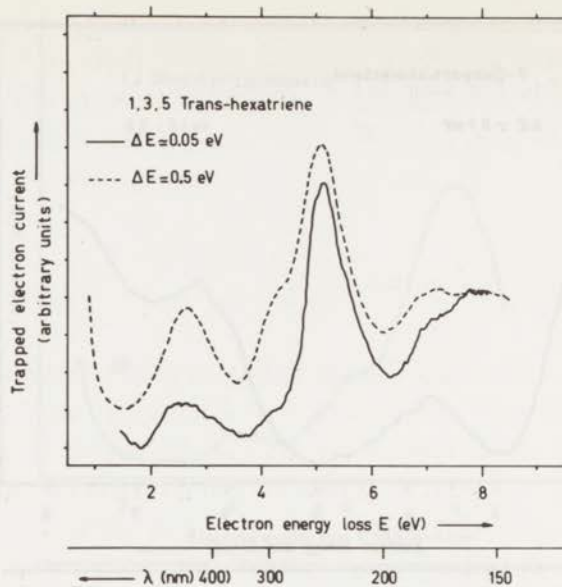
Fig. 7.3 – T.E. spectra of 1,3,5-trans-hexatriene measured at excess
energies of ΔE = 0.05 eV and 0.5 eV (dotted line).

TABLE 7.1

1,3,5-Trans-hexatriene (excitation energies in eV)[*]

	Theoretical values		Experimental data	
	Complete CI	Doubly CI[**] 0.01	Electron impact This research	Photon-impact
$S \rightarrow S$ ^1A_g	4.85	4.79		
^1B_u	5.26	5.28 (1.03)	5.1	5.13 (4.7)[a]
^1B_u	5.80	5.66	~ 5.7 (?)	
$S \rightarrow T$ ^3B_u	2.40	2.62	2.6	2.6[a,b]
^3A_g	3.87	4.01	~ 4.2	
^3B_u	4.76	4.87		
			7.2	

[*] The values between parentheses correspond to oscillator strengths
(calc.) or to the logarithm of extinction coefficients (exp.).

[**] Perturbation criterion 0.01 eV.

[a] Minnaard (1970);   [b] Evans (1960).

7.3   1,3,5 TRANS-HEXATRIENE

Threshold excitation spectra of 1,3,5 trans-hexatriene are pre-
sented in Fig. 7.3 for different excess energies (ΔE = 0.05 eV; ΔE =
0.5 eV). A rather intensive absorption is found at 2.6 eV which corres-
ponds to the first triplet state. A triplet state assignment is also
very probable for the shoulder appearing at ~ 4.2 eV. In Table 7.1
calculated excitation energies of 1,3,5 trans-hexatriene can be com-
pared with experimental values including the data resulting from our
measurements. Results of calculations with complete Configuration In-
teraction and with Configuration Interaction including singly and
doubly excited configurations (using the perturbation criterion value
of 0.01 eV) are presented. Details of the calculations and obtained
accuracy can be found in chapter II.

It appears that the predicted triplet excitation energies agree
rather well with the experimentally determined values of 2.6 eV and
4.2 eV. The most intense peak in our spectra, located at 5.1 eV is
probably characterized as the optically allowed singlet transition ex-
perimentally determined by photon-impact at 5.13 eV (Minnaard, 1970).
The very weak shoulder at ~ 5.7 eV (T.E. spectrum, ΔE = 0.05 eV)
probably corresponds to the third singlet state calculated at 5.80 eV
and 5.66 eV. A possible shoulder, it can also be explained by noise
fluctuations, might be distinguished just below the optically allowed
transition at 5.1 eV, thus corresponding to the first singlet excited
state (^1A_g) or to the third triplet transition (^3B_u) both calculated at
4.8 - 4.9 eV.

7.4   1,3,5,7 CYCLO-OCTATETRAENE
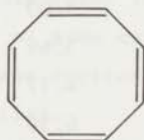
Extensive triplet excitation processes are observed below the
first excited singlet state $^1A_{2g}$ (4.4 eV) of this molecule (Knoop et
al., 1969). In Fig. 7.4 T.E. spectra of 1,3,5,7 cyclo-octatetraene
(COT) are shown measured at excess energies ΔE of 0.1 eV and 0.05 eV
(insert). In Table 7.2 the theoretical and experimental data are dis-
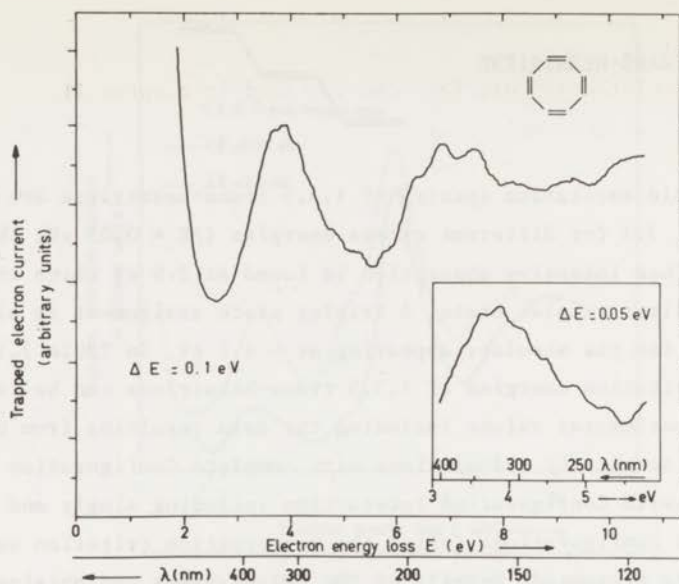played. A tentative assignment of the experimental data is based on the

Fig. 7.4 – T.E. spectra of 1,3,5,7-cyclo-octatetraene measured at excess energies ΔE of 0.1 eV and 0.05 eV (insert).

TABLE 7.2

1,3,5,7-Cyclo-octatetraene (excitation energies in eV)[*]

	Theoretical values		Experimental data	
	Doubly CI[**] 0.01	Singly CI	Electron impact This research	Photon impact
$S \rightarrow S$ $^1A_{2g}$	4.89	4.29	4.4	4.39 (2.6)[a]
^1E_u	6.41 (0)	5.91 (0)		
$^1A_{1g}$	6.97	7.11		
$^1B_{2g}$	7.07	6.71		
^1E_u	7.47 (1.40)	6.57 (1.44)		6.16 (4.4)[a]
$S \rightarrow T$ $^3A_{2g}$	3.63	3.00	3.4	
^3E_u	4.35	3.69	3.7	
$^3B_{2g}$	4.80	4.17	3.9 4.1	
^3E_u	6.62	6.50		
$^3A_{2g}$	6.70	6.70		

[*] The values between parentheses correspond to oscillator strengths (calc.) or to the logarithm of extinction coefficients (exp.).

[**] Perturbation criterion 0.01 eV.

[a] U.V. Atlas of Organic Compounds (1966).

best agreement with theoretical values. The used parametrizations and other details of the calculations can be found in chapter II.

Because of the small spacing between the energies of the excited states characterization is extremely difficult. At first sight it is rather surprising that calculations with Configuration Interaction of only singly excited configurations (singly CI) yield better agreement with the experimental data than those in which also doubly excited configurations (doubly CI - application of perturbation criterion, see chapter II) are included. This result can be explained along the following lines:

It has often been suggested that in the case of COT for the prediction of excited states inclusion of doubly excited configurations is essential because of the relatively small energy difference between the occupied and unoccupied degenerate molecular orbitals (both e_g symmetry). The ground state of the molecule will largely interact with those configurations in which two electrons are placed in a virtual MO (closed shell configuration). However, our point of view only partially agrees with these ideas. Certainly in the case of COT the inclusion of doubly excited configurations will affect the ground state energy relatively more than for other molecules. However, while the ground state is allowed to interact intensively with the doubly excited configurations, for the excited states this needs not to be true. In our calculations (doubly CI) the optically allowed state ^1E_u (observed at 6.16 eV with photon impact) is predicted ~ 1.3 eV too high in energy (Table 7.2). Inclusion of higher excited configurations, triply etc., will allow this state to interact to a larger extent with excited configurations thus leading to a lower energy (not always) for this state. Therefore the inclusion of doubly excited configurations in the case of COT leads to an energy decrease of the ground state which is much too large as compared with the decrease of energies of some excited states in the doubly CI calculations, so that for these excited states inclusion of higher excited configurations is essential.

This theory can be tested by inclusion of excited configurations higher than doubly. A complete CI calculation for COT is at the moment not possible for us. Even a calculation including all singly, doubly and triply excited configurations is difficult to handle (1750 configurations). Just as in the case of doubly CI calculations the selection of the essential configurations for triply CI is effected using a perturbation criterion with a value of 0.01 eV (chapter II).

TABLE 7.3

1,3,5,7-cyclo-octatetraene (excitation energies in eV)[*]

		Theoretical values[**]		Experimental values Photon-impact
		Doubly CI	Triply CI	
$S \rightarrow S$	$^1A_{2g}$	5.02	4.80	4.39 (2.6)[a]
	^1E_u	6.65	6.56	
	$^1A_{1g}$	7.33	7.28	
	$^1B_{2g}$	7.37	7.19	
	^1E_u	7.69	7.23	6.16 (4.4)[a]
Energy shift of ground state		−0.948	−0.948	

[*]   The values between parentheses correspond to the logarithm of extinction coefficients.

[**]   For both types of calculations (see also chapter II) the value for $k_\beta = 10.4$ is applied which give resonance integrals somewhat higher than in usual doubly CI type calculations. For the perturbation criterion the usual value of 0.01 eV is applied.

[a]   U.V. Atlas of Organic Compounds (1966).
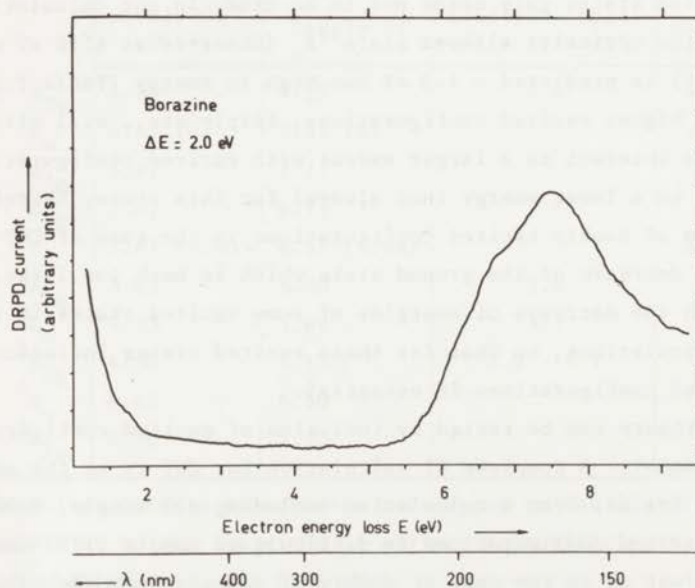
Fig. 7.5 - D.R.P.D. spectrum of borazine measured at an excess energy of $\Delta E = 2$ eV.

In Table 7.3 the theoretical results are listed for doubly CI
and triply CI using the same set of parameters. It appears that the
inclusion of triply excited configurations has no effect on the energy
of the ground state! The ^1E_u state which firstly was predicted 1.5 eV
too high is now only 1.0 eV too high compared with the experimental
value. It can be expected that the inclusion of even higher excited
configurations will give better agreement. An excellent agreement as
found for planar systems (chapter II) does not seem feasible because
of the possible partially break down of the $\sigma - \pi$ separability condition
due to the non-planarity of the molecule.

Intermolecular distances are taken from Traetteberg (1966).

7.5   BORAZINE $(B_3N_3H_6)$
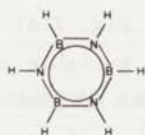
The study of borazine is of interest mainly because of the fact
that this compound and benzene are iso-electronic molecules. In Fig.
7.5 a D.R.P.D. spectrum of borazine is shown measured at an excess
energy of 2 eV. The broad absorption band, which is present in all our
spectra, peaks at $\sim$ 7.5 eV while at $\sim$ 6.7 eV a shoulder is found. From
photon-impact spectroscopy the singlet excited state $^1E'$ (strong, op-
tically allowed transition) of borazine has been determined at 7.55 eV
(Kaldor, 1971) while two weak absorptions were found at 6.28 eV ($^1A_2'$)
and at 6.56 eV ($^1A_1'$). Thus our absorption at $\sim$ 7.5 eV might be corre-
lated with the third singlet state of borazine at 7.55 eV ($^1E'$). A
similar picture was found for benzene, where the most prominent peak at
7.0 eV has been identified by the optically allowed transition to the
$^1E_{1u}$ state.

Below 5.5 eV no absorption was found in our spectra. This is in
agreement with the results of calculations performed by Peyerimhoff
and Buenker (1970). They predicted the three lowest triplet states of
borazine in the same energy range as where the three lowest singlet
states were calculated. Compared with benzene this means that the
energy differences between the excited states in borazine are much
smaller. This might result in a large overlap in intensity of the ab-
sorptions of the different states which explains why so little fine-
structure is present in our spectra. The absorption at $\sim$ 6.7 eV in our

spectra (Fig. 7.5) might be characterized as the second singlet state of borazine ($^1A_1'$) at 6.56 eV, though in analogy with benzene an assignment as a (second) triplet state can not be excluded.

7.6   ALLENE
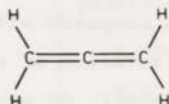
In a simplified model, allene can be considered as two double bonds having little interaction with each other. Then the two lowest triplet states of allene can be expected at excitation energies which are close to the triplet excitation energy of ethylene (4.4 – 4.6 eV; $\pi \rightarrow \pi^*$). In our spectra (e.g. Fig. 7.6) two absorptions at 4.4 eV and 4.8 eV are observed which are probably characterized by transitions to triplet states. By studying the MO picture of allene it appears that the lowest transitions in this molecule originate from excitation out of the highest, occupied degenerate molecular orbital to the lowest unoccupied, degenerate orbital both of e-symmetry leading to $^{1,3}B_1$, $^{1,3}B_2$, $^{1,3}A_1$ and $^{1,3}A_2$ states. Schaad et al. (1969) performed extensive calculations on allene. They predicted the $^1B_2$ state at higher energy than the other states. Using photon-impact, Sutcliffe et al. (1952) observed an intensive band peaking at 7.17 eV to which an assignment of the $^1B_2$ state (optically allowed) has been given. A weak absorption band was found at 6.1 – 6.9 eV.

Recently Rabalais et al. (1971) restudied the photon-impact spectrum of allene. A weak absorption at 6.70 eV (Table 7.4) was characterized as the ^1E state while for a small inflection at 5.76 eV and a weak absorption at somewhat lower energy tentatively the $^1A_1$ state and the $^1A_2$ state were assigned. However, the outcome of calculations performed by Schaad et al. (1969) contradict the assignment of ^1E for the 6.70 eV absorption. They calculated both the ^1E and ^3E states at higher excitation energies than the optically allowed transition to the $^1B_2$ state (7.2 eV). Moreover they predicted two triplet states $^3B_2$ (5.08 eV) and $^3A_1$ (4.98 eV) at much lower energy than the other two triplet states $^3B_1$ (6.52 eV) and $^3A_2$ (6.71 eV). Considering these values our peaks at 4.4 eV and 4.8 eV will be probably due to excitation to the $^3B_2$ and $^3A_1$ states. The accuracy of the calculations does not give a final answer regarding the sequence of
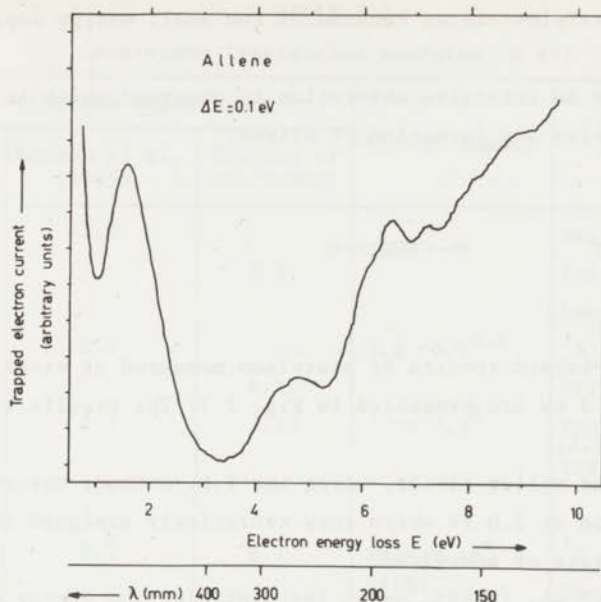
Fig. 7.6 – T.E. spectrum of allene measured at an excess energy
ΔE = 0.1 eV.

TABLE 7.4

Allene (excitation energies in eV)

Electron impact This research	Photon impact		Assignment
1.6			Neg. ion state
4.4 }			Triplet states $^3B_2$ and $^3A_1$
4.8			
~ 6.1			Triplet or singlet state
6.6	6.70[a]	6.11-6.89[b]	Probably singlet state(s) $^1A_1$, $^1A_2$, $^1B_1$ or ^1E
7.2	7.23[a]	7.17[b]	$^1B_2$ (optically allowed)
~ 8.1	7.8[a,b] ↓ Rydberg		Triplet
~ 9.0	bands		or singlet states

[a] Rabalais et al. (1971); [b] Sutcliffe et al. (1952).

the two lowest triplet states because of the small energy separation of these levels.

At 1.6 eV an intensive absorption is observed which is probably due to the negative ion formation of allene.

7.7   ACETYLENE $H-C\equiv C-H$

Electron-impact spectra of acetylene measured at excess energies $\Delta E = 0.2$ eV and 2 eV are presented in Fig. 7.7. The results are summarized in Table 7.5.

Bowman and Miller (1965), using the T.E. method, observed a prominent transition at 2.0 eV which they tentatively assigned to a low-lying triplet state of acetylene.

Trajmar et al. (1968), using incident electron energy of 25 eV, searched carefully for a transition in this energy region but found none. In our spectra we found an absorption at 1.9 eV ($\Delta E = 0$ eV) which
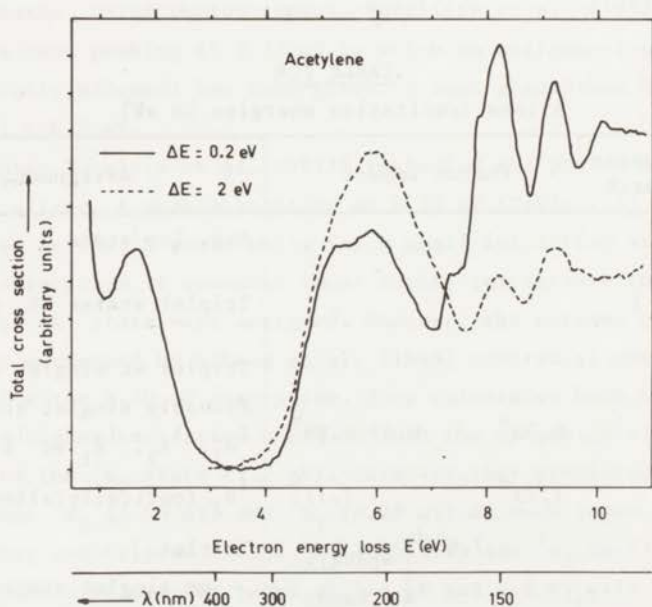
Fig. 7.7 - Excitation spectra of acetylene measured with the T.E. method ($\Delta E = 0.2$ eV) and with the D.R.P.D. technique ($\Delta E = 2$ eV; dotted line).

TABLE 7.5

Acetylene (excitation energies in eV)

Electron impact			Photon impact	Assignment
This research	Bowman et al. (1965)	Trajmar et al. (1968)		
1.9	2.0			Negative ion state
5.3		5.2		Triplet state, probably $^3\Sigma_u^+$
	} 6.2		5.2 –5.9[a,b]	$^1A_u(^1\Sigma_u^-)$
6.0		6.1		Triplet state ($^3\Pi_g$?)
7.3 – 7.4	7.7	7.15	7.19[c] 7.3[d]	Probably $^1\Pi_g$
~ 7.7				Triplet
	} 7.9			or
~ 7.9				singlet state
8.2	8.2	8.2	Ryd- 8.16[e]	$^1\Pi_u$
~ 8.6			berg	Singlet
9.2	9.2	9.2	states 9.23[e]	or
10.0	10.0		↓	triplet states

[a] Ingold and King (1953);   [c] Price (1935);   [e] Wilkinson (1958).
[b] Innes (1954);   [d] Nakayama et al. (1964);

shifts to lower energy with increasing excess energy. This behaviour implies an assignment of a negative ion state for this absorption (see chapter VI, section 6.3.3).

Trajmar et al. (1968) observed absorptions at 5.2 eV and 6.1 eV which they characterized both as triplet states by studying the behaviour of the intensity of the transitions as a function of scattering angle. They suggested assignment of these triplet states in correlation with the two lowest triplet states $^3\Sigma_u^+$ and $^3\Pi_g$ in nitrogen. The possible assignment of $^3\Sigma_u^+$ for the lowest triplet state of acetylene is not in agreement with the results of calculations performed by Dewar et al. (1961). Using the so-called Split-p-orbital method (allowing for vertical correlation of electrons) they calculated the two lowest triplet states $^3\Sigma_u^-$ at 4.5 – 5.3 eV and $^3\Delta_u$ at 4.4 – 5.8 eV, from which they assumed the $^3\Sigma_u^-$ to be the lower one.

Additional support for the 5.2 - 5.3 eV absorption as the lowest triplet state can be extracted from the work of Evans (1960) and Beer (1956) on the triplet states of poly-acetylenes. By interpolation of the 0-0 absorption band of these compounds we find the 0-0 band for acetylene at ∼ 4.5 eV from which an estimated value of ∼ 5.0 eV results for the Franck-Condon maximum of the lowest triplet state of acetylene.

7.8   PROPYNE (METHYL-ACETYLENE) $H-C\equiv C-C_{H_3}$

The substitution of a methyl group to acetylene changes the spectra (Fig. 7.8) significantly compared with those of acetylene (Fig. 7.7). The negative ion state observed at 2.8 eV is shifted over 0.9 eV to higher energy. The broad band located at ∼ 5.6 eV probably consists of two absorptions one at ∼ 5.2 eV and the other at ∼ 5.8 eV. Following the analogy with acetylene and allene triplet states as assignments are probably correct. From our spectra (Fig. 7.8) it appears that the
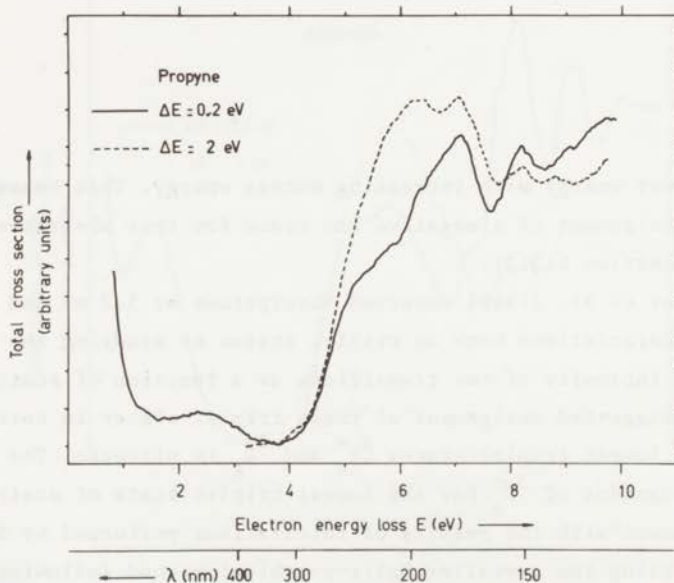
Fig. 7.8 - T.E. spectrum (ΔE = 0.2 eV) and D.R.P.D. spectrum (ΔE = 2 eV; dotted line) of propyne.

TABLE 7.6

Propyne (excitation energies in eV)

Electron impact		Photon impact Nakayama et al. (1964)	Assignment
This research	Bowman and Miller (1965)		
2.8	2.8		Negative ion state
~ 5.2			Triplet
~ 5.8	6.1		states
6.3			Probably triplet state
7.1	7.1	7.04	Singlet
8.2	8.3	8.05	states

absorption at 6.3 eV increases relatively fast with increasing excess energy. This behaviour indicates triplet assignment. The data resulting from T.E. and D.R.P.D. measurements are summarized in Table 7.6. These values can be compared with data obtained by Bowman and Miller (1965), using the T.E. method, or with photon-impact data (Nakayama et al., 1964).

R E F E R E N C E S

Aarts, J.F.M. and F.J. de Heer, Chem.Phys.Letters 4 (1969) 116.

Aarts, J.F.M. et al., to be published (1972).

Al-Joboury, M.I. and D.W. Turner, J.Chem.Soc.(1964) 4434.

Al-Joboury, M.I. and D.W. Turner, J.Chem.Soc.(1967) 373.

Allinger, N.L. and Th.W. Stuart, J.Chem.Phys. 47 (1967) 4611.

Anderson, N., P.P. Eggleton and R.G.W. Keesing, Rev.Sci.Instr. 38
        (1967) 924.

Bak, B., L. Hansen-Nygaard and J. Rastrup-Andersen, J.Mol.Spectr. 2
        (1958) 361.

Beer, M., J.Chem.Phys. 25 (1956) 745.

Berry, R.S., J.Chem.Phys. 38 (1963) 1934.

Berthod, H., J.Chem.Phys. 45 (1966) 1859.

Bowman, C.R. and W.D. Miller, J.Chem.Phys. 42 (1965) 681.

Brion, C.E. and G.E. Thomas, Int.J.Mass Spectr. 1 (1968) 25.

Brongersma, H.H. and L.J. Oosterhoff, Chem.Phys.Letters 1 (1967) 169.

Brongersma, H.H., Thesis, Leiden (1968).

Brongersma, H.H., A.J.H. Boerboom and J. Kistemaker, Physica 44 (1969)
        449.

Brongersma, H.H., F.W.E. Knoop and C. Backx, Chem.Phys.Letters 13
        (1972) 16.

Burke, P.G., J.W. Cooper and S. Ormonde, Phys.Rev. 183 (1969) 245.

Burland, D.M., G. Castro and G.W. Robinson, J.Chem.Phys. 52 (1970) 4100.

Burrow, P.D. and G.J. Schulz, Phys.Rev.Letters 22 (1969) 1271.

Callomon, J.H., T.M. Dunn and I.M. Mills, Phil.Trans.Roy.Soc. (London)
        259A (1966) 499.

Cermak, V., J.Chem.Phys. 44 (1966) 3774.

Chaimberlain, G.E. and H.G.M. Heideman, Phys.Rev.Letters 15 (1965) 337.

Claydon, C.R., G.A. Segal and H.S. Taylor, J.Chem.Phys. 54 (1971) 3799.

Colson, S.D. and E.R. Bernstein, J.Chem.Phys. 43 (1965) 2661.

Compton, R.N., R.H. Huebner, P.W. Reinhardt and L.G. Christophorou,
        J.Chem.Phys. 48 (1968) 901.

Coulson, C.A. and H.C. Longuet-Higgins, Proc.Roy.Soc. A 191 (1947) 39.

Cruickshank, D.W.J. and R.A. Sparks, Proc.Roy.Soc. A 258 (1960) 270.

Curran, R.K., J.Chem.Phys. 38 (1963) 780.

Dewar, M.J.S. and N.L. Hojvat, Proc.Roy.Soc. A 264 (1961) 431.

Doering, J.P. and A.J. Williams III, J.Chem.Phys. 47 (1967) 4180.

Doering, J.P., J.Chem.Phys. 51 (1969) 2866.

Dowell, J.T. and T.E. Sharp, J.Chem.Phys. 47 (1967) 5068.

Dunning, F.B. and A.C.H. Smith, J.Phys. B 3 (1970) L 60.

Ehrhardt, H., L. Langhans and F. Linder, Z.Physik 214 (1968) 179.

Ellison, F.O. and H. Shull, J.Chem.Phys. 23 (1955) 2348.

El-Sayed, M.A., J.Chem.Phys. 36 (1962) 552.

Evans, D.F., J.Chem.Soc. (1957) 1351.

Evans, D.F., J.Chem.Soc. (1957) 3885.

Evans, D.F., J.Chem.Soc. (1960) 1735.

Fano, U., Phys.Rev. 124 (1961) 1866.

Fano, U. and J.W. Cooper, Phys.Rev. A 138 (1965) 400.

Fayard, F., R. Azria and J.P. Ziesel, VII ICPEAC Abstracts (1971) 1172.

Feshbach, H., Ann.Phys. 5 (1958) 357.

Feshbach, H., Ann.Phys. 19 (1962) 287.

Fleming, R.J. and G.S. Higginson, Proc.Phys.Soc. (London) 84 (1964) 531.

Foner, S.N. and B.H. Nall, Phys.Rev. 122 (1961) 512.

Fox, R.E., W.M. Hickam, D.J. Grove and T. Kjeldaas, Rev.Sci.Instr. 26
      (1955) 1101.

Goddard, W.A., D.L. Huestis, D.C. Cartwright and S. Trajmar, Chem.Phys.
      Letters 11 (1971) 329.

Grissom, J.T., Thesis, OakRidge (1970).

Hagége, J., P.C. Roberge and C. Vermeil, Ber.Bunsenges.Phys.Chem. 72
      (1968) 138.

Hall, R.I., J. Mazeau, J. Reinhardt and C. Schermann, J.Phys. B 3
      (1970) 991.

Hall, R.I., Thesis, Paris (1971).

Hansen, D.M. and G.W. Robinson, J.Chem.Phys. 43 (1965) 4174.

Harrison, A.J., B.J. Cederholm and M.A. Terwilliger, J.Chem.Phys. 30
      (1959) 355.

Harrison, A.J. and D.R.W. Price, J.Chem.Phys. 30 (1959) 357.

Haugen, W. and M. Traetteberg, Acta Chem.Scand. 20 (1966) 1726.

Heitler, W. and F. London, Z.Physik 44 (1927) 455.

Henderson, J.R. and M. Muramoto, J.Chem.Phys. 43 (1965) 1215.

Hernandez, G.J., J.Chem.Phys. 38 (1963) 1644.

Herzberg, G., Molecular Spectra and Molecular Structure III, D. van
      Nostrand Comp.Inc., Princeton (1966).

Hillier, I.H. and V.R. Saunders, Chem.Phys.Letters 5 (1970) 384.

Hinze, J. and H.H. Jaffé, J.Am.Chem.Soc. 84 (1962) 540.

Holt, H.K. and R. Krotkov, Phys.Rev. 144 (1966) 82.

Horsley, J.A. and W.H. Fink, J.Chem.Phys. 50 (1969) 750.

Hubin-Franskin, M.J. and J.E. Collin, Int.J.Mass Spectr. 5 (1970) 163.

Hückel, E., Z.Physik 70 (1931) 204.

Huebner, R.N., Thesis, Oak Ridge (1968).

Hunt, W.J. and W.A. Goddard, Chem.Phys.Letters 3 (1969) 414.

Hunziker, H.E., J.Chem.Phys. 56 (1972) 400.

Ingold, C.K. and G.W. King, J.Chem.Soc.(1953) 2725.

Innes, K.K., J.Chem.Phys. 22 (1954) 863.

Jäger, K. and A. Henglein, Z.Naturfsch. 21A (1966) 1251.

Jones, L.C. and L.W. Taylor, Anal.Chem. 27 (1955) 228.

Jug, K., Theor.Chim.Acta 14 (1969) 91.

Kaldor, A., J.Chem.Phys. 55 (1971) 4641.

Knoop, F.W.E., J. Kistemaker and L.J. Oosterhoff, Chem.Phys.Letters
    3 (1969) 73.

Knoop, F.W.E., H.H. Brongersma, A.J.H. Boerboom and L.J. Oosterhoff,
    Advances in Mass Spectr. Vol. 5 (1970) 136.

Knoop, F.W.E., H.H. Brongersma and A.J.H. Boerboom, Chem.Phys.Letters
    5 (1970) 450.

Knoop, F.W.E., H.H. Brongersma and L.J. Oosterhoff, VII ICPEAC Ab-
    stracts (1971) 1077.

Knoop, F.W.E., H.H. Brongersma and L.J. Oosterhoff, Chem.Phys.Letters
    13 (1972) 20.

Koutecky, J., J. Cizek, J. Dubsky and K. Hlavaty, Theor.Chim.Acta 2
    (1964) 462.

Koutecky, J., K. Hlavaty and P. Hochmann, Theor.Chim.Acta 3 (1965) 341.

Kuppermann, A., J.K. Rice and S. Trajmar, J.Phys.Chem. 72 (1968) 3894.

Kuyatt, C.E., J.A. Simpson and S.R. Mielczarek, Phys.Rev. A 138 (1965)
    385.

Lassettre, E.N., A. Skerbele, M.A. Dillon and K.J. Ross, J.Chem.Phys.
    48 (1968) 5066.

Lugt, W.Th.A.M. van der, Thesis, Leiden (1968).

Lugt, W.Th.A.M. van der, and L.J. Oosterhoff, Mol.Physics 18 (1970) 177.

Maier-Leibnitz, H., Z.Physik 95 (1935) 499.

Marmet, P. and L. Kerwin, Can.J.Phys. 38 (1960) 787.

Marmet, P., Can.J.Phys. 42 (1964) 2102.

Mataga, N. and K. Nishimoto, Z.Phys.Chem. 13 (1957) 140.

Matsuzawa, M., J.Chem.Phys. 51 (1969) 4705.

McWeeny, R., Proc.Roy.Soc. A223 (1954) 63, 306.

Meyer, Y.H., R. Astier and J.M. Leclerq, J.Chem.Phys. 56 (1972) 801.

Miller, K.J., S.R. Mielczarek and M. Krauss, J.Chem.Phys. 51 (1969) 26.

Minnaard, N.G., Thesis, Leiden (1970).

Moccia, R., J.Chem.Phys. 40 (1964) 2186.

Mulliken, R.S., J.Chem.Phys. 3 (1935) 506.

Nakayama, T. and K. Watanabe, J.Chem.Phys. 40 (1964) 558.

Ochkur, V.I., Soviet Phys. JETP 18 (1964) 503.

Oldenberg, O. and F.F. Rieke, J.Chem.Phys. 6 (1938) 439.

Pariser, R. and R.G. Parr, J.Chem.Phys. 21 (1953) 466.

Pariser, R. and R.G. Parr, J.Chem.Phys. 21 (1953) 767.

Parr, R.G., The Quantum Theory of Molecular Electronic Structure,
        W.A. Benjamin Inc., New York (1964).

Peyerimhoff, S.D. and R.J. Buenker, Theor.Chim.Acta 19 (1970) 1.

Pichanick, F.M.J. and J.A. Simpson, Phys.Rev. 168 (1968) 64.

Pickett, L.W., M.E. Corning, G.M. Wieder, D.A. Semenow and J.M.
        Buckley, J.Am.Chem.Soc. 75 (1953) 1618.

Politiek, J., J. Los and P.G. Ikelaar, Vakuum-Technik 17 (1968) 150.

Pople, J.A., Trans.Far.Soc. 44 (1953) 1375.

Pople, J.A. and D.L. Beveridge, Approximate MO Theory, McGraw-Hill Book
        Comp., New York (1970).

Porter, G. and M.W. Windsor, Disc.Far.Soc. 17 (1954) 178.

Potts, W.J., J.Chem.Phys. 23 (1955) 65.

Price, W.C., Phys.Rev. 47 (1935) 444.

Price, W.C., J.Chem.Phys. 4 (1936) 147.

Rabalais, J.W., J.M. McDonald, V. Scherr and S.P. McGlynn, Chem.Rev.
        71 (1971) 73.

Rauk, A. and I.G. Csizmadia, Can.J.Chem. 46 (1968) 1205.

Richards, W.G. and J.A. Horsley, Ab Initio MO Calculations for Chemists,
        Clarendon Press, Oxford (1970).

Robin, H.B., R.R. Hart and N.A. Kuebler, J.Chem.Phys. 44 (1966) 1803.

Rudd, M.E., Phys.Rev.Letters 15 (1965) 580.

Rudge, M.R.H., Proc.Phys.Soc. 85 (1965) 607.

Santen, R.A. van, Thesis, Leiden (1971).

Schaad, L.J., L.A. Burnelle and K.P. Dressler, Theor.Chim.Acta 15
        (1969) 91.

Schiff, L.I., Quantum Mechanics, McGraw-Hill, INC., New York (1955).

Schulz, G.J., Phys.Rev. 112 (1958) 150.

Schulz, G.J., Phys.Rev. 116 (1959) 1141.

Schulz, G.J., J.Chem.Phys. 33 (1960) 1661.

Simpson, J.A., Rev.Sci.Instr. 35 (1964) 1698.

Skerbele, A., M.A. Dillon and E.N. Lassettre, J.Chem.Phys. 49 (1968)
        5042.

Smit, C., H.G.M. Heideman and J.A. Smit, Physica 29 (1963) 245.

Stamatovic, A. and G.J. Schulz, Rev.Sci.Instr. 39 (1968) 1752.

Stamatovic, A. and G.J. Schulz, Rev.Sci.Instr. 41 (1970) 423.

Stuart, Th.W. and N.L. Allinger, Theor.Chim.Acta 10 (1968) 247.

Sutcliffe, L.H. and A.D. Walsh, J.Chem.Soc. (1952) 899.

Temkin, A. and J.C. Lamkin, Phys.Rev. 121 (1961) 788.

Trajmar, S., J.K. Rice, P.S.P. Wei and A. Kuppermann, Chem.Phys.L.
        1 (1968) 703.

Trajmar, S., W. Williams and A. Kuppermann, J.Chem.Phys. 54 (1971) 2274.

Traetteberg, M., Acta Chem.Scand. 20 (1966) 1724.

U.V. Atlas of Organic Compounds, Vol. I (Butterworth Chemie Verlag,
        London, 1966).

Visscher, P.B. and L.M. Falicov, J.Chem.Phys. 52 (1970) 4217.

Watanabe, K. and M. Zelikoff, J. Opt.Soc.Am. 43 (1953) 753.

Watanabe, K. and A.S. Jursa, J.Chem.Phys. 41 (1964) 1650.

Whitten, J.L. and M. Hackmeyer, J.Chem.Phys. 51 (1969) 5584.

Wilkinson, P.G., Can.J.Phys. 34 (1956) 596.

Wilkinson, P.G., J.Mol.Spectr. 2 (1958) 387.

S U M M A R Y

This thesis deals with a study on the excited states of atoms and molecules, which consists of the following two parts:

I   The interaction of low-energy electrons with single atoms or molecules giving rise to excitation processes,

II   The calculation of excitation energies in the case of conjugated systems.

Chapter I sketches the current state of affairs regarding the detection of excited states. The information on excitation energies is rather scanty especially for triplet states. The application of low-energy electron-impact spectroscopy yields additional information for the excited states.

Chapter II describes the present state of electron-impact spectroscopy. While for high-energy electron impact the selection rules are very similar to those for optical excitation, practically all electronic transitions, including spin change, are allowed when low-energy electrons are used. The experimental procedures for the measurement of differential cross sections and total cross sections are summarized. Moreover a short survey is given of the theoretical methods employed in high-energy and low-energy electron impact spectroscopy.

Chapter III deals with the Molecular Orbital calculations on the excitation energies of molecules (singlet and triplet states). Within the frame-work of the Pariser, Parr and Pople -method for conjugated systems (π-electrons) extensive calculations were performed, studying the influence of singly, doubly and multiply excited configurations on the calculated energies. It appears that the calculations based on Configuration Interaction with only singly excited configurations in general predict reasonable triplet and singlet excitation energies. However, some optically forbidden transitions (^1A_g transition in 1,3 trans-butadiene and 1,3,5 trans-hexatriene) are badly predicted. It appears that the predicted energies for unsaturated hydrocarbons (planar) resulting from calculations in which singly and doubly excited configurations are included agree with experimental values

within 0.2 - 0.3 eV. In order to truncate the large number of excited configurations a criterion, based on perturbation theory, has been developed which allows to remove the non-essential configurations.

In chapter IV a spectrometer is described for the measurement of total excitation cross sections. Threshold excitation processes can be studied by means of the Trapped Electron (T.E.) method. However, with this technique the characterization of the observed transitions is difficult. A new technique is introduced the so-called Double Retarding Potential Difference (D.R.P.D.) method as suggested by Brongersma. This method allows to extend our measurements to 10 eV or more above the threshold of excitation. By studying the energy dependence of the excitation function in this energy region classification of the studied process may be obtained.

Apart from the conventional inlet system, introduction of samples obtained from gases or liquids into the spectrometer, a high-temperature inlet system has been used allowing the measurement of compounds of low volatility. A low-noise amplification system for the current of inelastically scattered electrons enables the use of very small primary beam currents (order of 10^{-9} A). This has the advantage that space charge effects are reduced considerably.

In chapter V helium and benzene are studied. For helium triplet excitation is very intensive near the threshold of excitation. Total cross sections of the 2^3S and 2^1S states of helium are measured in the 19 - 24 eV range. Several shape resonances (unstable negative ion states) are observed. An estimate for the 2^3P cross section is presented. Close coupling calculations of Burke et al. (1969) predict the correct structure but overestimate the magnitude of the cross sections as compared to the measured ones. Far above the first ionization potential a doubly excited state of helium is observed at 58.4 eV which is in agreement with other data. In the case of benzene singlet-triplet excitation processes appear also intensive near threshold. The 4.8 eV peak, firstly identified as the first singlet transition $^1B_{2u}$ in other studies, turns out to be due to excitation of the second triplet state of benzene $^3E_{1u}$. From the excitation function of this state we found evidence of two excited negative ion states of benzene at energies of ~ 5.2 eV and ~ 6.0 eV.

Chapter VI deals with water and related compounds. In the spectra of water the dominant peak at 7.2 eV is characterized as a triplet state

($^3B_1$) which is not in agreement with the assignments in other studies
($^1B_1$). For H_2S and methanol a similar absorption is found at 5.8 eV
and 6.5 eV. Triplet assignments seem likely. In our spectra of H_2O,
D_2O, CH_3OH, CD_3OD and di-methyl-ether a very weak absorption with its
maximum lying in the energy range of 4.4 – 4.8 eV is observed. This
mystery band might be due to excitation processes of the molecule it-
self (A_2 transitions in H_2O (?)) or is caused by the excitation of
contamination or decomposition products (OH radicals). The first possi-
bility is not in line with present theoretical thinking. The second
explanation does not look probable as no support was found experiment-
ally for such effects in the case of water.

In chapter VII the results for a number of molecules are given.
In the spectra of 1,2 di-methyl-cyclohexene two distinct absorptions
are observed at $\sim$ 5.4 eV and $\sim$ 6.2 eV, probably due to $\sigma \rightarrow \pi^*$ and/or
$\pi \rightarrow \sigma^*$ transitions. A triplet excitation process at 3.8 eV has been
observed for 7-dehydro-cholesterol which is at higher energy than the
corresponding triplet in 1,3 trans-butadiene ($\sim$ 3.3 eV), thus indica-
ting a non-planarity of the conjugated system. For 1,3,5 trans-
hexatriene two probable triplet states are observed at 2.6 eV and
$\sim$ 4.2 eV. The latter excitation process has not been found before.
Several absorptions were observed below the optically allowed state at
4.4 eV in the case of 1,3,5,7 cyclo-octatetraene. Triplet assignments
seem likely for most of them. It appears that calculations based on
Configuration Interaction of only singly excited configurations give
better agreement with experimental data compared with calculations in
which also doubly excited configurations are included. In the spectra
of borazine one prominent absorption band is observed peaking at $\sim$ 7.5
eV, which is the same energy where the optically allowed transition is
located. The low-energy absorptions observed in allene (1.6 eV), ace-
tylene (1.9 eV) and propyne (2.8 eV) are probably due to vibrationally
excited negative ion states. In the energy range of 4-6 eV intensive
triplet excitation is observed for these molecules.

S A M E N V A T T I N G

Het in dit proefschrift beschreven onderzoek betreft een studie
van aangeslagen toestanden van atomen en moleculen, die bestaat uit de
volgende twee gedeelten:

I   De wisselwerking van laag energetische electronen met atomen en
     moleculen aanleiding gevend tot aanslagprocessen,

II   De berekening van excitatie-energieen van geconjugeerde systemen.

Hoofdstuk I geeft in het kort aan op welke manieren aangeslagen
toestanden gemeten kunnen worden. De gegevens over aanslagenergieen zijn
tamelijk schaars, vooral voor triplettoestanden. Spectroscopie door
middel van botsingen met lage-energie electronen verschaft ons extra in-
formatie over aangeslagen toestanden.

Hoofdstuk II beschrijft de huidige stand van zaken in de spectros-
copie door middel van botsingen met electronen. Terwijl voor botsingen
met hoge-energie electronen de selectieregels vrijwel identiek zijn aan
de optische selectieregels, worden bijna alle electronische overgangen,
ook spin-verboden, toegestaan bij gebruik van lage-energie electronen.
De experimentele methodes die toegepast worden voor het meten van diffe-
rentiële en totale werkzame doorsneden worden aangegeven. Tevens wordt
een kort overzicht gegeven van de momenteel in gebruik zijnde theoreti-
sche beschrijvingsmethoden van aanslagprocessen tengevolge van botsingen
van zowel hoge- als lage-energie electronen.

Hoofdstuk III behandelt Molecular Orbital berekeningen van exci-
tatie-energieën van moleculen (singulet en triplet). Binnen het kader
van de Pariser-Parr-Pople methode voor geconjugeerde systemen (π-elec-
tronen) zijn uitvoerige berekeningen gedaan waarin de invloed van enkel,
dubbel en meervoudig aangeslagen configuraties op de excitatie-energieen
is bestudeerd. Het blijkt dat de berekeningen gebaseerd op Configuratie
Interactie met slechts enkel aangeslagen configuraties, in het algemeen
goede excitatie-energieën voor singulet- en triplettoestanden geven.
Enkele optisch verboden overgangen (^1A_g overgang in 1,3 trans-butadieen
en 1,3,5 trans-hexatrieen) worden echter slecht berekend. Tenslotte
blijkt dat de berekende energieen voor onverzadigde koolwaterstoffen (vlak)

resulterend uit berekeningen met enkel en dubbel aangeslagen con-
figuraties binnen 0.2 - 0.3 eV overeenkomen met experimentele waarden.
Teneinde het grote aantal aangeslagen configuraties te beperken is een
criterium gebaseerd op storingsrekening ontwikkeld, dat ons in staat
stelt alleen de belangrijke configuraties in de berekeningen mee te
nemen.

In hoofdstuk IV wordt een spectrometer beschreven die ontwikkeld
is voor de bepaling van totale werkzame doorsneden van aanslagprocessen.
De Trapped Electron (T.E.) methode stelt ons in staat excitatie-proces-
sen te meten dicht bij de drempel van aanslag. Met deze techniek is de
identificatie van de waargenomen overgangen meestal moeilijk. Een nieuwe
techniek is ontwikkeld, de zogeheten Double Retarding Potential Differ-
ence (D.R.P.D.) methode, welke gebaseerd is op ideeën van Brongersma.
Deze methode geeft ons de mogelijkheid de metingen uit te breiden tot
10 eV of meer boven de drempel van aanslag. Door de energie-afhankelijk-
heid van de excitatie-functie in dit energiegebied te bestuderen is
identificatie van het bestudeerde proces mogelijk.

Een inlaatsysteem speciaal voor vaste stoffen met lage damp-
spanning is in gebruik genomen buiten het gewone inlaatsysteem waarmee
gassen en vloeistoffen (dampvorm) in de spectrometer kunnen worden ge-
bracht. Een versterkingssysteem met een zeer laag ruisniveau voor de in-
elastisch verstrooide electronenstroom staat ons toe doorgaande bundel-
stromen te gebruiken in de orde van 10^{-9} A. Daardoor zullen ruimtela-
dingseffecten sterk worden beperkt.

In hoofdstuk V worden de resultaten van helium en benzeen gepre-
senteerd. Bij helium blijkt triplet excitatie zeer intensief in de buurt
van de drempel. Totale werkzame doorsneden van de 2^3S en 2^1S toestanden
van helium zijn gemeten voor het energiegebied van 19-24 eV. Diverse
shape resonanties (instabiele negatieve ion toestanden) zijn waarge-
nomen. Tevens is een schatting gemaakt van de totale werkzame doorsnede
voor de 2^3P toestand. De close coupling berekeningen uitgevoerd door
Burke et al. (1969) voorspellen de juiste structuur maar geven te grote
waarden vergeleken met onze waarnemingen. Een dubbel aangeslagen toe-
stand van helium werd gemeten bij 58.4 eV hetgeen in overeenstemming
was met metingen van anderen. Voor benzeen blijken singulet-triplet
overgangen ook vrij intensief in de buurt van de drempel van aanslag.
Aan de 4.8 eV piek werd op grond van onze meetresultaten besloten tot
een toekenning van een triplettoestand $^3E_{1u}$, hetgeen in strijd is met

de toekenning in andere studies ($^1B_{2u}$). Uit de excitatiefunctie van deze overgang zijn aanwijzingen gevonden voor twee aangeslagen negatieve ion toestanden bij ~ 5.2 eV en bij ~ 6.0 eV.

Hoofdstuk VI geeft resultaten over water en verwante verbindingen. In de spectra van water treedt een zeer intensieve piek op bij 7.2 eV die wij identificeerden als een triplet toestand met waarschijnlijke toekenning $^3B_1$. In andere studies werd aangenomen dat deze piek correspondeerde met een overgang naar de $^1B_1$ toestand. Bij H_2S en methanol zijn analoge absorpties waargenomen bij 5.8 eV en 6.5 eV. Hier lijken triplet toekenningen ook waarschijnlijk. In onze spectra van H_2O, D_2O, CH_3OH, CD_3OD en dimethyl-ether is een zeer zwakke absorptie waargenomen met een maximum liggend in het energiegebied 4.4 - 4.8 eV. Deze "mystery band" zou verklaard kunnen worden door een aanslagproces in het molecuul zelf (A_2 overgangen in H_2O (?)) of wordt veroorzaakt door een excitatieproces in verontreiniging of ontledingsproducten (OH radicalen). De eerste mogelijkheid is niet in overeenstemming met de huidige theoretische gedachtengang. De tweede verklaring lijkt niet waarschijnlijk daar experimenteel geen aanwijzingen werden gevonden voor zulke effecten in het geval van water.

In hoofdstuk VII worden de resultaten van een aantal moleculen van verschillend karakter gegeven. In de spectra van 1,2 dimethyl-cyclohexeen worden twee duidelijke absorpties gevonden bij ~ 5.4 eV en ~ 6.2 eV welke waarschijnlijk toegekend kunnen worden aan $\sigma \rightarrow \pi^*$ en/of $\pi \rightarrow \sigma^*$ overgangen. Een triplet excitatie proces bij 3.8 eV is waargenomen voor 7-dehydrocholesterol dat hoger ligt dan het corresponderend proces in 1,3 trans-butadieen (~ 3.3 eV) hetgeen wijst op een geconjugeerd systeem dat niet vlak is. Voor 1,3,5 trans-hexatrieen zijn twee waarschijnlijke triplet toestanden waargenomen bij 2.6 eV en ~ 4.2 eV. Het laatste proces is nog niet eerder gevonden. Verscheidene overgangen worden waargenomen beneden de optisch toegestane overgang (4.4 eV) in 1,3,5,7 cyclo-octatetraeen zodat voor de meeste, triplet karakter waarschijnlijk is. Het blijkt dat berekeningen met Configuratie Interactie van slechts enkel aangeslagen toestanden betere overeenstemming met experimentele waarden geeft dan berekeningen waarin bovendien dubbel aangeslagen toestanden worden meegenomen. In de spectra van borazine wordt een zeer intensieve absorptie gevonden bij ~ 7.5 eV, welke energie goed overeenkomt met de excitatie-energie voor de optisch toegestane overgang. De absorpties bij lage energie zoals gevonden in alleen (1.6 eV), acetyleen (1.9 eV) en propyn (2.8

eV) kunnen verklaard worden door vibratie aangeslagen negatieve ion toestanden. In het energiegebied van 4-6 eV wordt intensieve triplet aanslag waargenomen voor deze moleculen.

C U R R I C U L U M   V I T A E

Na het behalen van het einddiploma HBS-B aan de Rijks-HBS te
Deventer begon ik in september 1962 met de studie aan de Rijksuniversi-
teit te Leiden. Het candidaatsexamen in de scheikunde met bijvakken
natuurkunde en wiskunde (letter f) werd op 18 mei 1965 afgelegd. De
studie werd daarna voortgezet aan de afdeling voor Theoretisch Orga-
nische Chemie van Professor Dr. L.J. Oosterhoff. Onder leiding van
Dr. H.M. Buck werden enkele moleculen zoals N-picrylauramine gesynthe-
tiseerd en met verschillende physische methodieken onderzocht op hun
intra-moleculaire ladingsoverdracht. Op 2 oktober 1967 legde ik het
doctoraalexamen af in de Theoretisch Organische Chemie met als bijvakken
theoretische natuurkunde en wiskunde. Eind januari 1968 begon ik op het
F.O.M.-Instituut voor Atoom- en Molecuulfysica te Amsterdam met de
experimenten zoals beschreven in dit proefschrift.

Gedurende de periode september 1965 - oktober 1967 was ik als
candidaats-assistent in dienst van de Rijksuniversiteit te Leiden
(college-assistent). Hierna werd ik als wetenschappelijk medewerker ver-
bonden aan de afdeling Theoretisch Organische Chemie in dienst van
Z.W.O. (S.O.N.) tot 1 juli 1968, op welke datum ik in dezelfde functie
aangesteld werd bij de Rijksuniversiteit te Leiden.

De stimulerende gesprekken met de andere leden van de afdeling
Theoretisch Organische Chemie en met de andere medewerkers van het Gor-
laeus Laboratorium heb ik zeer op prijs gesteld. Vooral dient vermeld te
worden de stimulerende discussies die gevoerd zijn met Mevr. Drs. J.A.
v.d. Hart - v.d. Hoek, Dr. J. Lugtenburg, Drs. C.I.M. Beenakker, Drs.
M.C. van Hemert en Dr. J.J.C. Mulder. Laatstgenoemde ben ik veel dank
verschuldigd voor de hulp die hij verleend heeft bij het tot stand
komen van het theoretisch gedeelte van dit proefschrift. De staf van
het Centraal Rekeninstituut (C.R.I.) wil ik gaarne bedanken voor de
prettige medewerking. In het bijzonder de heer R.L. Zweerus ben ik zeer
erkentelijk voor de spontane en deskundige hulp bij Jobcontroll en
Fortran IV problemen.
De verbinding 1,3,5 trans-hexatrieen is met grote zuiverheid (98%) ver-
vaardigd door Mej. J.A. Duyndam.